DYNAMIC RESPONSE AND TRANSFER CHARACTERISTICS OF KNEE JOINT AFFERENTS IN SOMATOSENSORY THALAMUS OF THE CAT

by
Tom Chi Tien Yin

A dissertation submitted in partial fulfillment
of the requirements for the degree of
Doctor of Philosophy
(Electrical and Computer Engineering)
in The University of Michigan
1973

Doctoral Committee:

Professor William J. Williams, Chairman
Assistant Professor David J. Anderson
Associate Professor Spencer L. BeMent
Associate Professor Kenneth L. Casey
Assistant Professor Stephen S. Easter, Jr.

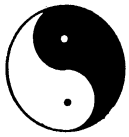

ACKNOWLEDGEMENTS

No thesis is the work of a single individual, and this thesis is no exception. To my advisor: Prof. W.J. Williams, whose enthusiasm initially led me to study the nervous system, I wish to express my wholehearted appreciation for his continual guidance, encouragement, and support of this work. He has been a generous teacher and friend throughout.

To my committee members: Prof. D.J. Anderson, who guided me into the study of stochastic point processes; Prof. S.L. BeMent, who helped in the experimental phase of this work and in preparing the text; Prof. K.L. Casey, who suggested the chronic preparation and gave much helpful advice on the clinical aspects of the problem; and Prof. S.S. Easter, Jr., who stimulated my interest in sensory physiology; I am grateful for their assistance and advice. To the Department of Physiology and Prof. L.T. Rutledge, I thank them for the use of the histology equipment and general help.

To Ms. Barbara Perkel and Ellen Zufall: who did yeoperson's (?) work in typing up the manuscript under trying conditions, a vote of thanks.

To my colleagues: Dr. J.W. Gesink, Dr. W.D. McCall, Mr. B.F. Belanger, Dr. M.M. Stern, and Ms. Lillian Tong, I look back with affection and appreciation for the long hours spent puzzling over problems on the blackboard, writing computer programs, and helping in the multitude of problems associated with such a work. To the latter, I am particularly grateful for her help in editing the manuscript as well as being a patient and loving wife, whose support and good cheer carried me through the study.

Financial support for this work was provided by a National Science Foundation traineeship and a U.S.P.H.S.-N.I.H. grant NS 08470.

TABLE OF CONTENTS

LIST OF TABLES

LIST OF FIGURES

LIST OF APPENDICES

LIST OF EQUATIONS

CHAPTER I

GENERAL INTRODUCTION

FOREWORD

In a general sense the jobs of an engineer and of a neurophysiologist are complementary. The engineer's job is synthetic, the neurophysiologist's job is analytic. The engineer is given a set of criteria and asked to design a system to meet these criteria. The neurophysiologist is given a system and asked to explain how the system works. Furthermore, modern technology and neurophysiology have progressed along roughly parallel lines. We have been very successful in designing systems that interact with our surroundings, either sensing minute details in the environment or moving objects precisely within the environment; but we are far from realizing a "thinking" or "learning" machine. Similarly we have progressed in our understanding of the sensory and motor processes by which an organism senses and reacts to the environment while memory and the cognitive processes of the nervous system remain wholly inexplicable. It seems reasonable, then, to believe that modern engineering principles may be helpful in studying the sensory and motor processes of the nervous system. In the last decade we have seen a growing interest in the application of engineering techniques to biological problems, especially in the realm of sensory physiology. The research described here utilizes the principles of communication and control theory to study a neural sensory system.

The process by which the organism is made aware of his environment involves several stages. The external energy (e.g. light, sound,

mechanical) must be transduced by a receptor, encoded into a form compatible with the nervous system, and transmitted into the central nervous system where, after passing through several synaptic relays, it reaches the cerebral cortex and higher centers where it is thought that "sensation" is first manifested. Spatial and temporal transformations of the signal can occur at any point along the pathway to the cortex. These transformations have been studied most successfully in the visual system where explanations of the changes in the response of receptor, bipolar, ganglion, lateral geniculate, and cortical cells are now beginning to emerge. In this thesis the transformations in the temporal domain are studied for the knee joint receptors of the somatosensory system at the level of the thalamus.

SYSTEM CHOSEN

The knee joint proprioceptor system of the cat was chosen for this study. This system has a number of properties that make it amenable for a study of this kind. The joint receptors in the knee of the cat have been studied extensively by a large number of investigators so that the properties of the first order receptors are reasonably well-known. The system is relatively simple: there is no efferent control on the receptors (Skoglund, 1956) as there is in muscle spindles. The adequate stimulus for these receptors is assumed to be the position or movement of the joint, both of which can be accurately controlled and monitored. The relevant somatosensory pathways are modality specific so that the thalamic cells are sensitive to the activity of only one type of receptor. Finally, although the sensation is an important one in terms of clinical dysfunctions, there is

an almost embarrassing lack of information about the physiology and anatomy of the system, especially at higher levels of the nervous system. Further information about the characteristics of the sensory processes at different levels of the nervous system can be potentially useful in the design of psychophysical tests for clinical situations.

RESEARCH OBJECTIVES

The objectives of this research are twofold: one, to determine the dynamic response of cells in the somatosensory thalamus that are sensitive to knee joint position and movement and two, to determine the filtering characteristics that these thalamic cells impose upon the afferent signal along the way to the cortex. Linear systems analysis techniques are used to find the frequency response of the thalamic neurons to sinusoidal movements of the joint. By knowing the dynamic response of the joint cells, the capacity of the animal to detect movements of the limb can be estimated and compared to the appropriate psychophysical data. The transfer characteristics of the cell can provide insight into the nature of information transmission along neural pathways and to the demodulation mechanisms by synaptic processes.

STRUCTURE OF THESIS

This thesis is organized into five chapters. After this introduction is a chapter containing a literature review of the anatomy and physiology of joint receptors. Chapter III describes in detail the experimental work and results of the dynamic properties of thalamic joint neurons. Chapter IV compares the results at the thalamus with

the results at the gracile nucleus, which is the level just preceding the thalamus, in order to ascertain the transfer properties of the thalamic cells. It also contains a discussion of the theoretical implications of these results in terms of neural communication. The final chapter is a general summary and conclusion. Much of the mathematical and theoretical results have been placed in the appendices.

CHAPTER II

ANATOMY, PHYSIOLOGY, AND CENTRAL PROJECTIONS OF JOINT RECEPTORS

INTRODUCTION

Physiologists have long known that humans are able to judge accurately the position and movement of their limbs in space without the aid of visual or tactile cues(Goldscheider, 1898). However, the mechanisms responsible for this position sense, or proprioception, have been the subject of some controversy, much of it of very recent origin. The controversy concerns the relative roles of muscle and joint receptors in conveying the position of the limb. The evolution of this debate is an interesting one and worth a short digression and review here.

The significance of this problem can be partially gauged by the prominence of the nineteenth and twentieth century physiologists who wrestled with it. In particular, Bell (1826), Helmholtz (1867), Sherrington (1900), James (1890), and Lashley (1917) all made contributions to the question at hand. Charles Bell (1826) was the first to postulate the existence of a position sense with its own receptor apparatus and afferent nerves comparable to the other senses, and it became known as the "sixth sense." Sherrington had made the great discovery in 1894 that muscle spindles are sensory endings and made the natural supposition that these receptors, along with the articular receptors, are responsible for the "muscular sense." In opposition to this view, at least in the case of eye muscles, Helmholtz (1867) had shown by his usual simple but powerful experiments that the eye muscles are not responsible for

the sense of position of the eyeball. Helmholtz held that our sense of position and movement of the eyeball must be determined by the efferent signals to the motoneurons of the oculomotor system; this sense was called the "sense of effort" and is now commonly called efferent copy.

Sherrington's greater influence on neurophysiology made his view the dominant one until the "modern" era when the functional properties of muscle spindles and Golgi tendon organs were studied with single unit analysis. It had become clear by the early 1950's that these receptors do not respond with any clear relationship to the length of the muscle, the condition seemingly necessary for signaling joint angle. Golgi tendon organs are connected in series with the extrafusal fibers and signal the tension in the muscle, which is a function of muscle length and load. Muscle spindles are connected in parallel with the extrafusal fibers which gives them the capacity for responding to muscle length, except that their discharge rate is biased by the efferent gamma activity as well as muscle length.

Furthermore, several other lines of evidence in both humans and animals seemed to show that muscle spindles and tendon organs could not be signaling the position of the limbs. In human subjects when a local anesthetic was applied to the finger (Provins, 1958; Merton, 1964) or toe joint (Browne et al., 1954), there was a gross loss of awareness of the position of the digit when it was moved passively, even though the anesthetic did not reach the spindles, which for these joints were located some distance away. Similarly, after anesthetizing the conjunctiva the eyeball could be moved 20° or more without any

sense of movement (Brindley and Merton, 1960). There did seem to be a difference between active (when the subject moved the digit himself) and passive (when the digit was moved by someone else) kinesthesia; the accuracy of estimates of limb position was relatively unimpaired when the subject was asked to move the limb actively (Paillard and Brouchon, 1968). In addition, passive stretch of the tendons at tensions adequate to stimulate the primary and secondary muscle spindles failed to evoke any clear sensation of muscle tension or joint movement (Gelfan and Carter, 1967). In animal experiments Freeman and Wyke (1966) found that transection of the posterior or medial articular nerve innervating the knee joint of the cat produced altered reflex behavior, and until recently electrophysiological recordings of evoked responses in the sensory cortex failed to show any response to stimulation of muscle nerves (McIntyre, 1962). Thus just three or four years ago, there was very compelling evidence that receptors within the joint capsule and not those within the muscles themselves are responsible for proprioception.

In the last few years, however, evidence has been presented showing that under suitable conditions muscle spindles do seem to contribute to our sense of position of the limbs. The most dramatic finding was the recent demonstration of a proprioceptive illusion induced by vibrating the tendon of the biceps or triceps muscle at 100 Hz (Goodwin et al., 1972a). Systematic misjudgements of up to 40° were induced in the elbow joint by this vibration which excited the muscle receptors maximally. No illusion was seen when the vibrator was placed directly over the joint so as to stimulate the joint receptors maximally. This same group of investigators also

found appreciable kinesthesia after the joint afferents had been anesthetized, particularly for rapid movements, passive or active (Goodwin et al., 1972b). In addition several investigators have now been able to elicit short latency responses in the cerebral cortex to electrical stimulation of Group I nerves in monkeys and cats (Oscarsson and Rosen, 1963; Mallart, 1968), so it would appear that signals from muscle spindles reach cortical levels. However, this does not necessarily imply that the signal has reached "conscious" levels. For the cat hindlimb muscle afferents the medullary relay is the nucleus Z of Brodal (Landgren and Silfvenius, 1971). To further cloud the picture, Lindström and Norrsell (1971) have been unable to replicate the experiments of Freeman and Wyke (1966). They denervated both the medial and posterior articular nerves and observed no readily discernible effect of the denervation.

Moreover, careful single unit studies of the characteristics of the joint receptors themselves have cast doubt on the ability of these receptors to code absolute joint position unambiguously. The slowly adapting joint receptors were found not only to have a double-valued "bell-shaped" static output frequency vs. angle curve, but also to exhibit severe non-repeatability by some investigators (Skoglund, 1956; McCall, 1971). Other investigators have found no bell-shaped static curve, but they have found that only an insignificant 2% of the slowly adapting receptors are active at intermediate angles of the joint when no twist is applied to the tibia, (Burgess and Clark, 1969b). All of the other receptors in their population responded only at extreme flexion or extension or both. This problem will be discussed in more detail later in this chapter when we discuss the physiology of the knee joint

receptors.

The question of the relative roles of muscle and joint receptors in the perception of position sense has been thrown open for re-examination by these recent findings. The most reasonable evaluation given the current evidence seems to be that muscle receptors, at least under certain experimental conditions, do indeed contribute to kinesthesia, particularly active kinesthesia, and that joint receptors, by themselves, are not capable of supplying all of the necessary information. Clearly further study of both the muscle and joint receptors and their central projections is needed if we are to understand this sensory function. The literature on the anatomy and physiology of muscle spindles and Golgi tendon organs is vast (Matthews, 1964; 1972; Eldred et al., 1967) whereas much less effort has been directed towards joint receptors, and even less towards their central afferents.

ANATOMY AND PHYSIOLOGY OF KNEE JOINT RECEPTORS

The joint receptors most often studied are those innervating the knee joint of the cat. The receptors lie in the synovial capsule of the knee joint and are innervated primarily by two small nerves: the medial and posterior articular nerves. Occasionally there exists a lateral articular nerve and some accessory nerves that course through muscle fibers (Gardner, 1944; Samuel, 1952; Skoglund, 1956; Freeman and Wyke, 1967).

There have been several histological investigations of the sense organs within the cat knee joint (Krause, 1874; Gardner, 1944; Samuel, 1952; Boyd, 1954; Skoglund, 1956; Freeman and Wyke, 1967). There is

general agreement on the types of endings found innervating the capsule. Within the capsule there are free nerve endings and two types of specialized endings. The tiny free nerve endings innervate both myelinated and unmyelinated fibers and are thought to be pain or sympathetic in function (Samuel, 1952). By far the most numerous ending is the Ruffini-type ending whose afferent axon typically divides once or twice into branches that break up into a series of fine sprays, each enclosed by a delicate capsule. The other type of ending within the capsule, but found much less frequently, is the lamellated Vater-Pacinian corpuscle with its axons ending in a small knob. External to the capsule there are Golgi endings on the cruciate, collateral, and patellar ligaments bound to the capsule. These endings are substantially larger than the Ruffini endings and are very similar to those found commonly in tendons.

The nerve fibers with these different types of endings are also differentiated by caliber. The Ruffini endings are associated with fibers between 7-10μ, the Golgi endings with fibers between 10-15μ, and the sparse Vater-Pacinian corpuscles with fibers between 7-12μ. As we shall see, the different endings also seem to be functionally distinct in the character of their sensory discharge.

ELECTROPHYSIOLOGY OF KNEE JOINT RECEPTORS

Numerous studies have investigated the properties of these joint receptors by recording discharges on the medial or posterior articular nerves or by recording from dorsal root filaments and sorting out single units by progressive splitting of the fibers. The majority of fibers are slowly adapting (tonic) and respond to position and move-

ment of the joint or to local pressure on the joint capsule. A much smaller number of fibers are rapidly adapting (phasic) and are very sensitive to any movement of the tibia. Boyd (1954) and Skoglund (1956) correlated a histological examination of the individual endings with their sensory discharge and found that the more numerous tonic responses originated from the abundant Ruffini and Golgi endings while the phasic responses emanated from the Vater-Pacinian corpuscles. Furthermore Andrew (1954) and Skoglund (1956) were able to distinguish two types of slowly adapting responses corresponding to the Ruffini and Golgi endings based upon their differential response to velocity of movement and to contraction of nearby muscles. The Golgi endings, like their counterparts in tendon organs, were not sensitive to velocity or muscle contraction.

The tonic receptors are the ones believed responsible for coding position of the joint (Andrew and Dodt, 1953; Boyd and Roberts, 1953; Skoglund, 1956; Cohen, 1955; Burgess and Clark, 1969b; McCall et al., 1973). Most of these reports agree upon the sensitivity of these receptors to externally applied stimuli. The usual response of the tonic receptors to static position of the joint is a very steady train of impulses with little or no adaptation. Cutting the muscle nerves severely inhibits the response of the joint afferents as recorded by gross recordings on the articular nerves, indicating that some of the receptors are sensitive to tension exerted on the joint by these leg muscles (Skoglund, 1956). This will be an important point when we contrast results obtained from the articular nerves with dorsal root recordings. Likewise, stimulating the muscle nerves of the elbow will produce a discharge in the elbow joint nerves even

when the ulna and humerous are rigidly clamped to the apparatus (Millar, 1972). Twisting of the tibia about its long axis affects the discharge of most single units and usually recruits more units. Increasing the intracapsular pressure by injecting fluid into the synovial cavity also greatly potentiates the discharge of most of the slowly adapting receptors.

The plot of discharge frequency vs. angle of the joint, or static curve, for a single ending shows that the receptors are excited over a comparatively small range of joint angle, usually 10-30°. This angle will be referred to as the receptive angle for a receptor or central joint afferent. The static curve of some of the tonic receptors has a monotonic character with a maximal response at one extreme of the receptive angle either at flexion or extension. Other units show a "bell-shaped" or double-valued static curve with the maximal response somewhere in the middle of the receptive angle. There is considerable overlap in the receptive angles of different units. Unfortunately there is no good estimate of the distribution of receptive angles over the entire range of movement of the knee joint, but all reports indicate that there are more units active at the extremes of extension and flexion than at intermediate angles. In fact, Burgess and Clark (1969b) found that only 2% of the fibers recorded at the dorsal roots were activated at intermediate angles, and the majority of the slowly adapting fibers were active at both extreme flexion and extension. This would seem to make it improbable that these receptors could be accurately conveying the position of the joint to the central nervous system. Moreover, McCall (1971) found that the static curves of most receptors exhibited a hysteresis-

like non-repeatability in traversing the receptive angle in one direction and then back.

It is clear that the physiological properties of these joint receptors are not ideal in terms of coding joint angle. The bell-shaped static curve, non-repeatability, and bidirectional response (discharge at both flexion and extension) are all characteristics that preclude unambiguous coding of joint position without more complex central processing. Given a suitable population of receptors, however, it would still be possible to accomplish the task even if the individual receptors themselves were not ideal. The most inexplicable result, then, is the observation by Burgess and Clark (1969b) that so few tonic receptors are active in the intermediate range between extreme flexion and extreme extension.

Much of the difference between the results of Burgess and Clark (1969b) and all other investigators is due to the fact that the former study recorded the joint afferents at the level of the dorsal roots and all other studies recorded directly on the peripheral nerves. The advantage of recording from the articular nerves is the relative ease with which joint afferents can be found. However, it suffers from the critical disadvantage that the receptors cannot be studied through the entire range of joint movement because of the placement of the electrodes. In addition, and possibly more crucial, by recording on the peripheral nerves, there is a natural sampling bias of joint units toward the few that are active at intermediate angles simply because it is easier to isolate a single unit in that range of joint angle where there are fewer active receptors. By contrast the dorsal root recordings permit investigation over the full range of

joint angle, but an extensive denervation of cutaneous and muscle nerves must be done in order to find the rare joint receptors among the numerous other types of afferents. The denervation causes an unloading of the tensions normally exerted upon the joint capsule, which possibly alters the response characteristics or sensitivity of the endings (Skoglund, 1956; Millar, 1972). This, no doubt, accounts for at least some of the discrepancies in the literature. Further work using dorsal root recording, preferably with no denervation, is needed to resolve these differences.

The slowly adapting receptors are also sensitive to the angular velocity and acceleration of movement. Steps, ramps, and sinusoidal waveforms have been applied to the joint in order to determine the dynamic behavior of the receptors (Andrew and Dodt, 1953; Boyd and Roberts, 1953; Cohen, 1955; Skoglund, 1956; Viernstein, 1969; Burgess and Clark, 1969b; McCall et al., 1973). The response of the tonic receptors to step or ramp inputs shows the typical proportional-plus-derivative or lead filter effect. In response to step inputs the receptor exhibits an initial burst that adapts within seconds to a steady frequency that is a function of the new position of the limb. Viernstein (1969) applied ramp inputs to the knee joint of monkeys and found that the resulting discharge could be fit by a lead filter with the form

$$H(s) = \frac{s + a}{s + b} \qquad (2.1)$$

in Laplace transform notation.

The frequency response of the tonic cat knee joint receptors to simusoidal inputs of angle displacement has been found by McCall et al.

(1973). The describing function for most of the tonic fibers was fit adequately with a fractional-order differentiator model (Chapman and Smith, 1963) of the form

$$H(s) = s^k \qquad (2.2)$$

where k = .25. The magnitude portion of this model has a positive slope of 20k db/decade and the phase has a constant lead of 90k degrees. Although the data could be fit with more complex models (e.g. alternating poles and zeroes), the s^k model is favored because it requires fewer parameters. This transfer function can be derived from a model with distributed, rather than lumped, parameters. In the time domain this model has a step response of the form

$$h(t) = G\,\Gamma(1 - k)t^{-k} \qquad (2.3)$$

which would be insensitive to absolute joint angle since $t^{-k} \to 0$ as $t \to \infty$. This type of response has been observed by some investigators in denervated preparations (Burgess and Clark, pers. comm.), but most studies have found that the endings are sensitive to joint angle even for very long adaptation times (McCall et al., 1973). This is still an open question that requires further study. Part of the problem is the slow convergence of t^{-k}, especially for small k.

Only a few investigators have studied the rapidly adapting receptors though most reports have mentioned their existence. Burgess and Clark (1969b) identified two types of rapidly adapting receptors, which they called phasic and Pacinian corpuscle-like. The phasic joint receptors produced a transient, bidirectional response, especially at extreme flexion or extension. They were capable of a low sustained discharge when stimulated strongly and responded to twisting of the

tibia. Some phasic receptors, which were insensitive to pressure applied to the back of the knee but responded to lateral pressure, were believed to be associated with the Golgi endings. The Pacinian-like endings were very sensitive to rapid joint movement in any direction and at any bias angle. They did not respond with a sustained discharge and appear to be the same as the phasic receptors described by Skoglund (1956). Farias (1973) found phasic joint receptors that phase-locked at low frequencies of sinusoidal stimulation. As the frequency increased, these receptors showed a bidirectional response in which spikes occurred within two narrow phase angles 180° apart.

Before we follow these joint afferents into the central nervous system, let us recapitulate what is known and what needs to be discovered about the peripheral receptors. There are two major groups of knee joint receptors; the majority are slowly adapting or tonic and the remainder are rapidly adapting or phasic. The tonic receptors are active only over a small receptive angle and most of them are active at flexion and/or extension rather than at intermediate angles. It is important to find out the distribution of receptive angles over the entire range of joint angle, preferably in an intact (nondenervated) hindlimb. If the population is indeed as biased to the extremes of flexion and extension as Burgess and Clark (1969b) found, then it is unlikely that these receptors can tell us the absolute joint angle without any additional information from muscle spindles, no matter how complex the central processor, because there are simply not enough receptors active at the intermediate angles. Also, the receptors are known to respond to twisting of the tibia with respect to the femur.

However, it is doubtful that an attempt to categorize the response of all the receptors to all possible torques will prove fruitful. The phasic receptor response has not been studied quantitatively; more precise judgements must be obtained about their sensitivity, receptive angles, bidirectionality, and response to different modes of stimulation.

PATHWAYS FOR KNEE JOINT AFFERENTS TO THE CEREBRAL CORTEX

Unfortunately the pathway for these knee joint afferents to the cerebral cortex is uncertain. Classical neuroanatomy identifies two major pathways for tactile and kinesthetic impulses; the dorsal column-medial lemniscal system and the ventral spinothalamic tracts (Crosby et al., 1962). The dorsal column fibers ascend in the ipsilateral fasciculus gracilis and cuneatus to synapse in the dorsal column nuclei (DCN). Fibers from these nuclei cross the midline, join the medial lemniscus, and ascend to the ventrobasal complex (VBC) of the thalamus. The ventral spinothalamic (or anterolateral) system has its first synapse in the spinal cord dorsal horn. The secondary fibers in the dorsal funicular grey decussate at the ventral white commissure and ascend along the ventrolateral margin of the spinal cord. They ascend to the posterior group of the thalamus but probably not to the VBC (Boivie, 1971a). In addition to these classical pathways, there now appears to be a third pathway that transmits tactile information to the somatosensory cortex: the spinocervical thalamic tract or Morin's pathway (Morin, 1955; Morin et al., 1962). Its second order afferents appear to derive from three sources:

dorsal grey matter, dorsal spinocerebellar tract, and ventral spinocerebellar tract (Ha and Liu, 1966). The afferents ascend in the dorsolateral funiculus, chiefly ipsilaterally, to the lateral cervical nucleus (LCN), which is located between the lower medulla and the third cervical root. The fibers from the LCN then cross and also project to the contralateral ventrobasal complex. Figure 2.1 shows a schematic diagram of these three pathways.

The classical view of the dorsal column is best described by Mountcastle (1968, p. 1377):

> "The distinguishing feature of the lemniscal system is that information concerning the location, spatial form, quality, and temporal sequence of stimuli that impinge upon the body is transmitted at each synaptic station with great fidelity...Certain of the spatial, particularly topographic, and temporal and intensive relations of events within this system are invariant across nuclear relays. This invariance derives from two special attributes. The first is that the peripheral sheet of receptors is projected through successive stages of the system and into the contralateral cortex. Second, the system encompasses within this single topographic pattern the several submodalities of mechanoreception. These properties define a lemniscal neuron, a cell of the lemniscal system that subtends a restricted receptive field, is activated by a single type of first-order mechanoreceptive afferent, and possesses through its synaptic relations powerful transmitting capacities in the temporal domain."

The mechanoreceptive submodalities subserved by the dorsal columns are touch, vibration, pressure, and kinesthesia. In cat the sacral, lumbar, and thoracic segments up to T_1 project to the gracile nucleus; the remaining thoracic and cervical roots project to the cuneate nucleus. Only 22-23% of the myelinated dorsal root fibers that enter the dorsal columns reach the DCN (Glees and Soler, 1951). The rest enter the spinal grey and make reflex connections with other tracts. At each relay of the dorsal column system, there is a convergence of the peripheral fibers such that at the DCN, for instance,

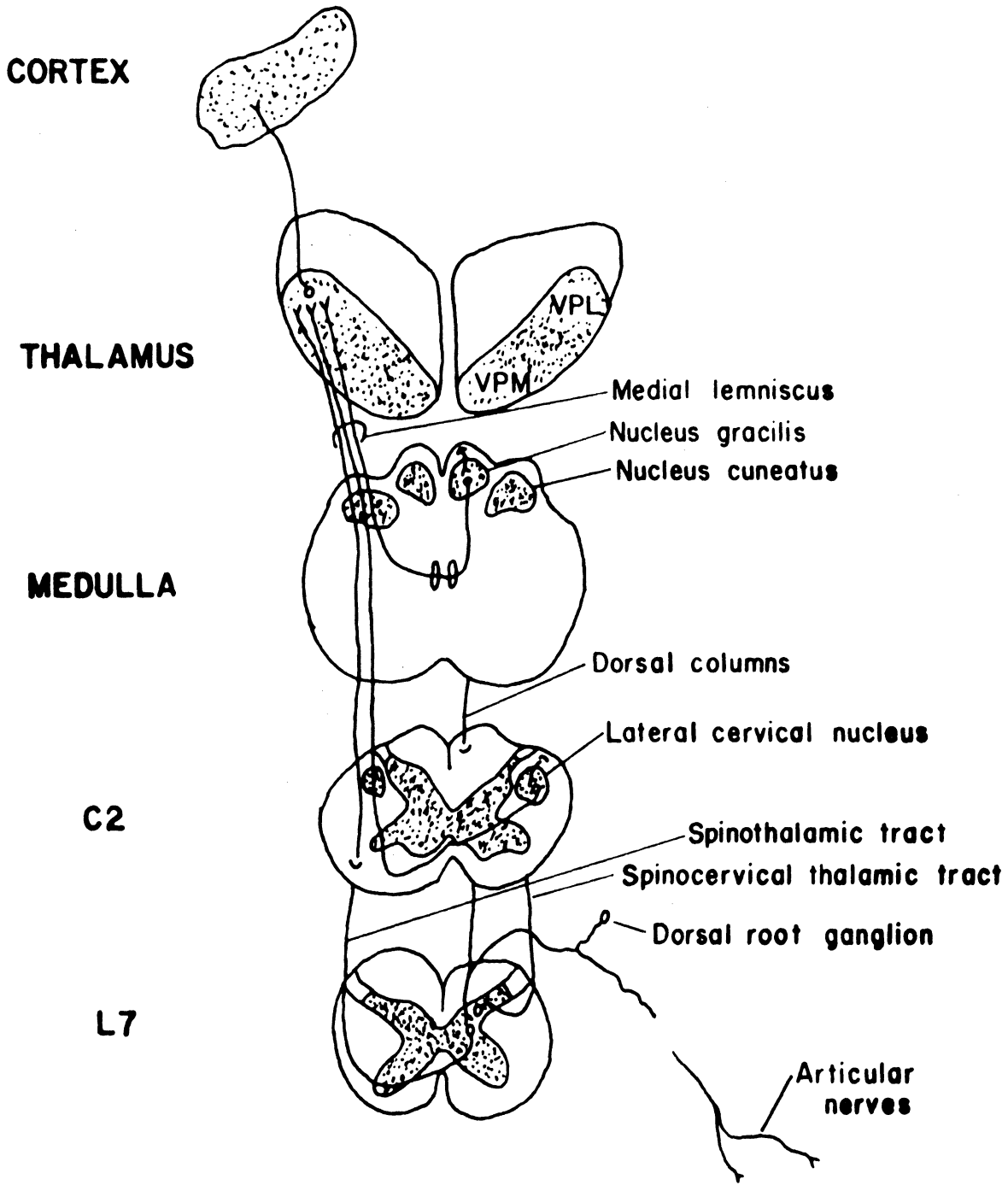

Figure 2.1. Possible pathways for knee joint afferents to the cerebral cortex. This schematic diagram shows the three major pathways for somatosensory transmission of hindlimb information: the dorsal columns, spinothalamic, and spino cervical thalamic systems.

the average receptive field of postsynaptic units is ten times larger than that of the first order fibers (Winter, 1965). Cells responsive to rotation of the joints have been found at all levels of the dorsal column system (Mountcastle and Henneman, 1949; Mountcastle, 1957; Kruger et al., 1961); and these cells preserve all properties of a lemniscal neuron, as defined by function rather than anatomy by Mountcastle and his colleagues (see quote above).

CENTRAL PROJECTION OF KNEE JOINT AFFERENTS

Recently controversy has arisen over this view of the lemniscal system. In particular, the concept that the slowly adapting joint receptors ascend in the dorsal columns to synapse in the DCN has come under serious attack (Gardner, 1969; Wall, 1970b). Briefly the argument against the classical view depends upon a re-examination of the earlier concepts in light of recent experiments. Essentially much of the classical view was based upon experiments in which the lesions and sections of dorsal column may not have been carefully controlled or monitored (Wall, 1970a; b). Meanwhile a large body of evidence has been accumulating suggesting that the dorsal column system does not mediate all fine discriminative sense. (Cook and Browder, 1965; Levitt and Schwartzmann, 1966; Kitai and Weinberg, 1968; Dobry and Casey, 1972). For the purposes of this study, the results of five recent experiments are particularly relevant. One, Burgess and Clark (1969a) found that no slowly adapting knee joint fibers could be activated by antidromic stimulation of the cervical dorsal columns. Two, Gardner and Noer (1952) found that cortical potentials from articular nerve stimulation persisted even after

dorsal column section. Three, Vierck (1966) found that dorsal column section in monkeys did not seriously impair position sense. Anterolateral section alone or even both dorsal column and anterolateral section did not result in serious loss. There was complete kinesthetic loss only after the posterior quadrants and opposite anterolateral tracts were sectioned. Four, Körner and Landgren (1969) found that cortical potentials from electrical stimulation of the posterior articular nerve were abolished by transection of the dorsolateral fascicle but not by transection of the dorsal columns at the C_4 level. Finally, experiments in our laboratory failed to find any tonic knee joint cells in the gracile nucleus (Williams et al., 1973). On the other hand, several investigators have reported finding slowly adapting joint units in the DCN (Kruger et al., 1961; Amassian et al., 1962). It is not clear, however, that all investigators equate the slowly adapting discharge with the tonic response as is done in this thesis. Kruger and coworkers, for example, reported that slow units occasionally maintained their discharge for greater than one minute in the absence of transient displacement, implying that most of their slow units did not fire a steady discharge. Instead they identified slow joint units with those neurons that displayed a steadily increasing discharge rate as the joint angle was increased or decreased, e.g. with the limb slowly in motion.

Williams et al. (1973) studied the frequency response of the phasic knee joint afferents found in the gracile nucleus. This was the only quantitative study of the response of central joint afferents to dynamic stimulation. Two general classes of knee joint

cells could be distinguished in the gracile nucleus both by their frequency response and adaptation characteristics. One type seemed to be responding to the acceleration of the joint angle and the other type to the velocity. A considerable degree of nonlinearity was present at this level in the form of phase-locking, a bi-directional response, and a dependence of the sensitivity on both the amplitude and bias angle of the input.

If some of the slowly adapting joint units do not ascend in the dorsal columns a likely transmission path for these impulses is the spinocervical tract (Gardner, 1969; Schwartzmann and Bogdonoff, 1969). The third order cells in the LCN receive most of their afferents from dorsal horn cells (Taub and Bishop, 1965) and the rest from the ventral and dorsal spinocerebellar tracts (Kitai and Morin, 1962; Ha and Liu, 1962, 1966). Joint afferents are known to project to dorsal spinocerebellar tract (Lundberg and Oscarsson, 1960; Lindström and Takata, 1972). Single unit studies in the LCN show that most of the cells are sensitive to light touch on small ipsi-lateral receptive fields with a small percentage sensitive to very large, sometimes discontinuous, and bilateral receptive fields (Oswaldo-Kruz and Kidd, 1964; Morin et al., 1963).

Whether or not joint afferents project to the LCN is an open question. Oswaldo-Kruz and Kidd (1964) found that none of their sample of 206 cells were true joint afferents whereas Morin et al. (1963) and Kitai et al. (1965) found a low percentage of hind limb joint cells in the cat and dog. All three of these studies utilized physiological stimuli;rejection or acceptance of a unit as a joint afferent was based on its response to joint angle change

and to probing of the area about the joint. The critcal experiment would be to stimulate the articular nerves and record from the LCN cells. The results cited earlier of Vierck (1966) and Körner and Landgren (1969) also implicated the spinocervical thalamic tract for conducting joint afferents.

The anatomical details at the next level of the central nervous system are in much less conflict. The ventrobasal complex (VBC) of the dorsal thalamus is composed of the ventroposterolateral nucleus (VPL) and the ventroposteromedial nucleus (VPM) (Rinvik, 1968). The VPL, or external component of the VBC, is larger than the VPM, or arcuate component, and receives the gracile and cuneate components of the medial lemniscus. The VPL lies rostral and lateral to the VPM. The gracile cells of the dorsal column system project to the lateral portion of VPL (VPL_l) and the cuneate fibers ascend to the medial portion (VPL_m) (Boivie, 1971b). Fibers from the LCN relay mainly in VPL_l but there may also be some overlap into the VPL_m dorsally and rostrally (Landgren et al., 1965; Boivie, 1970). Thus, at least two of the three major somatosensory systems project to the VBC with hindlimb and trunk afferents segregated to VPL_l and forelimb and cervical to VPL_m. The spinothalamic tract is believed to terminate partly in the VBC by most investigators . However, a recent careful study indicated that there was no degeneration in VBC after spinothalamic tracts were lesioned (Boivie, 1971a).

Many investigators have studied the activity of single cells in VPL using both extracellular and intracellular microelectrodes (Mountcastle and Henneman, 1949; 1952; Rose and Mountcastle, 1954; Poggio and Mountcastle, 1963; Mountcastle et al., 1963; Andersen

et al., 1964a; 1964b; Harris, 1970; Baker, 1971; Jabbur et al., 1972). In agreement with the anatomical studies, there is a consistent and functional topographical organization of cells in VPL and VPM as determined by the location of single neurons and of their peripheral receptive fields. Progressively more rostral segments project to the medial and posterior regions of the VBC. Each spinal segment projects a thin curving sheath of cells, convex laterally and concave medially. Poggio and Mountcastle (1963) found that almost all cells in the VPL of the unanesthetized monkey had lemniscal properties, i.e. they were modality specific and related to circumscribed, contralateral, and continuous receptive fields. These results were confirmed by Baker (1971) in the awake cat, except that the receptive fields were found to be larger than in the monkey. In contrast to these findings, Harris (1970) and Jabbur et al. (1972) found cells in chloralose cats that had large, bilateral, and discontinuous receptive fields. There is some evidence that chloralose tends to enhance the "nonlemniscal" properties of neurones in VPL (Bava et al., 1966), which may account for some of these discrepencies.

The only quantitative study of the response of cells in VPL that were sensitive to joint stimulation was by Mountcastle et al. (1963) in the unanesthetized, deafferented-head preparation of the macaque. In contrast to the bell-shaped static curve found at the periphery, all thalamic joint cells exhibited continuous and monotonic curves with the maximal discharge at the extremes of flexion or extension. The average active angle of these units was over 70°, about four times larger than those of the first-order afferents in the feline

knee joint. The shape of the static curve could be accurately described by a power function

$$\lambda = k\ S^n + \lambda_T \qquad (2.4)$$

where λ is the response in spikes/second, λ_T is the frequency of the spontaneous discharge, k is a constant scale factor, S is the stimulus intensity $(\theta - \theta_T)$ in terms of degrees of deflection (θ) of the joint away from the edge of the threshold angle (θ_T), and n is a constant. This is the same functional form as that found for many psychophysical measurements in other sensory modalities.

Stevens (1970) suggested that this power function is valuable for compressing the wide range of stimulus intensities into the physiological range of nerve discharge rates. This is especially pertinent in the visual and auditory systems where there is an enormous range of input intensities. For the joint receptor system, however, the utility of a power function is not so clear. Werner and Mountcastle (1963) related the compressive properties of the power law function with the often observed phenomenon that the standard deviation of the interspike interval histogram was linearly related to the mean interspike interval (Rodieck, 1967; Goldberg et al., 1964). Werner and Mountcastle (1963) showed that the decreasing slope of power functions as the stimulus intensity was increased could be offset by the decreasing standard deviation in interspike intervals, so that more nearly equal discrimination could be made between equal stimulus intensities. The test for this hypothesis involves a sequential probability test. The drawback to this conjecture is that in order to make a decision on the stimulus

intensity, the central nervous system must have prior knowledge of the shape of the interspike interval histogram as a function of the mean rate.

This study will be concerned with these cells in VPL_1 of the cat that are sensitive to stimulation of the knee joint. As we shall see, the rapidly adapting cells are believed to be relayed through the gracile nucleus on the strength of the similarity of response characteristics. The slowly adapting afferents are probably relayed through another pathway, the origin of which is uncertain. From the thalamus the impulses are then relayed to the primary somatosensory cortex (Mountcastle, 1957).

CHAPTER III

DYNAMIC RESPONSE OF KNEE JOINT AFFERENTS IN SOMATOSENSORY THALAMUS

INTRODUCTION

Impulses from at least two of the major somatosensory systems, the dorsal column-medial lemniscal and spinocervicothalamic systems, are known to project to the VPL of the dorsal thalamus (Boivie, 1971a). These pathways carry the impulses from the two general classes of mechanoreceptors: cutaneous and deep receptors. Within the category of deep receptors are included those described in Chapter II arising from the joint capsules. The majority of cells found in the VPL have lemniscal properties, i.e. they respond only to a single stimulus modality (hair, touch, pressure, joint) in a circumscribed and continuous receptive field (Poggio and Mountcastle, 1963; Baker, 1971).

Mountcastle et al. (1963) have studied the response of joint cells in the VPL of unanesthetized, paralyzed monkeys. In this work they studied in detail the properties of the tonic joint cells in response to static inputs of joint angle. The static curve of these cells was found to be best fit by a power function. The response of these cells to dynamic inputs was not studied in a quantitative manner, but their results for step and ramp inputs show a proportional-plus-derivative effect, similar to that for the peripheral receptors. In addition to these tonic units, a small number of phasic joint units, sensitive only to joint movement and not to static joint position, were also found but were not studied quantitatively.

Poggio and Mountcastle (1963) also studied the so-called "dynamic" properties of cells in the ventrobasal complex. By this they mean those properties concerned with "the temporal cadence of neural activity, the transformation of neural patterns of discharge at synaptic junctions, the quantitative relation of central response to peripheral stimuli" as distinguished from the static properties of modality and topography. By measuring the response (number of impulses) to the second of two brief supramaximal pulses applied to the periphery as a function of the interval between pulses, they showed that the recovery of a thalamic cell in unanesthetized monkeys was much faster than that in pentobarbital-anesthetized cats. This provided a measure of the depressing effect of anesthetics on the dynamic properties of the cell. By applying this same test and measuring responses at different levels of the somatosensory system, Angel (1967, 1969) found that much of the decreased responsiveness was due to failure of transmission through the ventrobasal complex of the thalamus. Clearly, then, the potential bias of anesthetics must be accounted for in a study of the quantitative response of VPL cells.

In recent years a growing number of investigators have begun to use systems theory to study the response of various biological receptors in an effort to quantify the response to dynamic stimulation. The response dynamics of muscle spindles (Matthews and Stein, 1969; Poppele and Bowman, 1970; Kirkwood, 1972), crustacean stretch receptors (Brown and Stein, 1966), joint receptors (McCall *et al.*, 1973), and other mechanoreceptors (Chapman and Smith, 1963; French *et al.*, 1973) have been studied. For all of these mechanoreceptors

the frequency response could be characterized as a high pass filter, i.e. the receptor showed a greater sensitivity to high frequency input signals than to low frequency signals. Presumably this provides the CNS with increased capability to respond to rapidly changing stimuli.

In this chapter we will describe responses of knee joint senstive neurons in the VPL of cats. The frequency response of these cells will be found by applying dynamic stimulation and using systems analysis techniques.

METHODS

Surgery

The data presented here were obtained from a total of 37 adult cats, (2.0 - 3.6 kg) obtained from the Laboratory of Animal Medicine at the University of Michigan Medical Center. The first set of cats (20 animals) were anesthetized, acute preparations that were prepared in the following manner. An initial anesthetic dose of sodium pentobarbital (Nembutal, 35 mg/kg) was administered intraperitoneally. In three experiments chloralose (α-d-tubochloralose, 50 mg/kg) was used for the initial dose. A cannula was inserted into the cephalic vein to administer supplementary doses of physiological saline and anesthetic in order to maintain a light analgesic state. Rectal temperature was monitored and maintained at 36-38° C by an electric heating pad. The left hind limb was skinned to the ankle and partially denervated in order to reduce the inputs from cutaneous receptors. The denervation entailed transecting the muscular branches of the

sciatic nerve before it divided into the tibial and peroneal nerves. Two pins were placed into the femur so that the leg could be held rigidly to the apparatus while the tibia could be rotated freely.

The animal was placed in a standard stereotaxic and a trephine hole 1.3 cm in diameter was made in the skull over the rostral half of the VPL (center at AP 10.0, LR 7.5). In order to reduce cerebral pulsations due to cardiovascular and respiratory movements, a closed head technique similar to that described by Amassian et al. (1959) was employed. A lucite cylinder, machined to taper snugly into the trephine hole, was mounted atop the skull with dental acrylic to form a chamber. The outer surface of the cylinder was threaded to accommodate a brass ring that could be screwed onto the chamber. The two femur pins were clamped rigidly to the apparatus thereby immobilizing the femur while leaving the tibia free to rotate. The preparation was then ready for microelectrode recordings.

In order to verify the projection of knee joint afferents to VPL, the medial articular nerve in one animal was dissected free from the connective tissue and exposed for stimulation. A silver wire electrode connected to a Grass pulse stimulator was wrapped around the nerve. In this animal no femur pins were inserted and the only stimulation applied was a train of pulses to the articular nerve. The closed chamber was mounted on the skull in the usual manner for microelectrode recording from VPL.

In the remaining 17 animals, an unanesthetized, semi-chronic animal was prepared in a manner similar to that described by Hayward et al. (1964). An effort was made to use only docile and friendly animals; more aggressive cats were avoided. One week before

the recording sessions, the animal was anesthetized with a dose of ketalar (5 mg/kg, i.p.) and sodium pentobarbital (25 mg/kg) and placed in a standard stereotaxic unit. The next step was to mount a platform on the skull so that the animal could be held rigidly in the Horsley-Clarke plane during recording sessions without earbars or face clamps but with aluminum rods anchored to the stereotaxic and passed through acrylic cylinders on the platform. Under sterile procedures the skull was exposed and the trephine hole was made over the rostral VPL. The dura was left intact. The lucite chamber was placed into the hole. In addition two acrylic cylinders (i.d. 6.25 mm, o.d. 9.37 mm, 3 cm long) were placed transversely on the skull, one just rostral and one just caudal to the chamber. Aluminum rods of 6.25 mm diameter, which fit snugly inside the acrylic cylinders, were slipped inside the cylinders and the cylinders were pushed flush against the skull. The rods were then fastened rigidly to a specially machined fixture that was anchored to the stereotaxic frame. In order to prevent lateral movements a small screw was placed through the middle of the rostral cylinder and two aluminum rods, one from either side, were used in that cylinder. Several small stainless steel screws were placed part way into the skull bone, and numerous small holes were made randomly on the exposed skull to roughen the surface. The lucite chamber and acrylic cylinders were then cemented onto the skull with dental acrylic. A small amount of warmed sterile mineral oil was placed into the chamber, and it was closed with a tight-fitting threaded lucite cap. Hot paraffin was poured into the chamber to complete the seal. Fig 3.1 shows a diagram of the

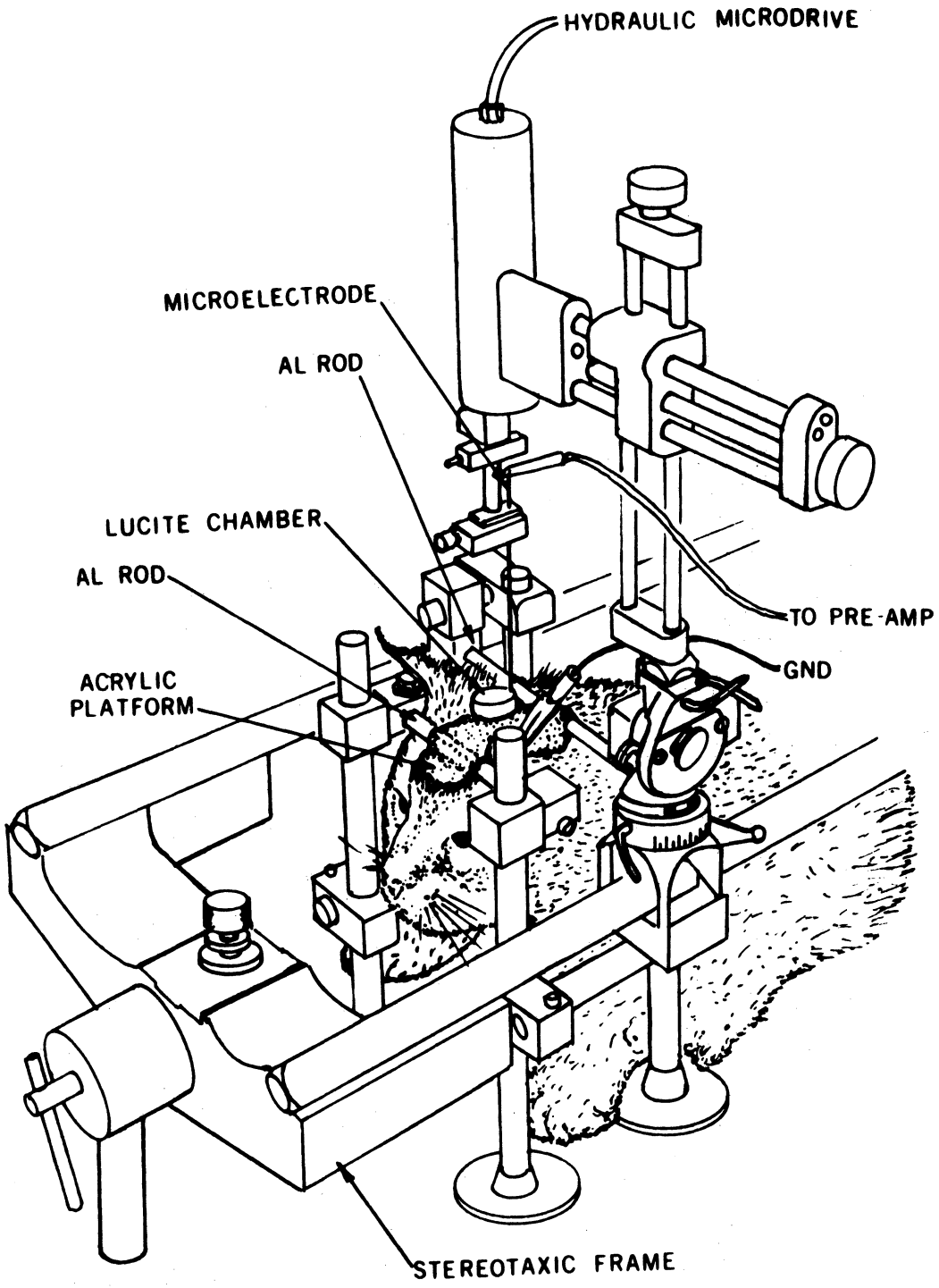

Figure 3.1. Diagram of the semi-chronic preparation during a recording session. The head is held rigid by the aluminum rods that are slipped through the lucite cylinders embedded in the acrylic platform. The lucite chamber serves as a closed chamber for the microelectrode.

apparatus and closed chamber.

The sterile surgery was finished by threading a stainless steel Steinman pin of the type commonly used by veterinarians to set fractures into the femur. The wound was closed with sutures. A long-acting antibiotic (Bicillin) was administered to reduce chances of infection.

The animal was then allowed to recover from the anesthetic. Usually by the second day after surgery, the effects of anesthetic had worn off and the cats appeared normal in almost all respects. Particular attention was paid to see if the cats were suffering any discomfort from either the pin in the femur or the chamber on the head. At no time did the animals show any apparent discomfort from the leg pin. Animals usually behaved as if it were absent, although a few showed a noticeable limp while walking. However, the animals invariably moved about normally even jumping up and down off tables with alacrity. The animals often would try to rub their heads against the experimenter, probably because the head wound itched. The animals all slept and ate normally and were not particularly vocal. In sum, the chronic preparations behaved normally postsurgery with no apparent pain or discomfort.

After the animals had returned to normal, they were placed in the fixture with the aluminum rods in order to acclimate them to the apparatus. The acclimating sessions initially were 10-15 minutes long and eventually lasted several hours. After several sessions the animals usually adapted to the apparatus and would often fall asleep soon after being placed in the head mount.

Recording

In the anesthetized preparations the recording sessions commenced immediately after the surgery was completed. The animal was placed in a Faraday cage. After the dura was removed, tungsten microelectrodes of ≃1μ tip diameter and insulated with resin or Epoxylite (Transidyne or Fred Haer) were used to record the extracellular unit activity. The electrode was positioned with a microdrive to a point just above the cortical surface. A small amount of warmed mineral oil was poured into the chamber. Warm, liquid paraffin was then poured into the chamber to the top of the brass ring. The wax was allowed to solidify before driving the microelectrode into the VPL. Subsequent penetrations were made by withdrawing the microelectrode, unscrewing the brass ring, removing the hardened wax and liquid mineral oil, repositioning the microelectrode, and repeating the above procedures.

Standard techniques for recording extracellular single units were employed. The neural signal was amplified by a pre-amplifier (Tektronix 122) with a bandwidth of 80 Hz to 5 kHz. An active 60 Hz notch filter was sometimes used to improve the signal isolation. The spike trains were monitored on an oscilloscope (Tektronix 502A) and with a loudspeaker, and were recorded on an AM channel of a four channel AM/FM tape recorder (Hewlett-Packard 3960A) at 3 3/4 i.p.s. (bandwidth: 50 Hz to 15 kHz, S/N: 38 db). Fig. 3.2 shows a diagram of the recording arrangement.

In the semi-chronic preparations recordings would begin about a week after the operation and after the animal had been acclimated to the fixture. With sterile procedures a small piece of dura mater was

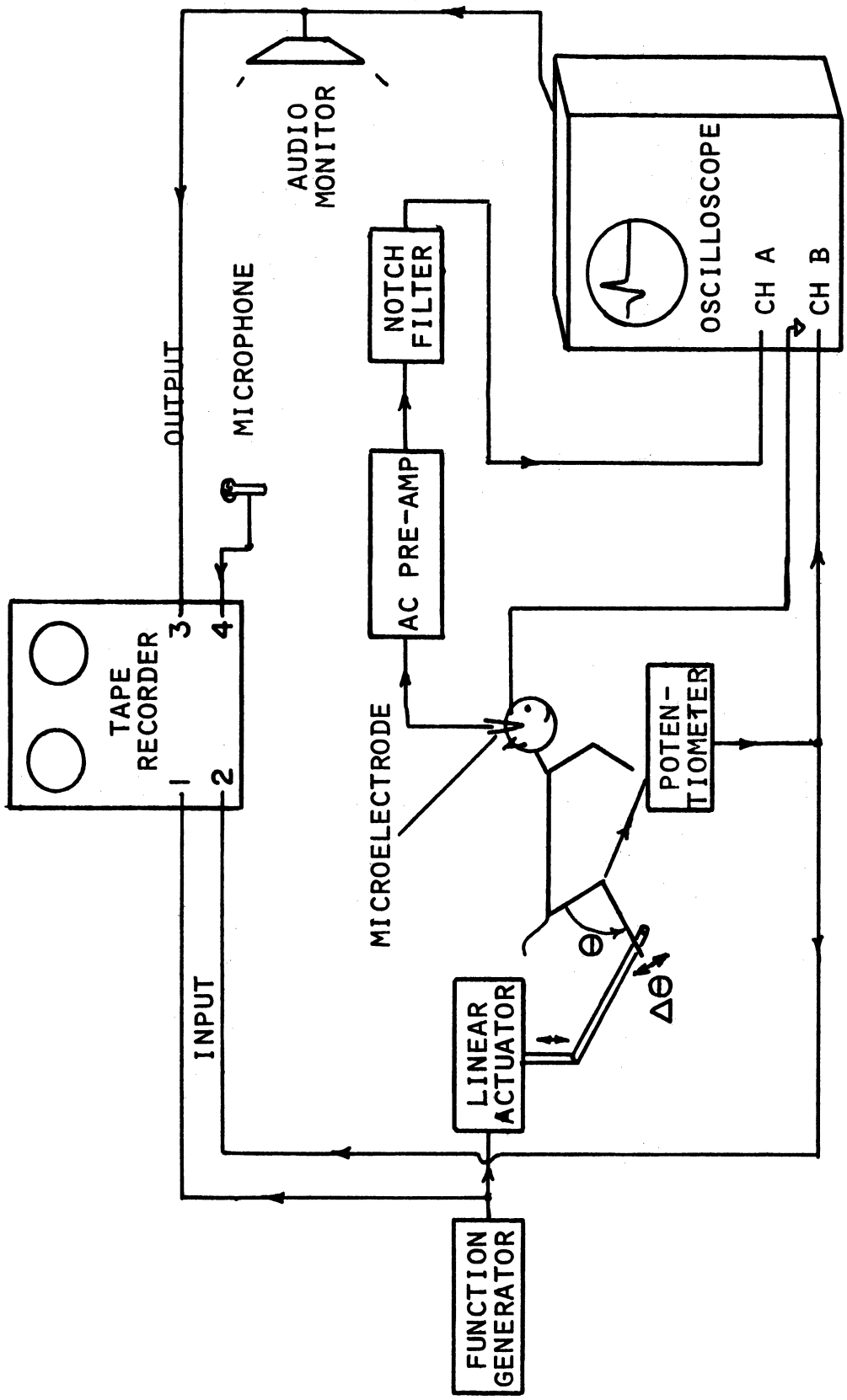

Figure 3.2. Schematic diagram of the recording arrangement. The stick figure shows that the bias angle θ is the angle between the tibia and the femur and the excursion angle Δθ is the amplitude of the peak-to-peak movement al

reflected and a microelectrode was inserted into the VPL using the same closed head recording techniques described above. In some of the earlier semi-chronic animals the animal was supported at the chest and trunk by a hammock, but this was found to be unneccessary if the frame was low enough to permit the animal to rest comfortably on it. The left hind limb was held securely by clamps onto the Steinman pin and was placed in a natural position. The more obstreperous animals were given a small dose of Acepromazine (1.5 mg/kg) to tranquilize them. The recording sessions lasted no longer than four hours at a time, and the animals could be used for several sessions. Most of the animals were sacrificed after 3 or 4 sessions, and none were kept longer than 12 days after the initial surgery.

Stimulation

The input parameter to the system was knee joint angle. Precise movements of joint angle were applied with a voltage-controlled electromechanical actuator (Gesink and Williams, 1968). The actuator had a flat frequency response out to about 10 Hz (+1 db at 5 Hz) and had negligible phase lag ($< 4°$ at 5 Hz). The harmonic distortion of the actuator and its electronics was from 2 - 4% (harmonic distortion was taken to be the root mean square of the first four harmonics as a percentage of the fundamental). The linear actuator was coupled to one end of a hinge, the other end of which was rigidly clamped to the apparatus. The axis of the hinge was aligned with the axis of rotation of the knee joint. The ankle of the cat was fastened to the moveable end of the hinge so that it could be rotated by the actuator. A potentiometer positioned at the axis of the hinge was used to

monitor joint angle. With this arrangement very precise movements of joint angle could be applied. The excursion angle $\Delta\theta$ was the peak-to-peak amplitude that the joint could be moved by the application of suitable signals into the actuator. Within a 10° range, $\Delta\theta$ could be easily and quickly changed by the input signal from a function generator. However, a change of the bias angle θ, the absolute angle of the tibia with respect to the femur, required a manual movement of the actuator and was not as easily implemented (see Fig 3.2 for a diagram of θ and $\Delta\theta$). The signal driving the actuator and the potentiometer signal were recorded on the two FM channels of the tape recorder (bandwidths: 0 to 1250 Hz, S/N: 48 db). A Hewlett-Packard 3300 signal generator with a 3305 plug-in unit provided the ability to apply discrete and swept sine, triangle, and square wave inputs from .1 to 100 kHz. In practice, frequencies greater than 6 or 7 Hz were not used since the resulting vibrations induced at these frequencies made it difficult to hold a single unit. The recording conditions were sufficiently stable to hold a single cell for several hours in the anesthetized or asleep preparations. However, cells could not be held for long if the animal awakened and moved about.

As the tip of the microelectrode entered the VPL, the background activity increased. Single units were identified on the basis of spike shape, and all the data were recorded from soma spikes. Action potentials recorded from fibers were identified by their shape (usually monophasic and of shorter duration, $\simeq$.5 msec) and were not used. Once a single cell was isolated, the

peripheral receptive field was determined by brushing hairs, stroking skin, probing deep tissues, and manipulating joints over the body of the animal. Cells were separated into four categories by modality: hair, touch, deep, and joint. Determination of the adequate stimulus for a cell was made in the following manner. If the cell responded to a gentle stimulus applied to only the hairs, it was considered to be a hair cell. If the unit was unresponsive to hair stimulation but responded to gentle stroking of the skin, it was considered to be a touch cell. If the unit was neither a hair nor touch cell but responded to probing of the deep tissue or movements of the limbs, it was classified as a deep afferent. The size of the peripheral receptive field was estimated and classified as small (approximately < 5 cm^2 and usually on the paws), medium (5 - 100 cm^2) and large (> 100 cm^2 and usually an entire limb). If the unit was not a knee joint cell, no further tests were performed and subsequent penetrations were designed to reach the hind limb area of VPL with the aid of the topography described by Mountcastle and Henneman (1949).

Knee joint cells were identified by the following criteria: one, phasic response to movement of the joint or graded response to position of joint; two, no response to stroking of the hairs or to light touch around the joint; and three, high sensitivity to squeezing the joint capsule and to twisting the tibia. By these guidelines, cells that were stimulated by receptors in the deep fascia about the knee joint could not be distinguished from those stimulated by the knee joint receptors described in Chapter II. However, I am confident that the cells identified as knee joint

receptors were not afferents from muscle receptors for several reasons. One, the thalamic projection area of hindlimb muscle spindles, at least the one relayed through nucleus Z, was shown to be primarily the ventral lateral nucleus with a very small projection to the rostral tip of VPL (Grant et al., 1973). Most of the penetrations were caudal to this position. Two, my experience with recordings on the medial articular nerve have shown that all of the units were very sensitive to even slight squeezing of the joint capsule or twisting of the tibia, and these criteria were used as the definitive test. Cells that were sensitive to squeezing the gastrocnemius or quadriceps were considered to be muscle receptors. Finally, any cells that were considered questionable were not classified as knee joint afferents. It is probable that some joint receptors were missed under these stringent conditions and that may explain the relatively small number of joint receptors found.

Once a cell was identified as a knee joint cell, the extent of its peripheral receptive angle was determined. For the phasic units this was sometimes a difficult judgment. Since the response usually was dependent upon the frequency at which the leg was moved, often the cell could be made to respond over the entire range from flexion to extension provided a sufficiently high frequency stimulus was applied. However, most units showed a distinct range of maximal sensitivity, and the initial experiments were done with the leg positioned in this range. For the phasic units, their response to dynamic inputs was determined by applying

discrete or swept sinusiodal inputs of joint angle. In order to examine the linearity and the extent of the response of the joint units, the response was also tested with different excursions $\Delta\Theta$ at the same bias angle Θ or at different bias angles for the same excursion. In addition step inputs were applied in order to measure the latency of the response in VPL.

Data analysis

The response of a neuron in the VPL is a train of virtually identical action potentials that is conducted on to the somatosensory cortex. If the occurrence of a spike rather than, say, its duration or amplitude is considered to be the information-carrying parameter, then the response can be described as a stochastic point process, each spike being associated with a unique instant of time (Perkel et al., 1967). It is sufficient, then, to know the time at which each spike occurs. The impulses recorded on magnetic tape were detected by a discriminator with both time and amplitude windows and converted into standard pulses during computer processing.

All of the initial computer processing was done on a Hewlett-Packard 2115a minicomputer in the Bioelectrical Sciences Laboratory. This facility is equipped with an A/D and D/A converter, high speed paper tape reader and punch, and teleprinter and lineprinter devices. The memory size is 8,192 16 bit words. The crystal clock of the time base generator of the computer was used to time occurrences of the spikes. In addition the university IBM 360/67 was used for much of the data processing and CalComp plotting.

The primary objective of this experiment was to find the frequency response function of thalamic knee joint cells to sinu-

soidal movements of joint angle. Two kinds of input waveforms were used to extract the frequency response functions. The first employed the classical method of sine waves at discrete frequencies spaced over the bandwidth from .1 to 7 Hz. The second used a logarithmically swept sinusoid over the same bandwidth. The input parameter was the angle between the tibia and the femur as monitored by the potentiometer at the knee joint, and the output was assumed to be the average firing rate of the neuron.

For the discrete sinusoidal inputs cycle histograms were used to find the frequency response $H(j\omega)$. The histogram was triggered by the positive-going zero-crossing of the input signal. The period of the sinusoid was divided into 72 equal bins (5° each). The last bin was constrained to be equal to the average of the 71st and 1st bin because the reference zero crossings were more precisely detected when sampling the A/D continuously on the input channel during this 72nd bin. Fourier analysis was used to compute the fundamental and higher harmonics (up to the 18th). Non-harmonic distortion was averaged out by the histogram program since it had no constant phase relation to the input. This was equivalent to viewing the data through a spectral window of the shape $\sin \omega T/\omega T$, where T was the period of the input signal. Therefore, all non-harmonic coefficients were biased by the window, but harmonic coefficients were not biased by the non-harmonic components, which were averaged to zero. The amount of distortion was computed as the ratio of the root mean square of the second to sixth harmonic to the amplitude of the fundamental. The magnitude $H(\omega)$ and

phase $\phi(\omega)$ of the response were easily computed from the sine and cosine components of the fundamental frequency. In addition, qualitative judgments of the response could be made from cycle histograms, particularly for the phasic responses, e.g. peaks in the histogram indicated a phase-locking response.

For the swept sinusoids a novel technique using correlation and spectral analysis made it possible to obtain a complete frequency response profile of 128 points in almost the same amount of time that it would take to obtain just a single point with discrete sinusoids. The technique utilizes the following relationships: for a linear, time-invariant system with input x(t), impulse response h(t), and output y(t)

$$y(t) = \int_0^\infty h(u)\, x(t-u)\, du \qquad (3.1)$$

$$R_{xy}(t) = \int_0^\infty h(u)\, R_{xx}(t-u)\, du \qquad (3.2)$$

$$S_{xy}(j\omega) = H(j\omega)\, S_{xx}(j\omega) \qquad (3.3)$$

where $R_{xy}(t)$ is the cross-correlation of x(t) and y(t), $H(j\omega)$ is the system frequency response, and $S_{xy}(j\omega)$ is the output-input cross power spectral density. Cross-correlation is a powerful tool for extracting the signal when a great deal of uncorrelated noise is present. (See Appendix A for a more detailed discussion of correlation analysis.) From (3.3) it can be seen that the frequency response can be found by the ratio of the cross power spectral density and the input power spectral density. Fig. 3.3 shows a diagram of the technique used to extract the system response. Theoretically any input can be used to extract the frequency response as long as the

Figure 3.3. Schematic diagram of the technique used to find the describing function frequency response. The neural pulse train y(t) is shaped into standard pulses, and the average discharge rate is found by the fourth order low pass filter with corner frequency set at 7 Hz. In order to cancel the dynamic effects of the low pass filter, the input x(t) is also passed through an identical filter so that the same filter effects are present in S_{xx}, and S_{yx}. Further details of this technique are given in Williams et al. (1972).

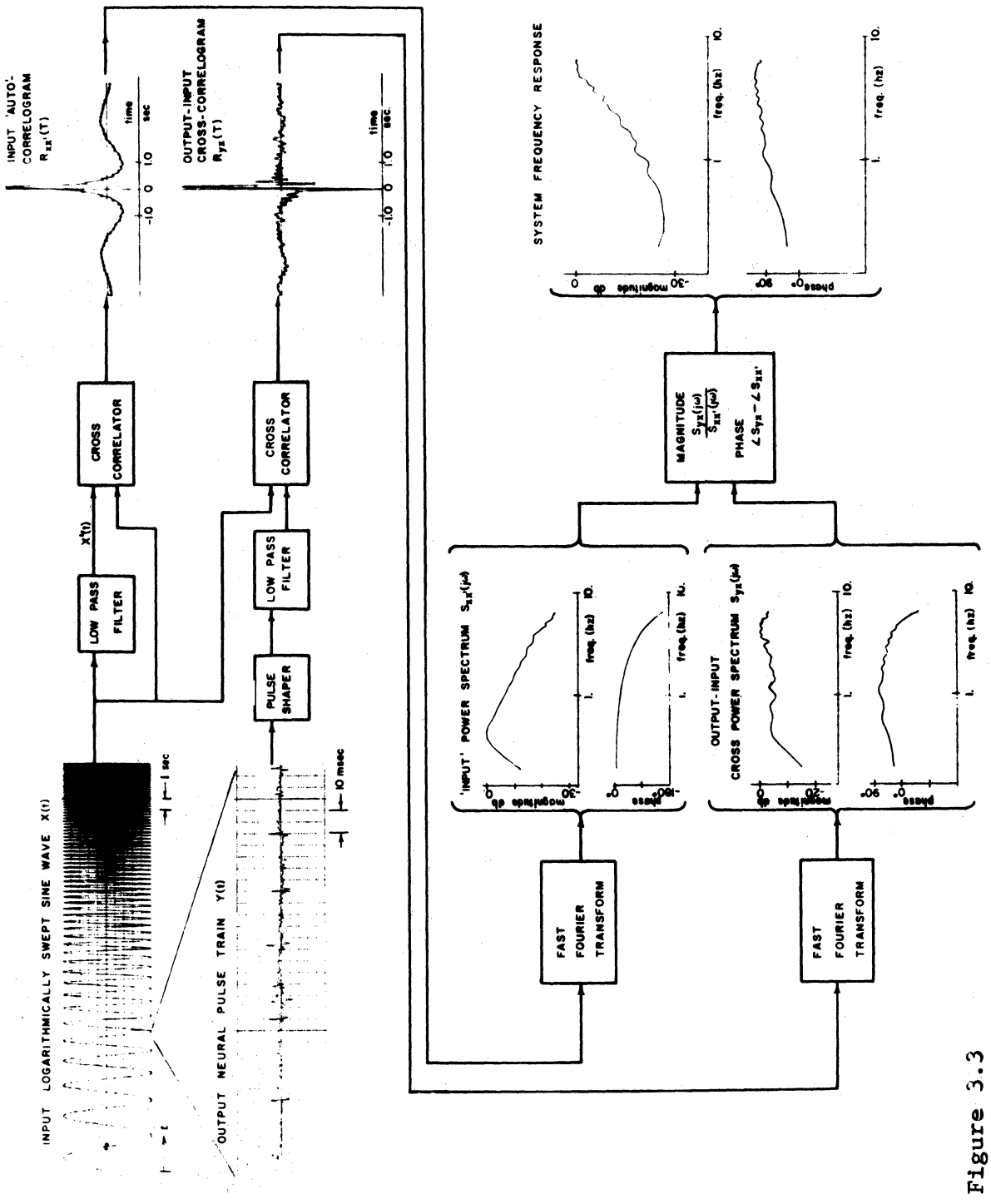
INPUT LOGARITHMICALLY SWEPT SINE WAVE X(t)
1 sec
t
OUTPUT NEURAL PULSE TRAIN Y(t)
10 msec
LOW PASS FILTER
X'(t)
CROSS CORRELATOR
PULSE SHAPER
LOW PASS FILTER
CROSS CORRELATOR
INPUT 'AUTO'-CORRELOGRAM
$R_{xx'}(T)$
time
sec
-1.0
0
1.0
OUTPUT-INPUT CROSS-CORRELOGRAM
$R_{yx}(T)$
time
sec
FAST FOURIER TRANSFORM
FAST FOURIER TRANSFORM
'INPUT' POWER SPECTRUM $S_{xx'}(j\omega)$
OUTPUT-INPUT CROSS POWER SPECTRUM $S_{yx}(j\omega)$
magnitude db
phase
freq. (hz)
MAGNITUDE $\frac{S_{yx}(j\omega)}{S_{xx'}(j\omega)}$
PHASE $\angle S_{yx} - \angle S_{xx'}$
SYSTEM FREQUENCY RESPONSE
magnitude db
phase
freq. (hz)

Figure 3.3

bandwidth of $S_{xx}(j\omega)$ is wide enough to encompass all frequencies of interest in $H(j\omega)$. Commonly, band limited white noise is used (Lee, 1960; Bendat and Piersol, 1966; Mannard and Stein, 1973). The logarithmically swept sinusoid used in this study combines the attributes of using a sinusoidal input with the requirement of a finite bandwidth. This technique incorporates the powerful noise rejecting properties of cross-correlation with a tremendous increase in the data acquisition rate. Cross-correlation can also be used for discrete sine-wave inputs as discussed in Appendix A, but there is no improvement in the data acquisition rate.

The analysis outlined above can be used to find the exact transfer function for a linear, time-invariant system. Biological systems are, however, invariably nonlinear, but describing function analysis can be used if the nonlinearity is time-invariant. The output of a nonlinear system can be considered to be composed of a quasi-linear factor and nonlinear noise term

$$y(t) = \int_0^\infty h_1(x,u)\, x(t-u)\, du + n(t). \qquad (3.4)$$

The Laplace transform $H_1(x,s)$ of the impulse response $h_1(x, t)$ in the linear term is known as the describing function. The value of $h_1(x, t)$ is chosen to minimize the mean square error $n^2(t)$ (Jenkins and Watts, 1968; Appendix A) for the given input $x(t)$, i.e. unlike linear systems, the describing function will, in general, be a function of the input $x(t)$ (Thaler and Pastel, 1962).

Most often describing functions are found for sinusoidal inputs. In this case the linear term is considered to be the fundamental of the response and the nonlinear term contains any of the higher

harmonic or nonharmonic contributions. The describing function obtained will be characterized by a magnitude $H(x,\omega)$ and a phase $\phi(x,\omega)$ that are, in general functions of both frequency and input amplitude. This technique can be used to advantage if the higher-order harmonics are small in comparison to the fundamental, if the system is not interested in the higher harmonics, or if the system has a considerable amount of low pass filtering. Appendix B contains a more detailed discussion of the describing function technique as applied to swept inputs and also gives the results of a simulated system whose frequency response was found in this manner.

The input to the system was the angle of the joint and the output was the average spike rate, determined by demodulating the standard pulses (10 volts, 1 msec) with a fourth-order low pass filter (Krohn-Hite 3750) at a corner frequency of 7 Hz. The effects of the filter were compensated by cross-correlating the input waveform across the identical filter, as shown in Fig 3.3. The appropriate cross-and auto-correlograms were computed by sampling the signals at 33 Hz over 256 points for a data window of 7.67 sec and calculating the correlogram with Fast Fourier Transform techniques. The power spectral densities were likewise calculated by Fast Fourier Transform after smoothing with a Bartlett spectral window. The frequency response was computed by the ratio of $S_{xy}(j\omega)/S_{xx}(j\omega)$ so that the magnitude of the response was

$$H(\omega) = |S_{xy}(j\omega)|/S_{xx}(j\omega) \tag{3.5}$$

and the phase was

$$\phi(\omega) = \measuredangle S_{xy}(j\omega) - \measuredangle S_{xx}(j\omega) \tag{3.6}$$

The spectral analysis programs were written by Dr. M. M. Stern. The frequency responses were displayed as Bode plots on a CalComp plotter with magnitude in db and phase in degrees vs. log frequency. The phase angles were sometimes 180° apart depending upon whether the unit responded on flexion or extension of the joint. For ease of comparison, all of the phase angles were plotted as leading angles.

Once the describing function was found, it was useful to know the degree to which it characterized the input-output relations of the system. The coherence function $\gamma^2(\omega)$ gives a measure of the degree of causality between the input and the output (Roth, 1971).

$$\gamma^2(\omega) = |S_{xy}(j\omega)|^2/[S_{xx}(j\omega)S_{yy}(j\omega)] \qquad (3.7)$$

If the system can be described by (3.4),

$$\gamma^2(\omega) = \frac{|H_1(\omega)|^2 S_{xx}(\omega)}{|H_1(\omega)|^2 S_{xx}(\omega) + S_{nn}(\omega)} \qquad (3.8)$$

In effect, the coherence function is the ratio of signal power to signal power plus noise power if the signal is the response of the linear describing function and noise is all other components of the output. From (3.8) it can be seen that $0 \leq \gamma^2(\omega) \leq 1$. If the system is linear and noise free, $\gamma^2(\omega) = 1$. If x(t) and y(t) are unrelated, $H_1(\omega) = 0$ and $\gamma^2(\omega) = 0$. For $0 < \gamma^2(\omega) < 1$ there are three possible factors: one, the system is nonlinear; two, extraneous noise is present; and three, the output is due to inputs in addition to x(t) (Bendat and Piersol, 1966).

In order to relate the swept frequency response of the units to

the discrete sinusoidal response, a special scatter diagram was implemented on the minicomputer. The scatter diagram contains the same information for the logarithmically swept inputs as cycle histograms do for discrete sinusoidal inputs. Each spike causes a dot to be displayed on the D/A converter at the appropriate phase angle (along the abscissa) and at the particular modulation frequency (along the ordinate) corresponding to the period of the swept frequency in which it occurred. Each row represents one cycle of the swept input and the dots in that row are equivalent to a single cycle histogram. For the logarithmic sweeps with suitably long sweep times, it turns out fortuitously that the ordinate is a linear frequency axis over the bandwidth of the sweep. (See Appendix D) Fig. 3.4 shows an example of the scatter diagram.

Some more conventional measures of spike train activity were also used to analyze the data. Interspike interval histograms were used to estimate the probability density function. Serial correlation coefficients to order n were calculated from 500 successive interspike intervals by

$$\rho_n = \{1/\sigma^2\}\, E_i[(T_i - m)(T_{i+n} - m)] \qquad (3.9)$$

where m is the sample mean, σ^2 the sample variance, E_i the expected value operator over i, and T_i the ith interspike interval. Non-zero deviations of ρ_j for any j is indicative of correlation between interspike intervals of order j apart (Moore et al., 1966). Positive values of ρ_j indicate that long intervals tend to be followed j spikes later by long intervals and short intervals tend to be followed j spikes later by short intervals. Negative values

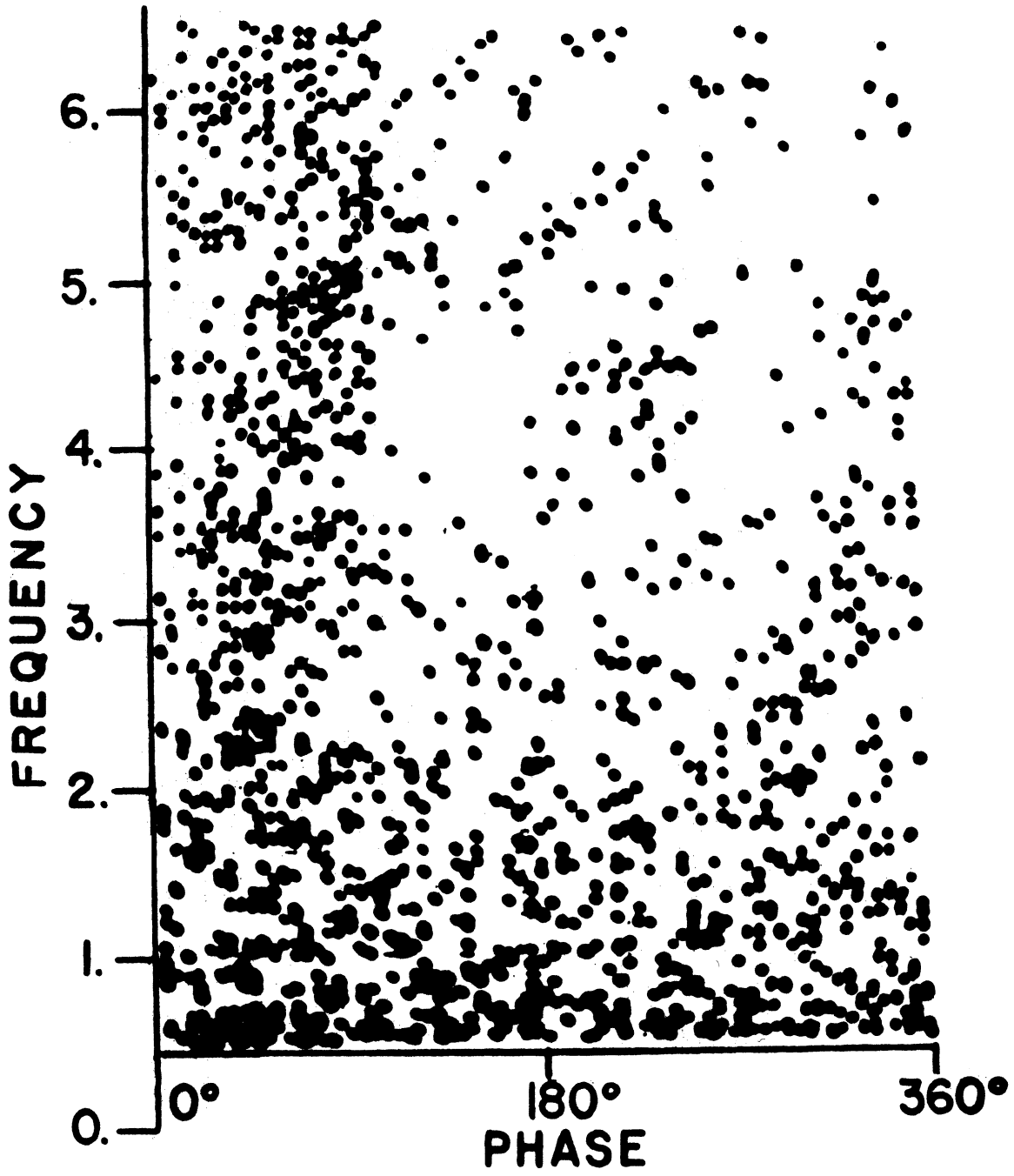

Figure 3.4. Example of the scatter diagram for the swept frequency input applied to cell C12-4 in an unanesthetized animal. Each row represents one cycle of the log swept input and each dot gives the phase at which an impulse occurred within that cycle. The frequency is the reciprocal of the period between the positive going zero-crossings, which are at 0° phase. 90° phase is extension; 270° is flexion. The bias angle was 127° and the excursion angle was 2.8°. Dots were retouched.

of ρ_j indicate that long intervals tend to be followed by short and short intervals by long. These calculations were performed on the university IBM 360/67 computer.

Square wave inputs were applied in order to measure the latency of the response. Post-stimulus histograms were used to analyze the data. Fig. 3.5 shows a general flow diagram of the data analyses used for the different inputs.

For some of the frequency response curves, a linear transfer function consisting of real poles, zeroes, and a time delay was found that fit the data points in a least squares sense. The optimization used a conjugate gradient optimization technique in the IBM Scientific Subroutine Package and was written by Dr. J. W. Gesink.

Histology

The positions of some of the joint cells were marked by a small lesion at the site of recording made by passing DC current, electrode positive. Not all sites were marked since the procedure often rendered the electrode inoperative for further recording and some of the lesions were too small or too large. However, usually all of the electrode tracks could be identified. Animals in which successful recordings were made were sacrificed and perfused with physiological saline and a 10% formalin solution. The head was removed and placed in the formalin solution for at least one month. The brain was removed and blocked so that it could be cut into frontal sections of 40μ width by a freezing microtome. Near the rostral VPL every section was mounted and stained with cresyl violet. Up to 10 mm on either side of the electrode penetrations fewer sections were stained and their positions were carefully noted. Since the region of interest has no

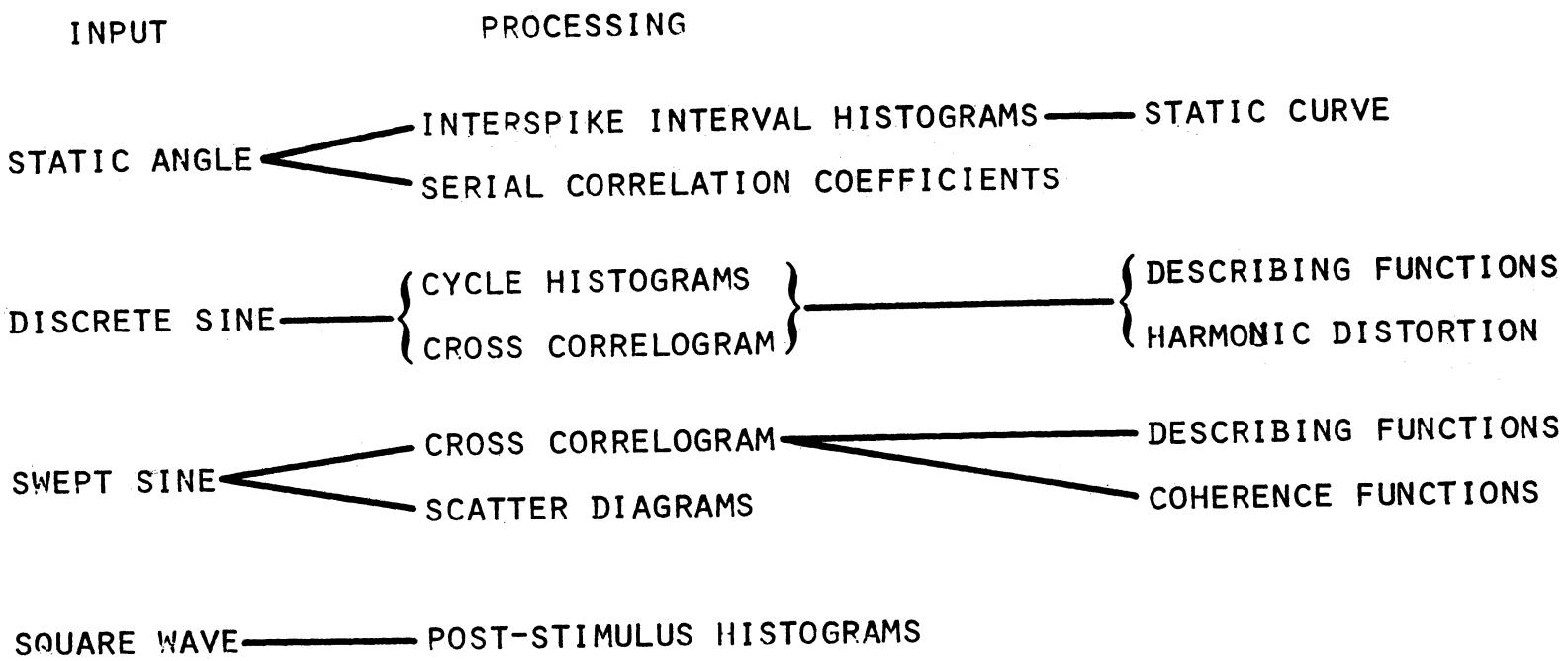

Figure 3.5. Flow diagram of the data processing used for the different input waveforms.

clear identifiable feature in frontal sections, it was sometimes helpful to use the sections in the more caudal portions of VPL to verify positions of the microelectrode tracks or lesions. The rostral pole of the lateral geniculate body was most often used as a reference point since it was easily identified. No penetrations were made caudal to this position. The atlases of Jasper and Ajmone-Marsan (1954) and Rinvik (1968) were used to verify microelectrode positions.

RESULTS

Out of the total of 418 cells isolated in this study, 387 of them could be driven by the proper stimulation of a peripheral receptive field. Out of this sample 42 were identified as knee joint cells by the criteria outlined above. These cells were selected for detailed study in order to characterize the response of thalamic knee joint afferents.

Rapidly adapting response

The majority (35/42) of these joint neurons were rapidly adapting and responded only when the limb was moved. In 31 of these cells, the unit was held long enough to stimulate it with discrete or swept sinusoidal inputs and to make a quantitative determination of its response to dynamic stimulation.

The response of the phasic joint units to discrete sinusoidal stimulation was analyzed by cycle histograms. Fig 3.6 shows the response of a typical cell to sinusoidal inputs of different frequencies at the same bias angle and excursion. At low frequencies

Figure 3.6. Cycle histograms of cell A12-1 for discrete sinusoidal inputs of different frequencies at the same bias angle (80°) and excursion angle (5°). The animal was anesthetized N = total number of impulses counted, B = total number of complete cycles of the input averaged, F = frequency of the input sine wave. The histogram was triggered by the positive-going, zero-crossing of the input stimulus. For this unit the first half cycle represents flexion of the limb, and the last half cycle represents extension of the limb.

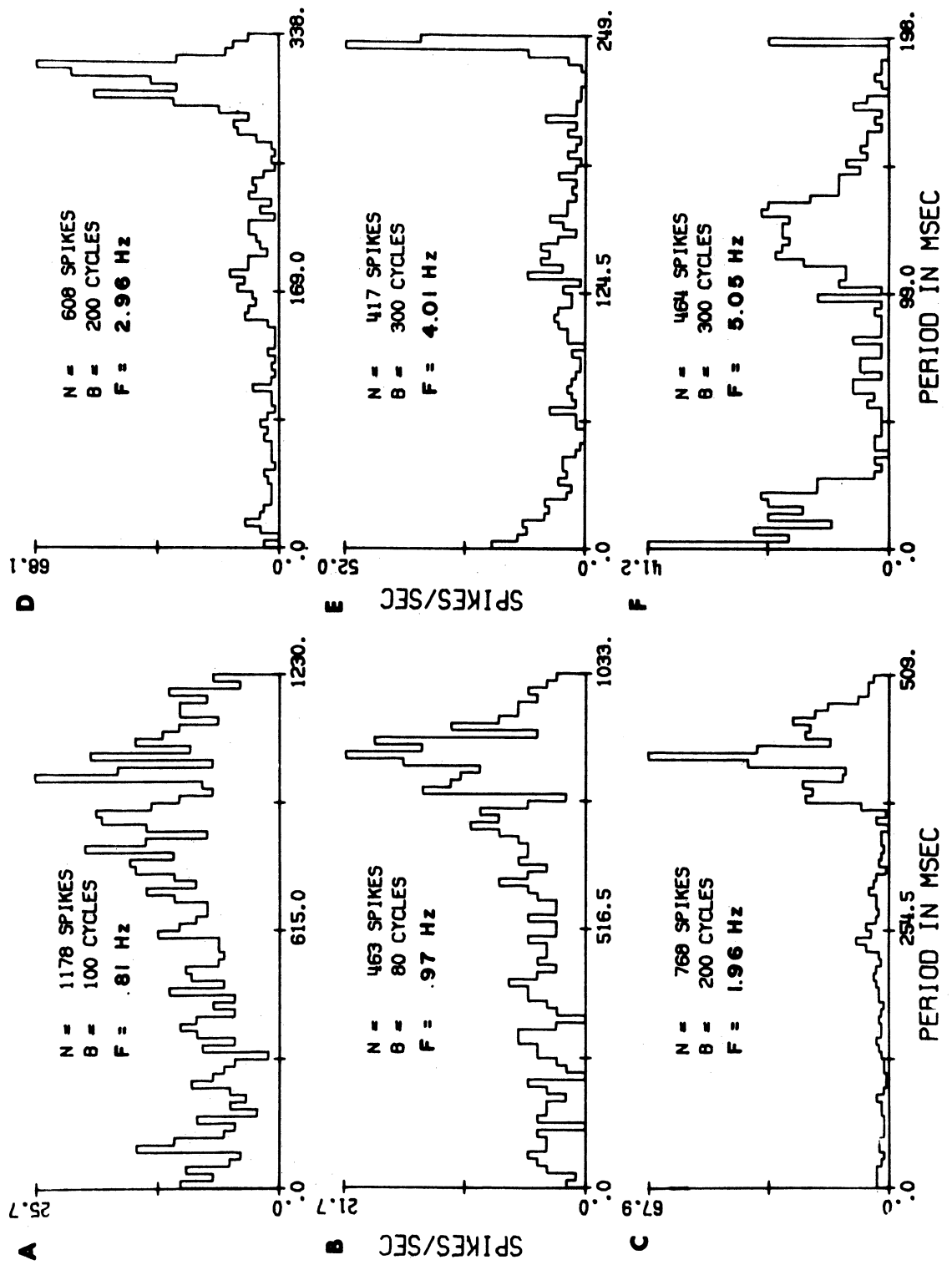
A
N = 1178 SPIKES
B = 100 CYCLES
F = .81 Hz
25.7
0.0
615.0
1230.
B
N = 463 SPIKES
B = 80 CYCLES
F = .97 Hz
21.7
0.0
516.5
1033.
C
N = 768 SPIKES
B = 200 CYCLES
F = 1.96 Hz
67.9
0.0
254.5
509.
PERIOD IN MSEC
SPIKES/SEC
D
N = 608 SPIKES
B = 200 CYCLES
F = 2.96 Hz
68.1
0.0
169.0
338.
E
N = 417 SPIKES
B = 300 CYCLES
F = 4.01 Hz
52.0
0.0
124.5
249.
F
N = 464 SPIKES
B = 300 CYCLES
F = 5.05 Hz
41.2
0.0
99.0
198.
PERIOD IN MSEC

Figure 3.6

(.8 Hz) the response was modulated by the input such that the cycle histogram had an approximately sinusoidal shape. As the frequency increased, the response became less and less sinusoidal and began to show a phase-locked component as the spikes tended to occur only within a narrow range of phase angles. This was evidenced by a peak in the cycle histogram. At the highest frequency shown (5 Hz), the cell began to show a bidirectional response, i.e. spikes tended to occur at two different phase angles approximately 180° apart. Fig 3.7 shows the response of another phasic cell that began to phase-lock at a low frequency (.5 Hz) and showed no evidence of a bidirectional response even at the highest frequency (6 Hz).

Notice that in both units the peaks of the cycle histograms began to lag in phase as the frequency increased. This lag in the peak of the cycle histogram was exhibited in all units with a phase-locked response. If the receptor responded at a particular phase angle of the input stimulus and there was a pure time delay (e.g. a transport delay) before the thalamic response, then one could expect a similar lag in the cycle histogram peaks because the time delay represented larger phase angles at higher frequencies. However, the delays in the cycle histograms were larger than time delays measured by applying step inputs to the knee joint. Fig. 3.8 shows the post-stimulus histogram of a step input to a thalamic joint unit. The initial burst of activity occurred with a latency of 23.0 ± 2.2 msec. Fig 3.9 shows a graph of the phase angle at which the peak occurs in the cycle histogram as a function of the input modulation frequency. Since the peaks of the cycle histogram to, say, a 1 Hz input stimulus occurred over a wide range of phase

Figure 3.7. Cycle histograms of cell A12-2 for discrete sinusoidal inputs of different frequencies at the same bias angle (74°) and excursion angle (6°). The animal was anesthetized. N = total number of impulses counted, B = total number of complete cycles of the input averaged, F = frequency of the input sine wave. For this unit the first half cycle represents flexion of the limb, and the last half cycle represents extension.

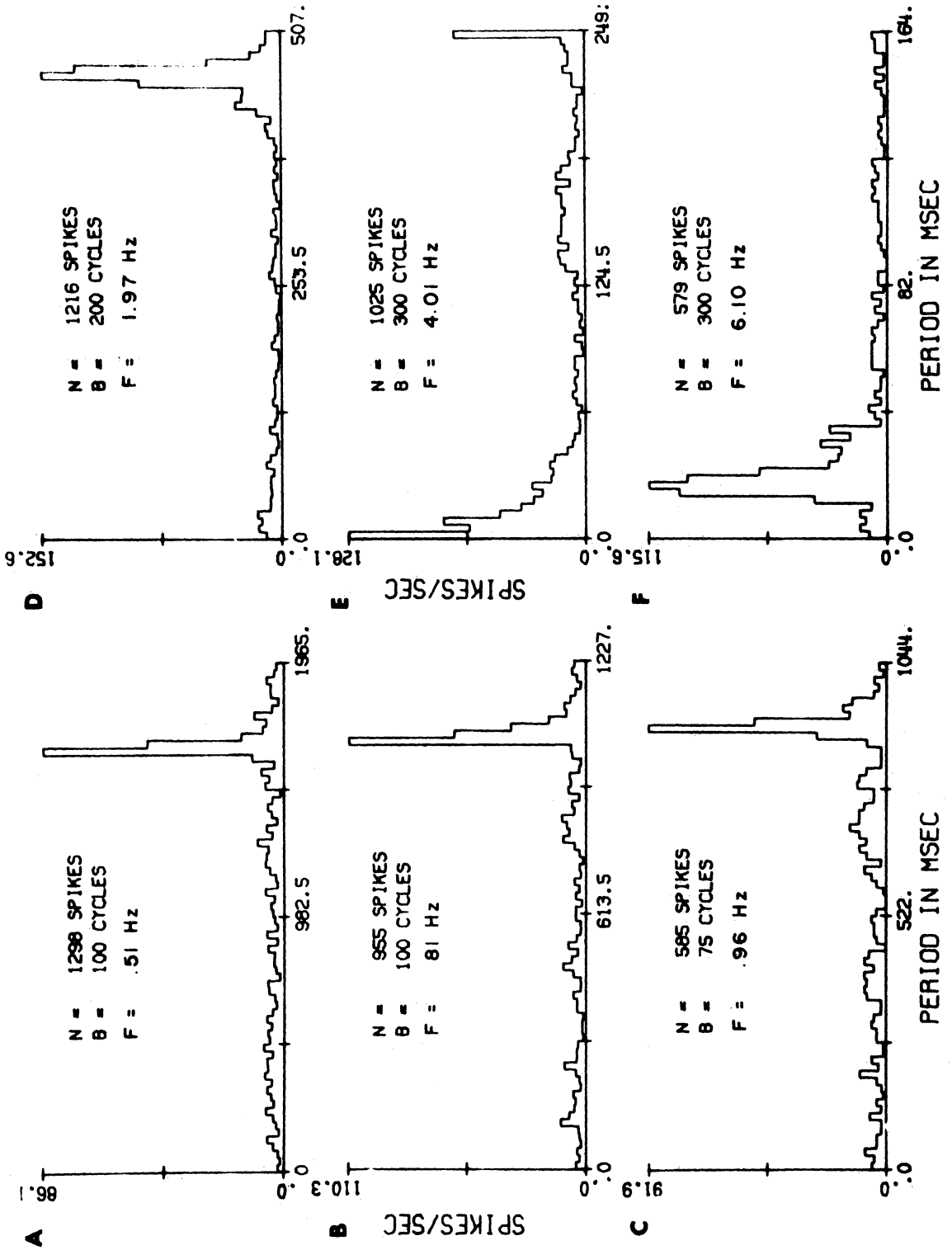
A
N = 1298 SPIKES
B = 100 CYCLES
F = .51 Hz
86.1
0
992.5
1985.
B
N = 955 SPIKES
B = 100 CYCLES
F = 81 Hz
110.3
0
613.5
1227.
C
N = 585 SPIKES
B = 75 CYCLES
F = .96 Hz
91.9
0
522.
1044.
SPIKES/SEC
PERIOD IN MSEC
D
N = 1216 SPIKES
B = 200 CYCLES
F = 1.97 Hz
152.6
0
253.5
507.
E
N = 1025 SPIKES
B = 300 CYCLES
F = 4.01 Hz
128.1
0
124.5
249.
F
N = 579 SPIKES
B = 300 CYCLES
F = 6.10 Hz
115.6
0
82.
164.
SPIKES/SEC
PERIOD IN MSEC

Figure 3.7

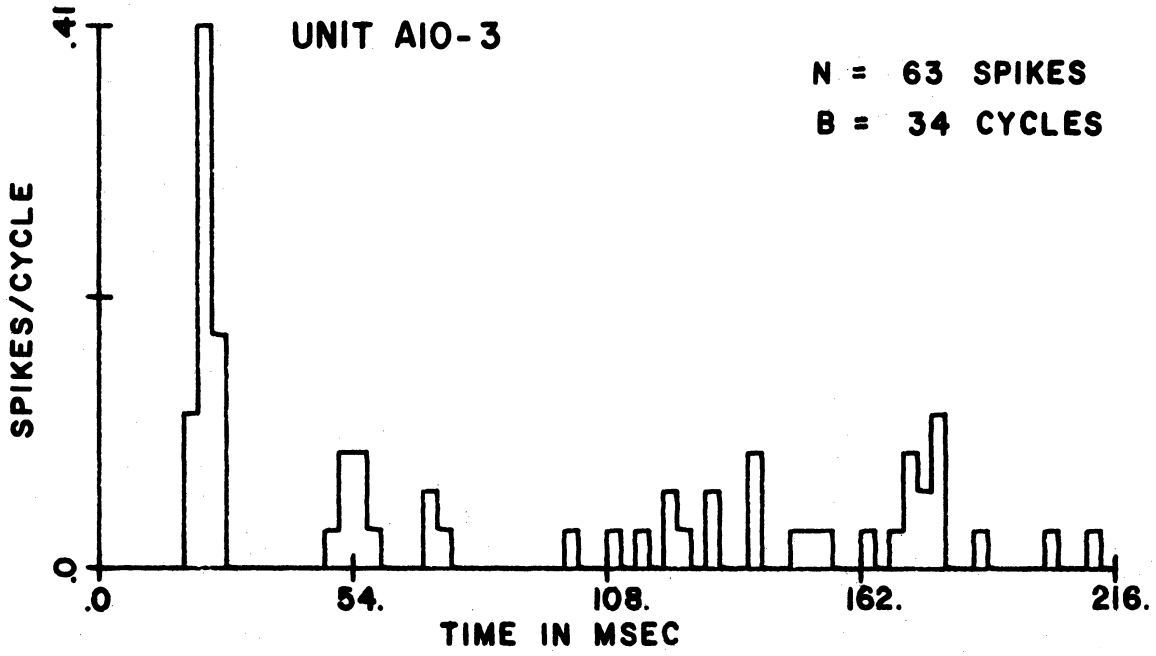

Figure 3.8. Post-stimulus histogram of cell A10-3 for a step input of 4°. Histogram was triggered by the step input. N = total number of impulses counted, B = total number of cycles applied.

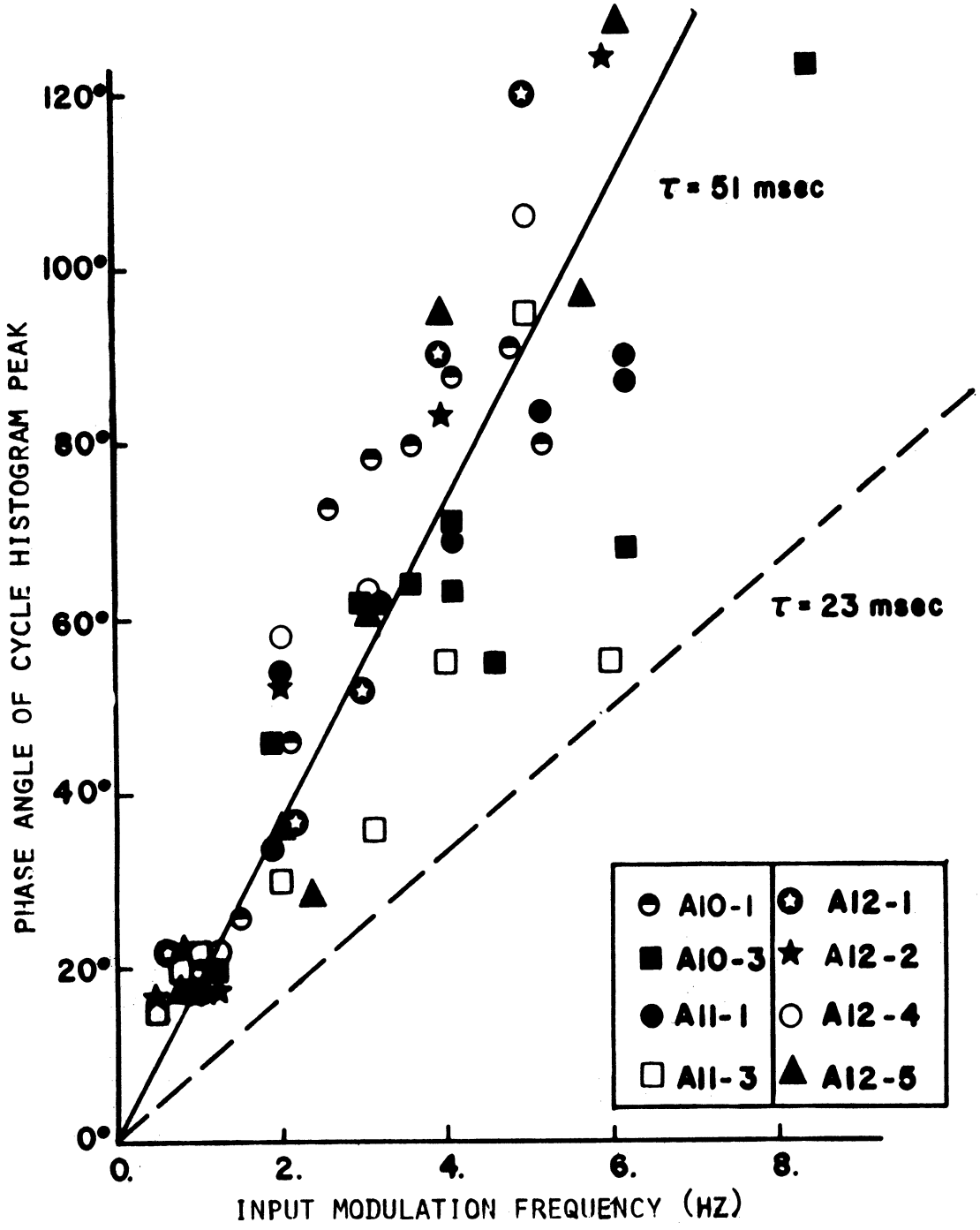

Figure 3.9. Graph of phase angle of the peaks of cycle histograms vs. input modulation frequency for phasic cells that showed phase locking. The graph was normalized by making the phase angle 20° at 1 Hz. The solid line is the linear regression for the data points and represents a time delay of 51 msec. The dotted line is the 23 msec delay predicted from the latency to step inputs.

angles for all the different units, the graph of Fig. 3.9 was normalized such that the phase at 1 Hz was 20° so that the relative delays of all the units could be compared. The clustering of points about 1 Hz was then artificial. A pure time delay can be plotted as a straight line on this graph, the slope of which is equal to the delay. It is clear that the delays measured by the cycle histograms are considerably greater than the 23 msec conduction delay. If the data points were fit linearly, a 50.7 msec delay is obtained with a correlation coefficient of .89. The relatively low correlation coefficient indicates that the effect is probably not due solely to a time delay, or at least the delays are different for different units.

Clearly the phasic units are not linear transducers of joint position. The phase-locking displayed by most of these cells is evidence of an essential nonlinear behavior that cannot be made linear by use of small signal analysis (Spekreijse and Oosting, 1970). However, it is often profitable to study nonlinear systems with linear analysis as long as the proper assumptions are considered. Since the phasic cells respond only to movements of the joint, it is reasonable to assume that they are coding the first or second derivatives of position, albeit in a nonlinear fashion. If we assume that the nervous system is only interested in the fundamental component of the response, then the describing function analysis can be employed. The higher harmonics of the response are considered to be noise and only the fundamental response is computed. For the cycle histograms the degree of distortion was measured by computing the contributions of the higher harmonics relative to the fundamental.

The amplitude of the fundamental component of the response was computed from the cosine and sine Fourier coefficients at the frequency of the driving waveform. This was equivalent to the least mean square or best fitting sine wave to the entire period of the waveform. It represented the signal that was actually transmitted forward by the cell through the average rate of discharge. Other investigators have used an expression that was the best fitting sine wave over the active portion of the period, by artificially filling in the output sine wave with "negative frequencies" (Chapman and Smith, 1963; Jones and Milsum, 1970; Schneider, 1973). This latter measure was more appropriate when the input characteristics of the cell, i.e. the depolarization potential generating the action potentials, rather than the output signal was of interest.

The describing function for a phasic joint cell is shown in Fig. 3.10. The data points represented by dots were calculated from the cycle histograms as described above. The data points represented by the line were calculated from the swept frequency method for the same cell. The correspondence in the results obtained from the two different methods showed that either one could be used to derive the frequency response of the cell. However, there was a vast difference in the time required to implement the two techniques. The swept frequency curve of 100 data points was obtained in one sweep of 150 seconds. The cycle histogram data of 8 data points required over 1800 seconds. Obviously there was a tremendous increase in the data acquisition rate in using the swept frequency technique. For this reason most of the frequency response

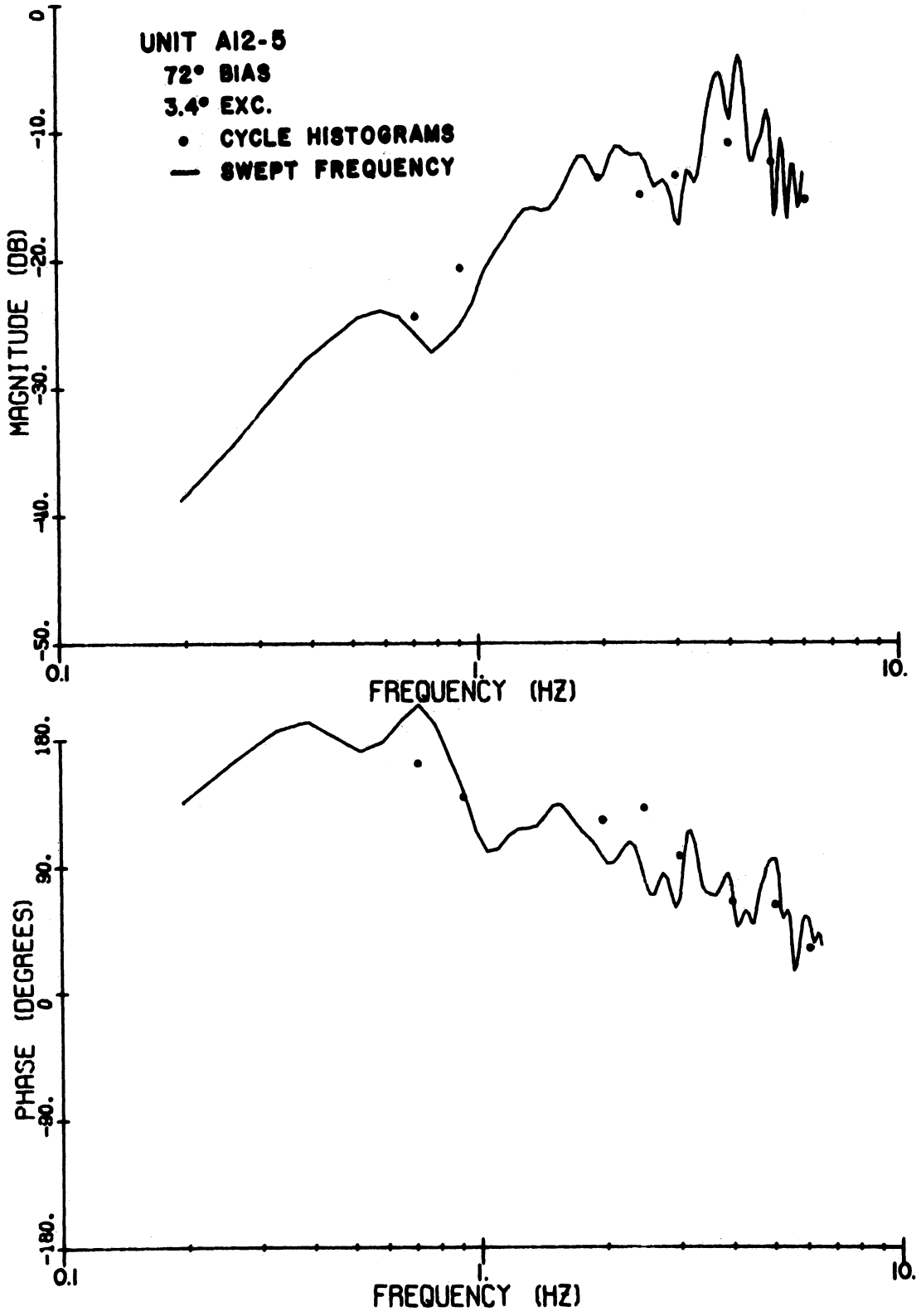

Figure 3.10. Describing function for cell A12-5 using discrete sinusoidal and swept frequency inputs in an acute animal. The Fourier analysis of the cycle histograms was used to obtain the 8 data points for discrete inputs. Correlation and spectral analysis was used for the swept inputs. 0 db represents 28.8 pps/deg. and a phase angle of 90° is flexion.

curves were obtained using this swept frequency technique.

The describing functions for both the anesthetized and unanesthetized phasic joint cells can be characterized as high pass filters. Fig. 3.11 shows a result found in an anesthetized preparation. The magnitude portion of the describing function has a steep positive slope on the order of 30 db/decade and the phase angle has a lead at low frequencies that gradually decreases as the frequency increases. The same general features are evident in the results shown in Fig. 3.10. The curve labeled "model" in Fig. 3.11 is a least square fit of the data with an optimized linear transfer function. The general form of the model is

$$H(s) = G \frac{(s + z_1)^2}{(s + p_1)} e^{-s\tau} \qquad (3.10)$$

The unit shown in Fig. 3.11 was not really typical in that the decrease in phase with increasing frequency was considerably larger than for most of the other cells. This was reflected in the large value of a time delay needed to fit the data.

The positive slope of the gain curve indicates that the phasic knee joint neurons at the thalamic level are sensitive to the higher derivatives of the joint position. A pure velocity transducer would have a slope of 20 db/decade in the magnitude curve and a 90° phase lead at all frequencies. A pure acceleration transducer would have a 40 db/decade slope with a 180° lead. The response of the thalamic joint cell of Fig. 3.11 indicates that the fundamental component of the response can be responding to the acceleration of the input stimulus in the frequency range from

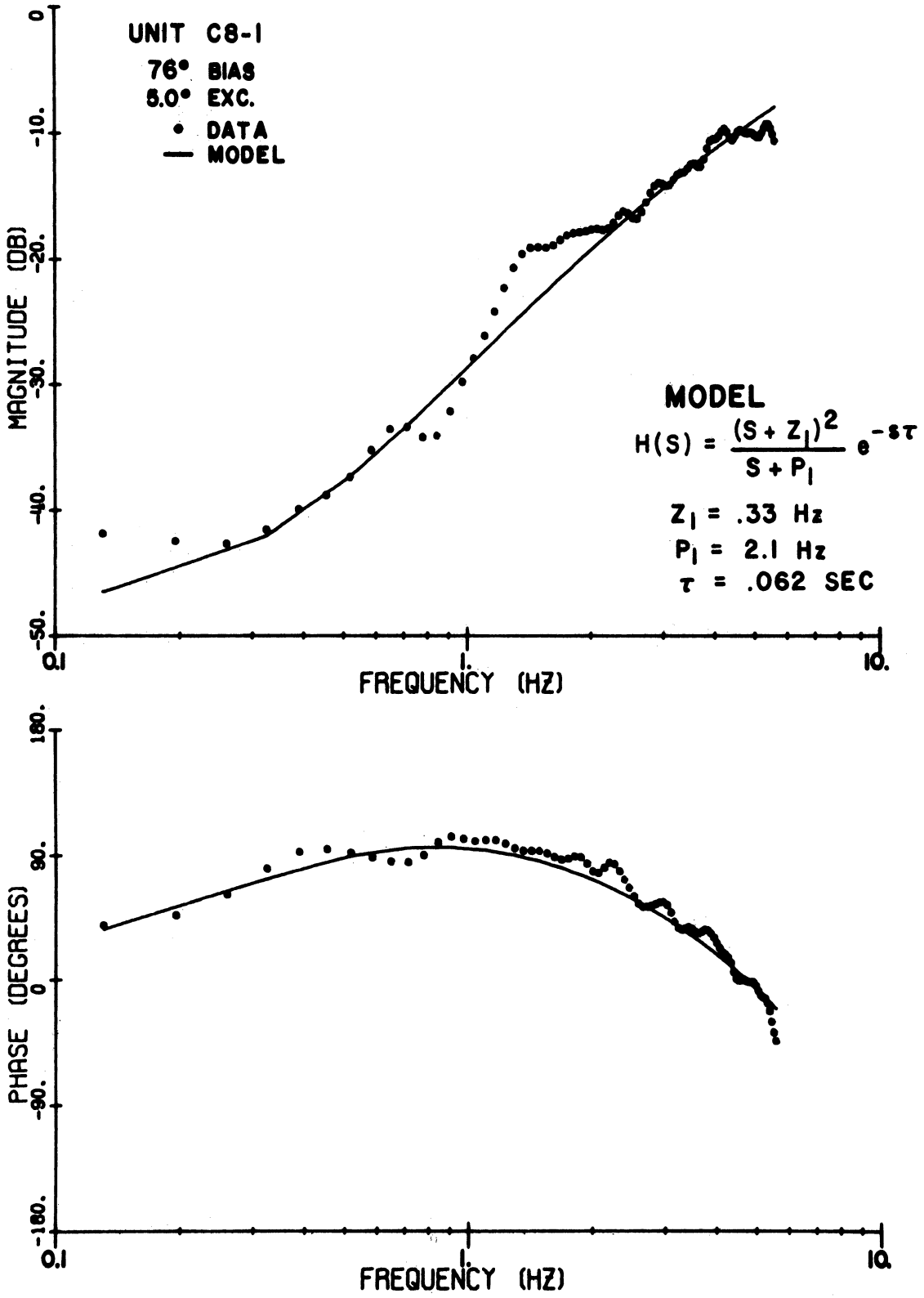

Figure 3.11. Describing function for cell C8-1. The solid line is a model with the transfer function and optimized parameters as shown. The animal was anesthetized. 0 db represents 35.6 pps/deg. and 90° phase is flexion.

.3 to 2 Hz.

An examination of the results for all units in which a describing function could be found showed the following general deviations from the data shown in Fig. 3.11. One, the slope of the gain curve varied from as low as 20 db/decade to as high as 35 db/decade. Two, the low frequency portion of the magnitude curve often leveled out at frequencies ranging from .1 to 1.0 Hz. Three, the high frequency portion of the gain curve attenuated at frequencies from 4 to 6 Hz. Four, the low frequency portion of the phase curve varied from +180° to +45°. Five, the rate at which the lead in the phase curve decreased varied considerably. In terms of a linear transfer function some of these variations could be consistent with differences in the positions of the two corner frequencies z_1 and p_1. For example if z_1 were larger than that found for Fig. 3.11, the low frequency gain curve will tend to flatten out, the slope will decrease, and the low frequency phase will show less lead. An example of this is shown in Fig. 3.12 for a cell in an unanesthetized preparation. It was apparent, however, that not all of the units could be fit with a transfer function of the general form of (3.10). Many of the response curves with a flatter gain curve could be characterized by a transfer function with a lead filter response, i.e.

$$H(s) = G \frac{s + z_2}{s + p_2} e^{-s\tau} \qquad (3.11)$$

where $z_2 < p_2$. This transfer function can be termed velocity-sensitive in the bandwidth between z_2 and p_2. The phasic cells found in the VPL showed a continuum of deviations between the two models of (3.10) and (3.11), and some could not be fit with either

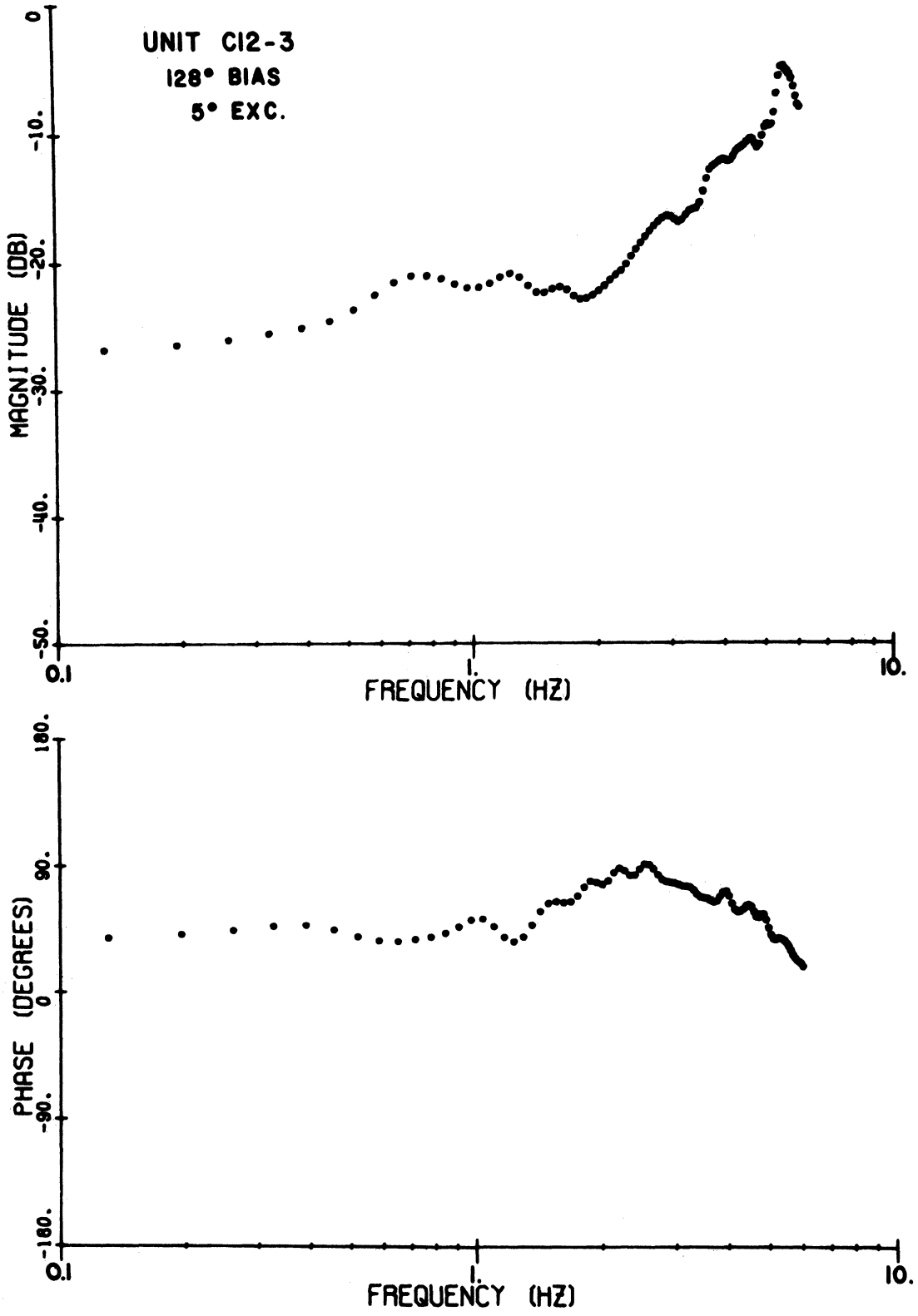

Figure 3.12. Describing function for cell C12-3. Animal was unanesthetized. 0 db represents 35.6 pps/deg. and 90° phase is extension.

model. For example, Fig. 3.13 shows the describing function for a cell found in an anesthetized preparation that could not be fit well by a transfer function of this form. However, it exhibited many of the same characteristics seen in the other thalamic units, namely a steep gain curve (≃30 db/decade slope) and a prominent phase lead at low frequencies that gradually decreased at higher frequencies. The decrease in lead of the phase angle was a consistent feature of all units.

The coherence function $\gamma^2(\omega)$ estimates the degree to which the output is linearly related to the input by the frequency response. Equivalently $\gamma^2(\omega)$ is also an estimate of the ratio of signal power to signal plus noise power if all of the output not contained in the fundamental component is considered to be noise. Fig. 3.14 shows the coherence function for the data in Fig. 3.13. At low frequencies there is very low coherency since the signal component is small. As the frequency increases the signal component also increases and the coherency becomes larger. For cells that have a random component to the carrier or spontaneous discharge, the coherence function is also dependent upon the average pulse rate (Appendix B). The higher the average rate, the larger the signal-to-noise ratio and the larger the coherency.

As attempt was made to estimate the accuracy to which the describing function of Fig. 3.13 represented the true frequency response, or equivalently to find the confidence interval for the frequency response estimate. For stationary white noise inputs, Jenkins and Watts (1968) have derived an analytic expression for the 95% confidence interval of frequency response estimates found by spectral

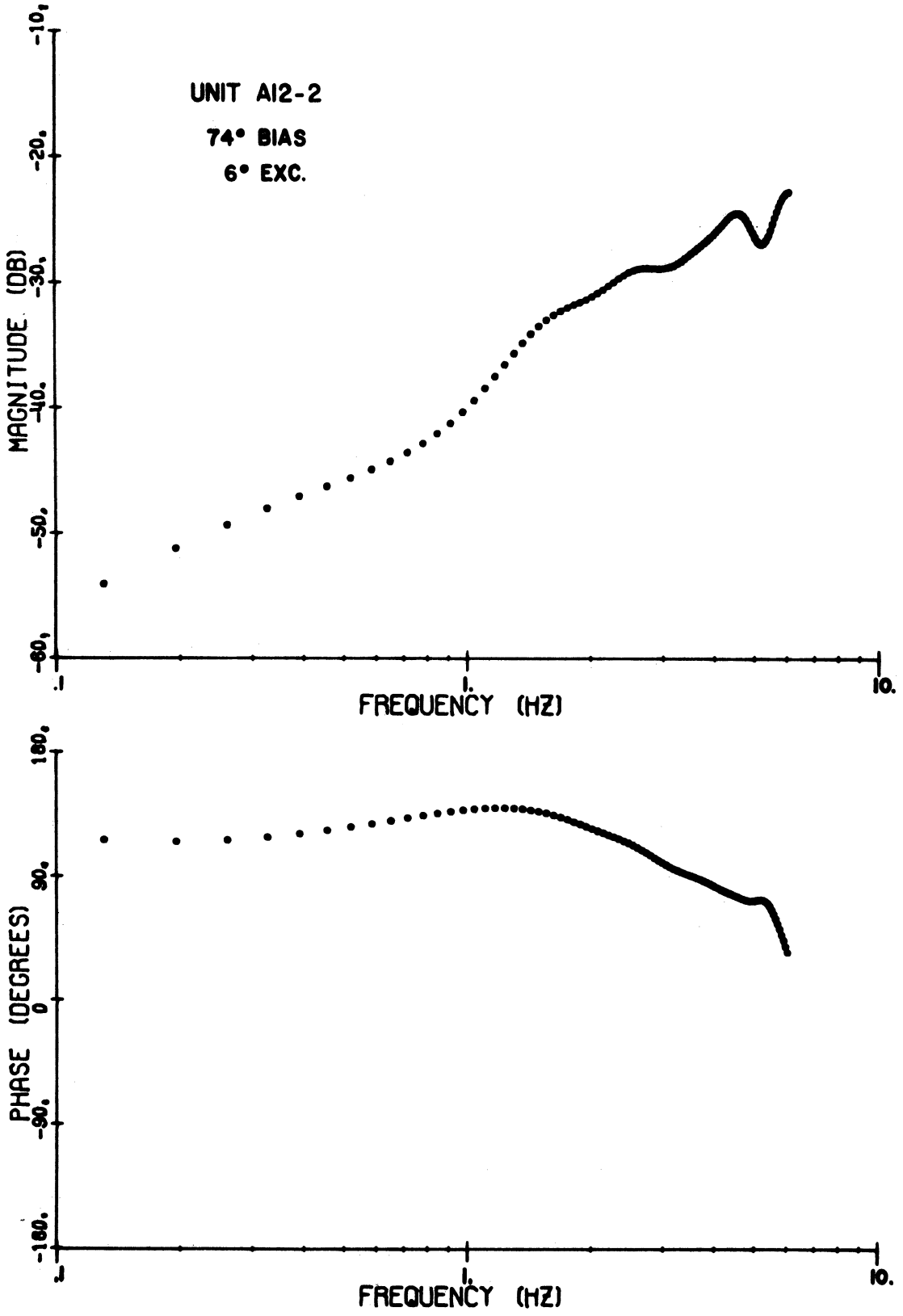

Figure 3.13. Describing function for cell A12-2. Animal was anesthetized. -20 db represents 2.5 pps/deg. and 90° phase is extension.

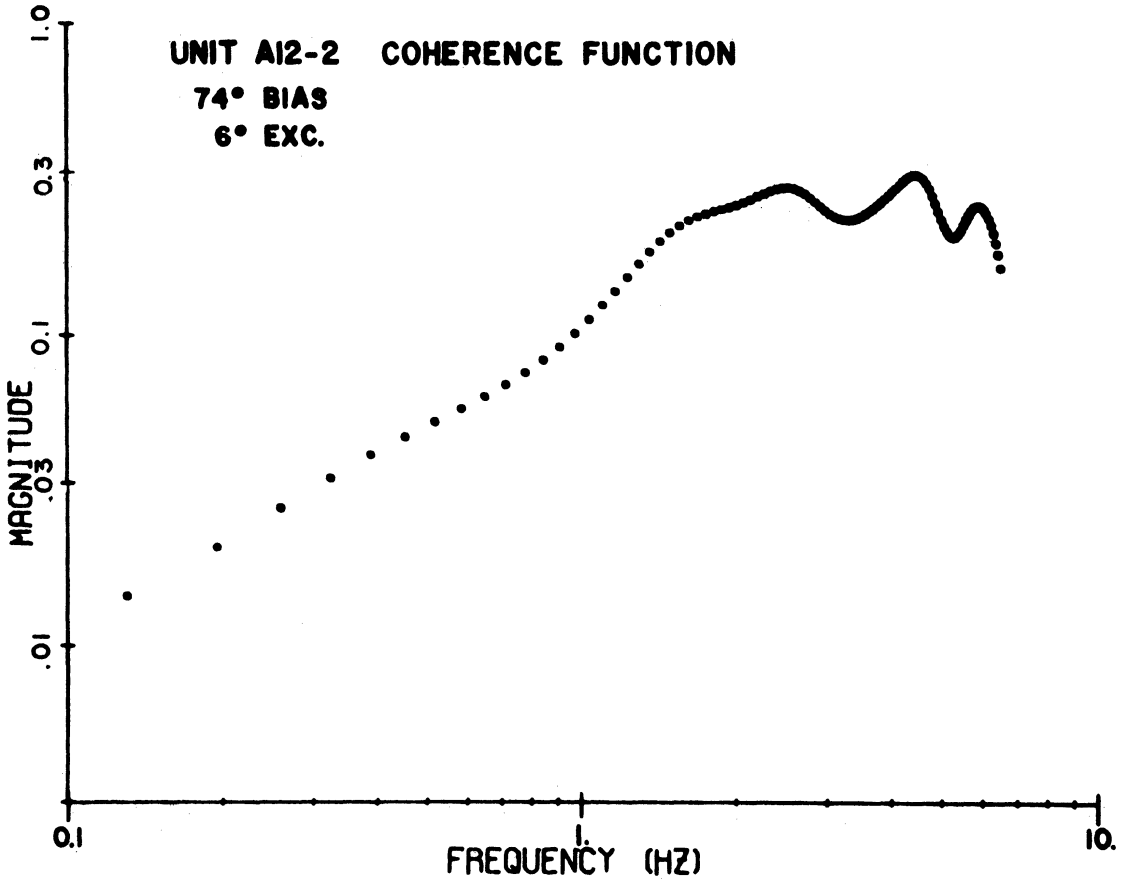

Figure 3.14. Coherence function for cell A12-2. The describing function from which the coherency was calculated is shown in Fig. 3.13.

analysis. These estimates are formally a least squares regression analysis at each frequency of the linear system represented by (3.4). Linear least squares estimation can then be used in the frequency domain if the random variables are assumed to be distributed as chi-squared. The expression is a function of the number of degrees of freedom ν of the smoothed spectrum estimates, the $F_{2,\nu-2}$ distribution, and the coherency $\gamma^2(\omega)$ at each point.

Unfortunately this derivation could not be used or easily transformed for use in the case of the nonstationary swept frequency inputs. Instead estimates of the confidence intervals were made by calculating an ensemble averaged estimate of the describing function. The input to the cell was 20 sweeps from .1 - 6 Hz of 10 seconds each. The data were processed in two ways. First, the 20 sweeps were processed together to obtain a time averaged estimate of the describing function. This was the method used in all the other data processing. Secondly, the sweeps were separated into ten different records of two sweeps each. Each record of two sweeps was processed individually to obtain ten different estimates of the describing function. The ten frequency response curves were then averaged together to obtain an ensemble average estimate of the describing function along with standard deviations of the estimate. The results are shown in Fig. 3.15. For both the gain and phase curves, the confidence intervals for the data are wide at low frequencies and become progressively narrower as the frequency increases. The magnitude of the standard deviation is well correlated to the inverse of the coherence function in Fig. 3.14.

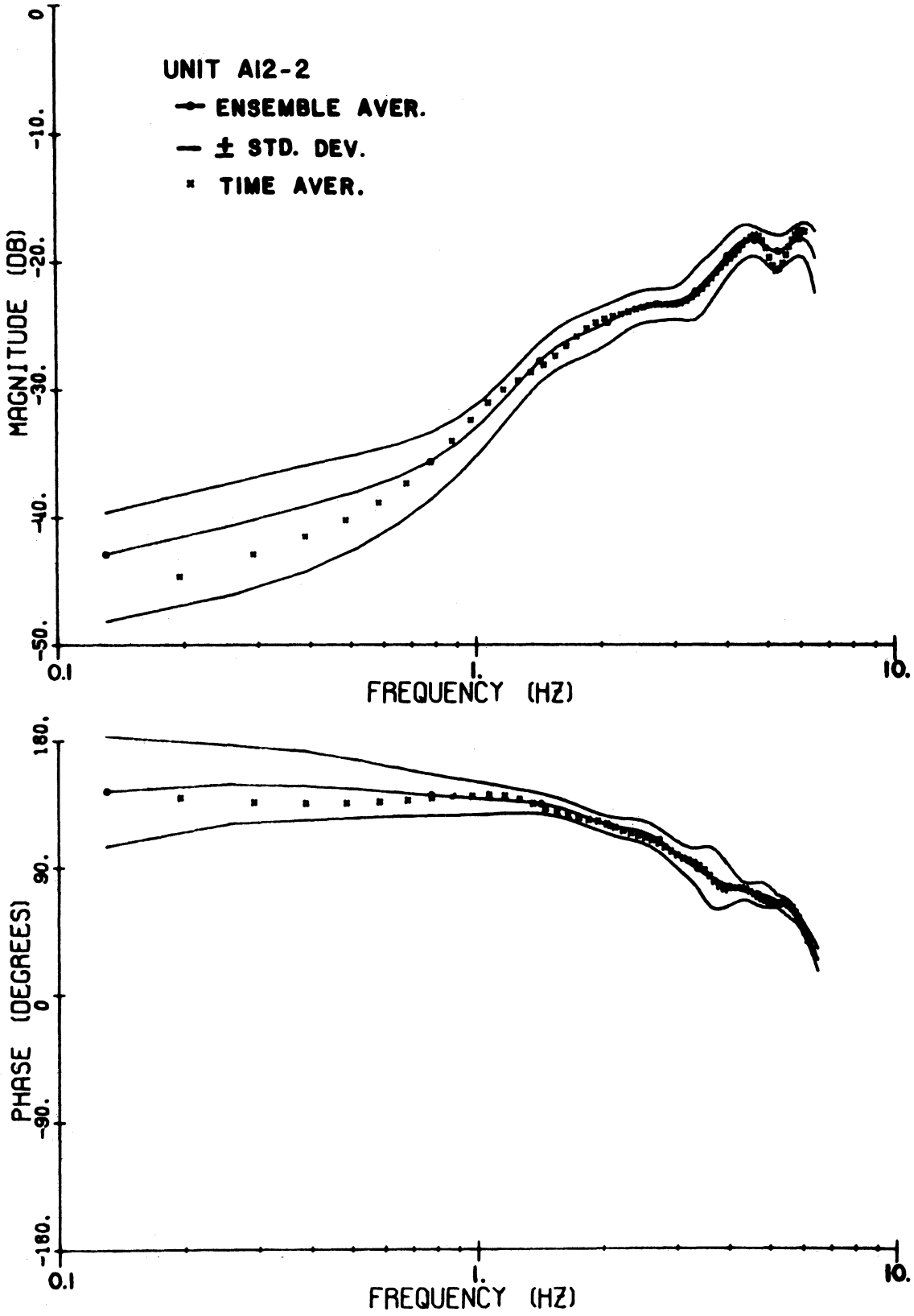

Figure 3.15. Estimate of the confidence intervals for the describing function of cell A12-2. The ensemble average and standard deviations were calculated by averaging ten different estimates of the describing function. See text for details.

This provides an estimate of the confidence intervals for the describing functions, given the values of ν and $\gamma^2(\omega)$. The values for $\gamma^2(\omega)$ shown in Fig. 3.14 are typical of results found in the other frequency response estimates.

Scatter diagrams showing each spike at the phase and frequency at which it occurred were used to gain some insight into the nature of the response to swept frequencies. Two such diagrams are shown in Fig. 3.16. Fig. 3.16a shows one sweep of the unit for which the frequency response is shown in Fig. 3.12, and Fig. 3.16b shows one sweep of the unit for which the cycle histograms and frequency response curves are shown in Fig. 3.7 and 3.13 respectively. Fig. 3.16a shows that for this cell in a semi-chronic animal there is no severe phase-locking or bidirectional response even at the highest frequency. The predominant response between 0° and 90° corresponds to the phase of the describing function (Fig. 3.12) starting with a 45° lead while the slight shift in the dots to increasing delays is seen in the Bode plot as a decrease in lead at frequencies above 3 Hz. The phase-locking seen in the cycle histograms of Fig. 3.7 is manifested as a row of dots with a positive slope in Fig. 3.16b. The slope of the dots corresponds to the beforementioned delay in the cycle histogram peak at increasing frequencies. The phase-locked response goes from +360° to 0° at about 4 Hz in Fig. 3.16b just as in Fig. 3.7e. Thus, examination of the scatter diagrams can yield almost all the information contained in the cycle histograms in a much more compact and efficient form, and what cannot be discerned from the scatter diagrams (e.g. Fourier

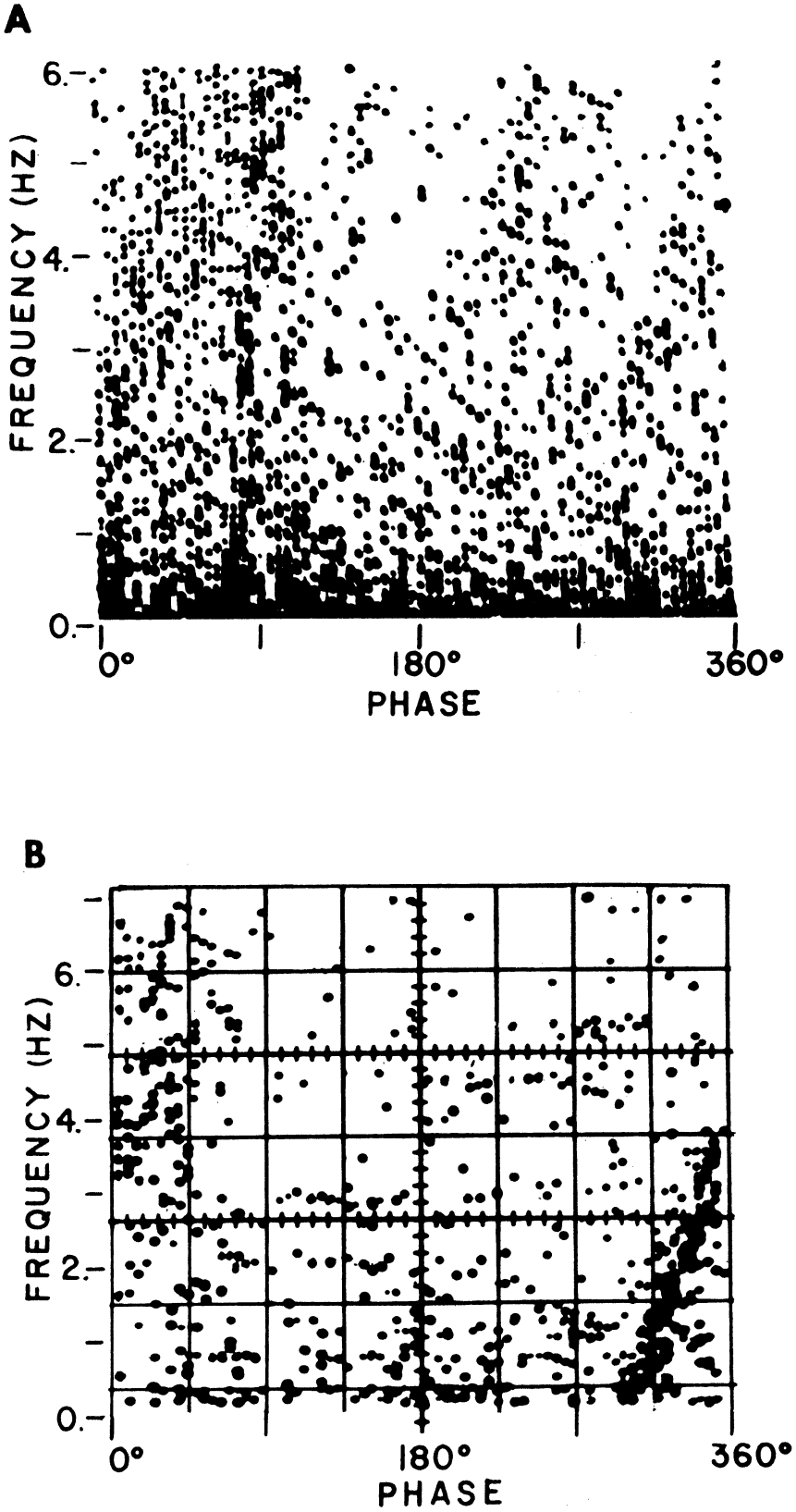

Figure 3.16. Scatter diagrams for cells C12-3 and A12 2. A). Response of cell C12-3 in an unanesthetized animal. 90° phase is extension. B). Response of cell A12-2 in an acute animal. 90° phase is flexion. Dots have been retouched by hand.

analysis) can be derived from the describing functions.

Fig. 3.16 also shows one of the differences between the unanesthetized and anesthetized preparations. The greater number of dots in Fig. 3.16a as compared with Fig. 3.16b shows that the average level of activity is much higher in the unanesthetized preparations. This was a frequent observation in comparing the spontaneous activity of VPL cells in the two preparations. However, in so far as the frequency response data were concerned, there appeared to be no significant differences between the two conditions. The describing functions for the two classes of cells seemed to be indistinguishable except that the phase angles in the acute animals tended to exhibit more lead at low frequencies.

In one unit the frequency response when the animal was asleep could be compared with the response in an awake animal. This is believed to be the first time that a quantitative response of this type has been compared in a single unit under the two conditions. The responses are shown in Fig. 3.17. The state of the animal was judged by its behavior, i.e. whether or not its eyes were open and looking about. In general the differences in the two responses are slight. The dip in the gain curve between 1 and 2 Hz in the awake preparation is an artifact caused by movements of the animal. Otherwise the two responses are virtually identical. Units in chronic preparations were much harder to keep for long periods of time in the awake animal. As a result most of the frequency response determinations were made in sleeping animals.

The linearity of the system was examined by comparing the frequency responses of a unit for three different bias angles Θ

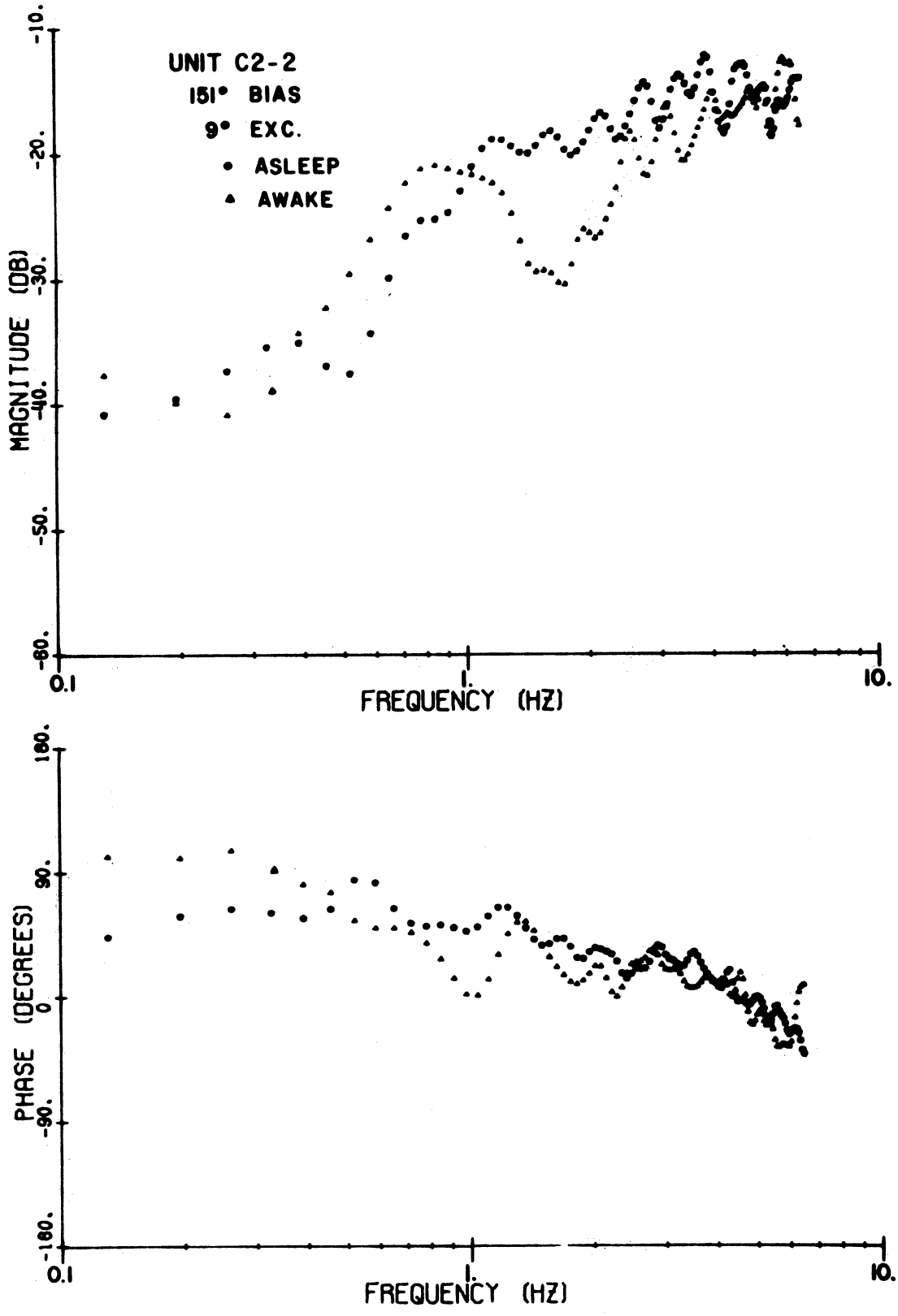

Figure 3.17. Describing functions for cell C2-2 in an awake and asleep animal. Identical stimuli were applied to the animal. -20 db represents 2.0 pps/deg. and 90° phase is extension.

at the same excursion amplitude $\Delta\Theta$ and for three different amplitudes at the same bias. The results are shown in Fig. 3.18 and 3.19. In Fig. 3.18 the three frequency response curves were very similar except at low frequencies. The gain sensitivity of the cell when the limb was biased near flexion (Θ = 107°) was about 3 db less than that of the other two responses. The differences in the gain curves at low frequency were probably not significant since the coherence function at these frequencies was also low. From the error analysis shown in Fig. 3.14 and 3.15 the low coherency at these frequencies implies larger variability in the describing function estimates. In Fig. 3.19 the response at the smallest imput amplitude of 1.5° was markedly different from the two responses at larger excursions. This was indicative of a threshold nonlinearity in which the input had to be greater than a certain threshold amplitude before the unit responded. Although it was not evident in Fig. 3.19, other cells in which this experiment was attempted sometimes showed a saturation effect in which the sensitivity decreased for very large input excursions.

In general, the qualitative characteristics of all the phasic knee joint cells taken as a whole can be summarized as follows. Most of the cells were sensitive to joint movement over a broad range of angles, and could be activated at almost all bias angles by sufficiently high frequency inputs. However, there was a range in which the joint cell seemed to be maximally sensitive. Most of the cells responded to either flexion or extension of the limb while a small percentage (12%) were bidirectional even at low input frequencies. Most of the units also showed a phase-locked

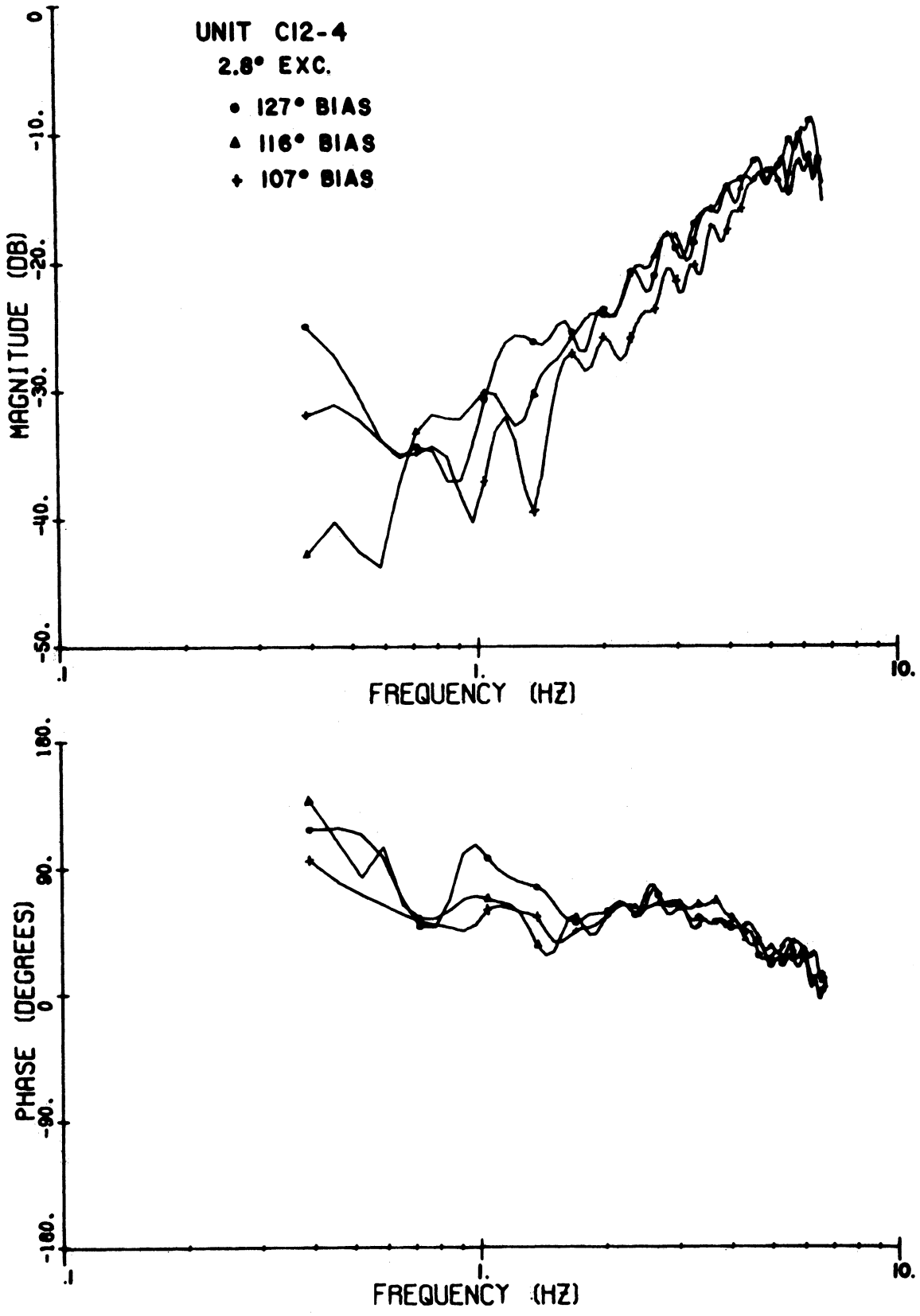

Figure 3.18. Describing functions for cell C12-4 for 3 different bias angles. Animal was unanesthetized and excursion angle was held constant. 0db represents 57.8 pps/deg. and 90° phase is flexion.

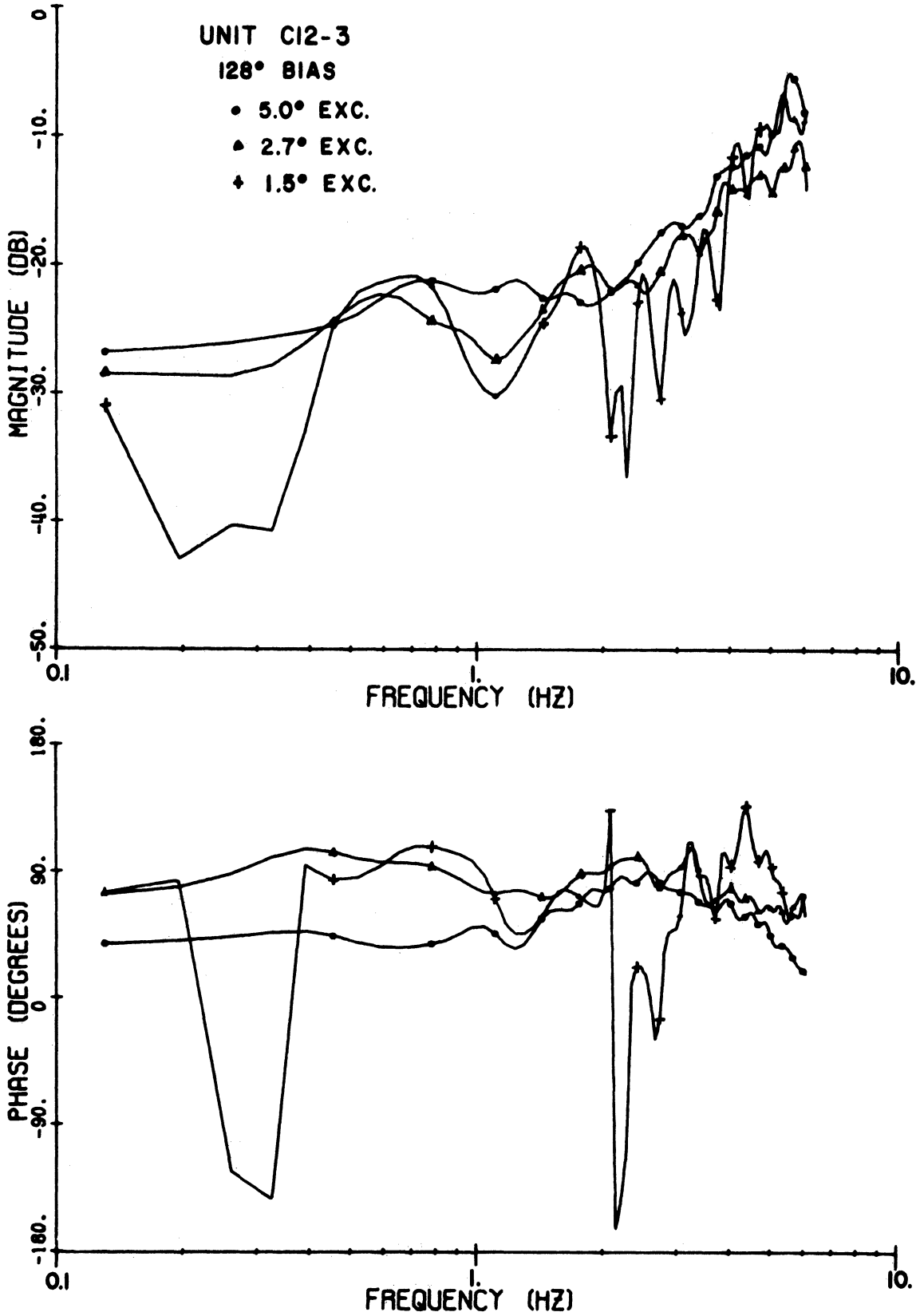

Figure 3.19. Describing functions for cell C12-3 for 3 different input amplitudes. Animal was unanesthetized and bias angle was held constant. 0 db represents 34 pps/deg. and 90° phase is flexion.

response, particularly at frequencies above 3 Hz.

Slowly adapting response

The original goal of this study was to find the dynamic response characteristics of the slowly adapting knee joint cells. Unfortunately only 7 out of the 438 cells isolated during the course of the study were identified as tonic knee joint cells and a detailed quantitative study was completed for only one of these cells. Obviously any conclusions that are drawn from this meager sample are subject to valid criticism. With this precaution in mind, the data are presented because they demonstrate some interesting and worthwhile results, but they are not meant to indicate the response of a "typical" slowly adapting joint cell.

Only one of the seven tonic joint cells was found in the acute preparations. In fact, it was for precisely this reason that the later experiments were performed on semi-chronic animals. It was felt that the action of the anesthetic agent in depressing the spontaneous activity of the VPL cells could be responsible for silencing or otherwise distorting the tonic discharge of the slowly adapting responses. Although more slowly adapting knee joint cells were found in the chronic preparations, they were still not found in large numbers. Only 6 out of the 281 cells isolated in the unanesthetized animals were found to be tonic knee joint cells.

The response of a tonic knee joint cell to discrete sinusoidal stimulation is shown in Fig. 3.20. The cycle histograms show the response to different frequencies of sine wave inputs at the same bias angle and excursion. The solid curve in each histogram is the fundamental component of the response. The output response is

Figure 3.20. Cycle histograms for cell C10-6 for different frequencies of stimulation at the same bias angle and excursion. N = total number of impulses counted, B = total number of cycles averaged, λ_o = average discharge rate of the output pulse train, λ_m = amplitude of the fundamental component of the output, ϕ = phase angle of the fundamental component, F = frequency of the input sine wave. Animal was unanesthetized and the first half cycle of the histogram represents flexion of the limb.

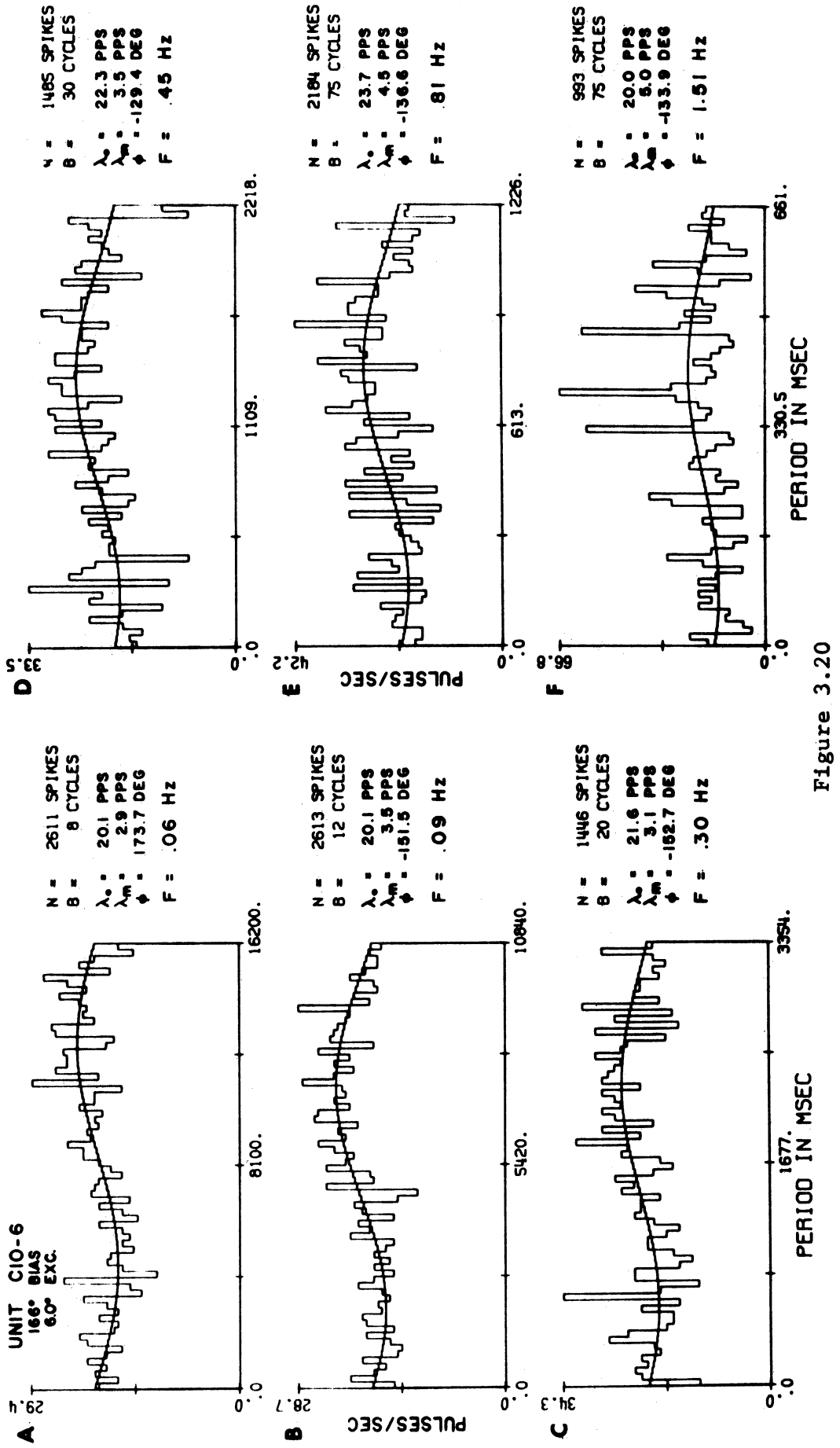
UNIT C10-6
166° BIAS
6.0° EXC.
A
N = 2611 SPIKES
B = 8 CYCLES
λo = 20.1 PPS
λm = 2.9 PPS
φ = 173.7 DEG
F = .06 Hz
29.4
0.0
8100.
16200.
B
N = 2613 SPIKES
B = 12 CYCLES
λo = 20.1 PPS
λm = 3.5 PPS
φ = -151.5 DEG
F = .09 Hz
28.7
0.0
5420.
10840.
C
N = 1446 SPIKES
B = 20 CYCLES
λo = 21.6 PPS
λm = 3.1 PPS
φ = -162.7 DEG
F = .30 Hz
34.3
0.0
1677.
3354.
PERIOD IN MSEC
PULSES/SEC
D
N = 1485 SPIKES
B = 30 CYCLES
λo = 22.3 PPS
λm = 3.5 PPS
φ = -129.4 DEG
F = .45 Hz
33.5
0.0
1109.
2218.
E
N = 2184 SPIKES
B = 75 CYCLES
λo = 23.7 PPS
λm = 4.8 PPS
φ = -136.6 DEG
F = .81 Hz
42.2
0.0
613.
1226.
F
N = 993 SPIKES
B = 75 CYCLES
λo = 20.0 PPS
λm = 6.0 PPS
φ = -133.9 DEG
F = 1.51 Hz
66.8
0.0
330.5
661.
PERIOD IN MSEC

Figure 3.20

assumed to have the general form

$$y(t) = \lambda_o + \lambda_m \sin(\omega_m t + \phi) \qquad (3.12)$$

and the values for λ_o, λ_m, and ϕ are given. The response of this unit to low frequency sinusoidal stimulation was well described by a frequency modulated pulse train. However, at the highest frequency shown (1.5 Hz) the response already exhibited considerable harmonic distortion. At higher frequencies the distortion was even more pronounced. The gain of the response increased gradually as the frequency increased while the phase showed a slight leading angle (relative to extension of the limb) that remained approximately constant over all frequencies.

The describing function calculated in three different ways for this unit is shown in Fig. 21. The data represented by "+" is the describing function calculated from a swept frequency input. In this case a linear sweep from .01 to 2.0 Hz was used since the function generator for logarithmic sweeps could not go below .1 Hz. The linear sweep was generated by putting a very low frequency triangular waveform into the voltage-controlled oscillator input of a sine wave generator biased at .1 Hz. The linear sweep had the disadvantage that higher harmonics may be correlated with the response within the data window, particularly at low frequencies (see Appendix B), but fortunately the harmonic distortion at low frequencies was small as can be seen from Fig. 3.20. The data in Fig. 3.21 represented by "." show the frequency response calculated from the cycle histogram data, part of which is shown in Fig. 3.20. The data represented by "▲" is the response calculated from the

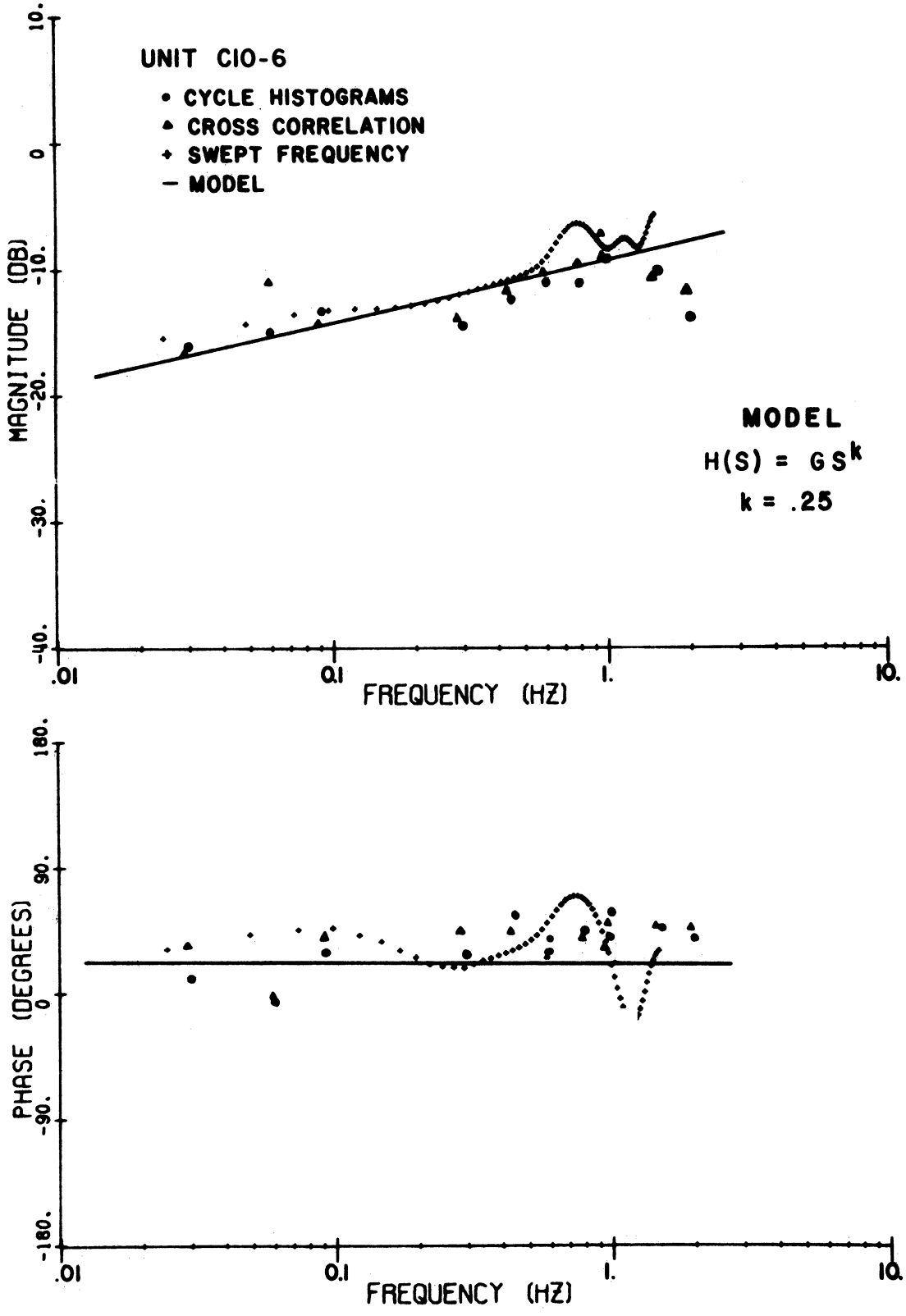

Figure 3.21. Describing functions for cell C10-6 calculated by the cycle histogram, discrete frequency cross-correlation, and swept frequency data. Solid line is the model found for knee joint receptors 0 db represents 2.4 pps/deg. and 90° phase is extension. See text for details.

discrete sinusoidal inputs but processed by the cross correlation technique described in Appendix A. Theoretically the curves obtained from the two different techniques of processing the discrete sinusoidal inputs would superimpose, and excellent correspondence is seen in Fig. 3.21. The line drawn in Fig. 3.21 is a model for a transfer function of the form

$$H(s) = G\, s^{k} \qquad (3.13)$$

where k = .25. This is the form of the dynamic response of tonic knee joint receptors (McCall et al., 1973) and is drawn here for comparison purposes. As can be seen in Fig. 3.21 the thalamic data show the same general features as the model, i.e. a slowly increasing gain curve with a leading phase.

The linearity of this unit was examined by stimulating the joint with different excursion amplitudes of a .6 Hz sine wave while it was biased at the same angle. The results are shown in Fig. 3.22. If the system was linear, the amplitude of the response λ_m should have been linearly related to the input amplitude $\Delta\Theta$ while the phase ϕ and average spike rate λ_o remained unchanged. From Fig. 3.22 it can be seen that ϕ and λ_o remain approximately equal over all values of $\Delta\Theta$. The graph of λ_m vs $\Delta\Theta$ is shown in Fig. 3.23, and it shows that the response is linear over the amplitudes used.

The static curve of this unit is shown in Fig. 3.24. From Fig. 3.24a it can be seen that the active angle for this unit was only 35° and that the cell was maximally sensitive at extreme extension. In Fig. 3.24b the static curve was replotted over the receptive angle on log-log coordinates. The spontaneous discharge λ_T and the

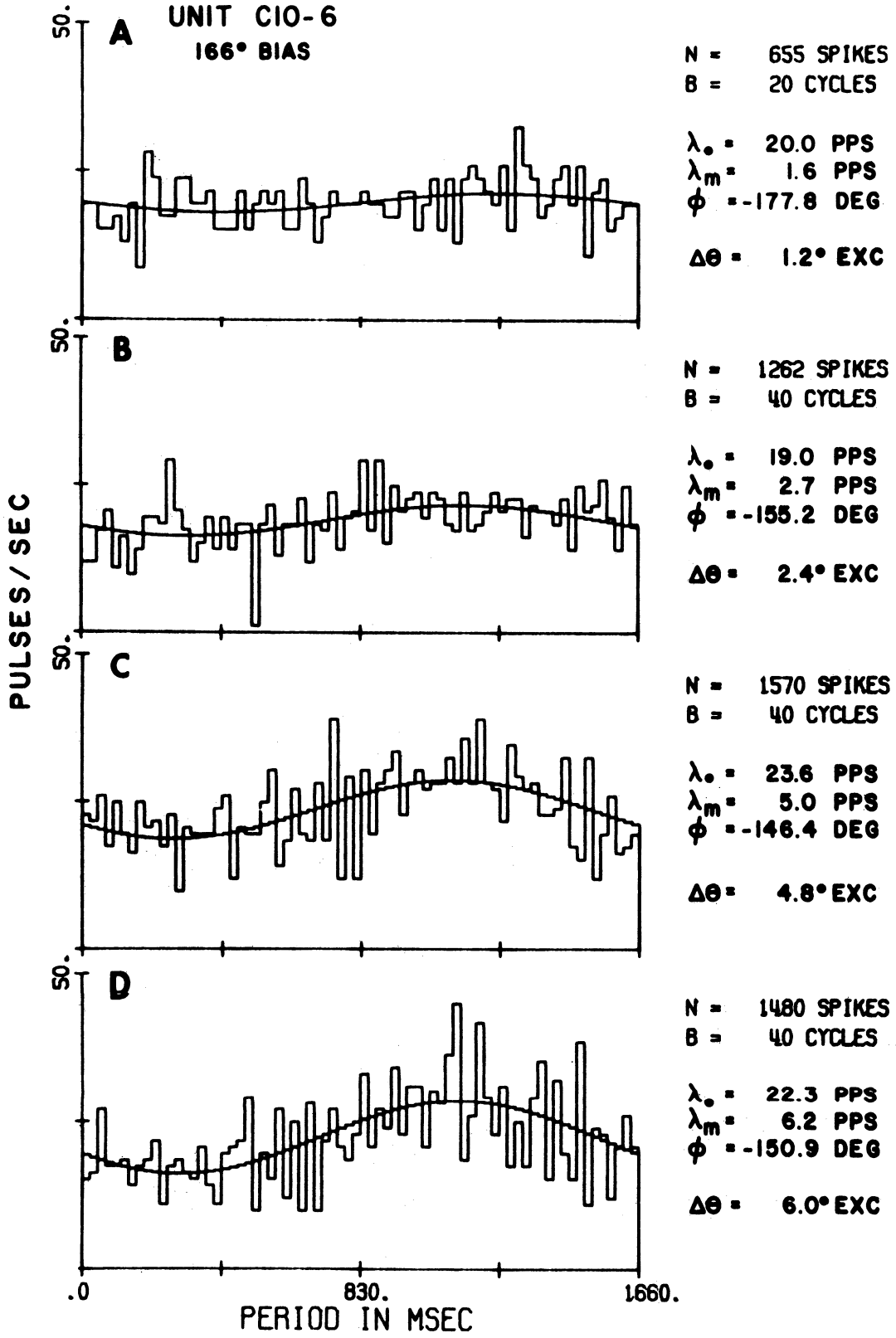

Figure 3.22. Cycle histograms for cell C10-6 for different excursion angles. Stimulus frequency and bias angle were held constant. Positive phase angles are flexion.

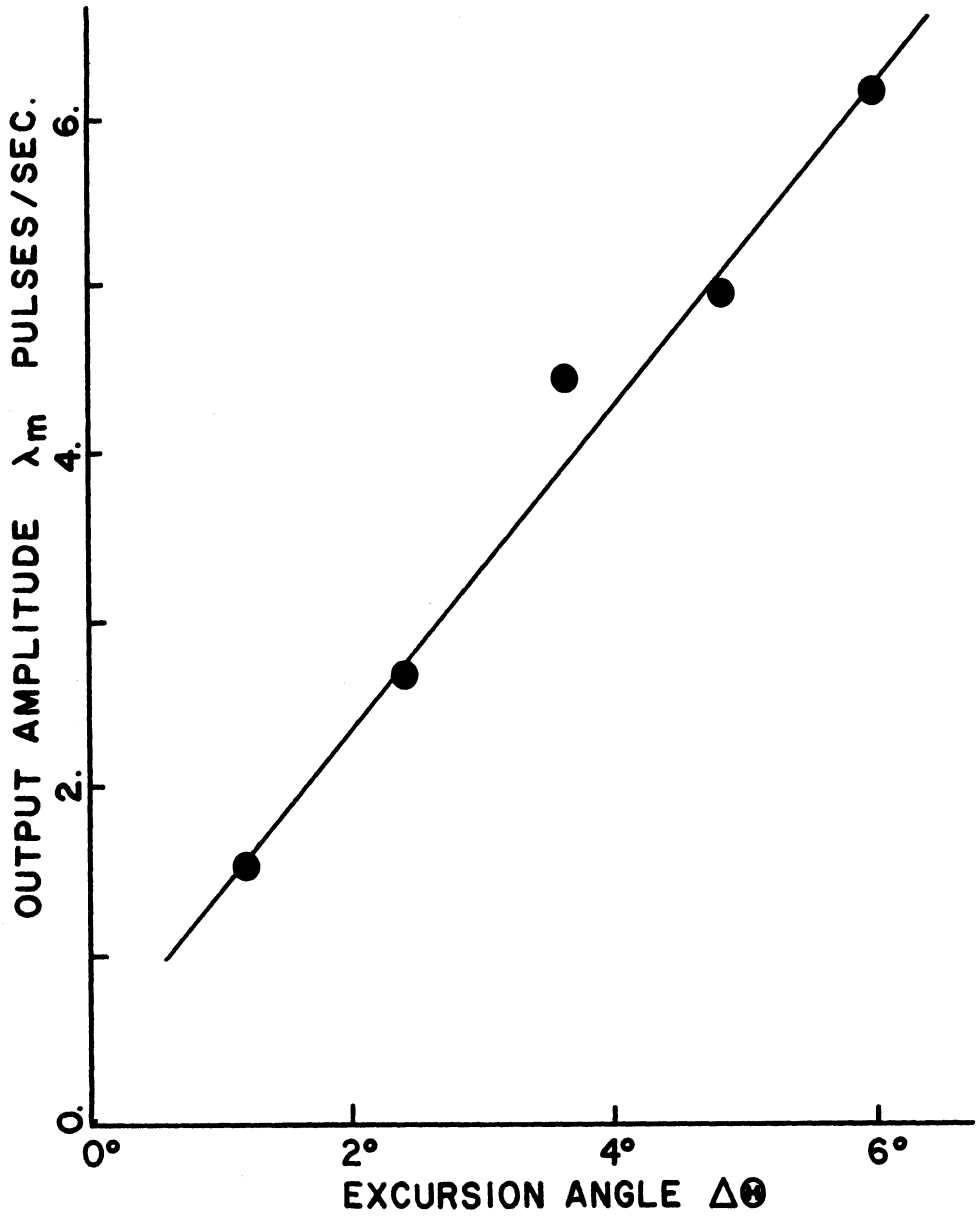

Figure 3.23. Graph of excursion angle vs. amplitude of fundamental harmonic of output for cell C10-6. Data points were calculated from cycle histograms of Fig. 3.22. Frequency of stimulus was .6 Hz. Line was drawn by eye.

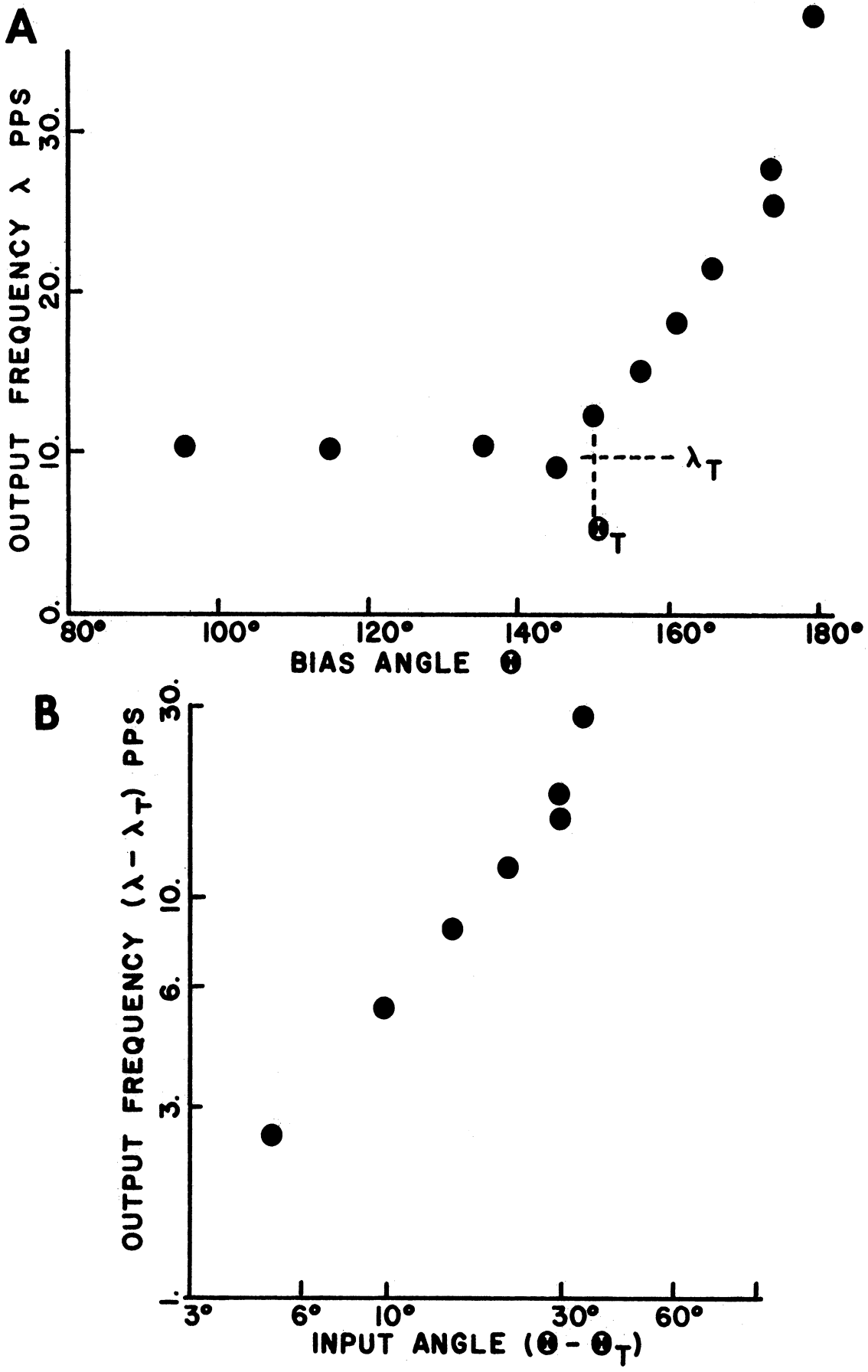

Figure 3.24. Static curves for cell C10-6 on A) linear and B) log-log coordinates. See text for details.

threshold angle θ_T have been subtracted out. A straight line on this graph indicates that the response is described by a power function (Mountcastle et al., 1963). The data showed that the response for this unit was roughly a power function with exponent one. The average firing rate of the cell was calculated from the means of the interspike interval histograms shown in Fig. 3.25. The interspike interval histograms for this cell in Fig. 3.25a-c can be fit with exponential curves as shown. The histogram in Fig. 3.25d-f are results from another tonic joint cell in an anesthetized preparation. The large first bins in the interval histograms for this acute preparation show the tendency for the cell to respond in bursts of 3-5 spikes. Although the static curve for this unit was also monotonic, it was clear that the character of the discharge was different from that in the chronic animal. The serial correlation coefficients of the two units shown in Fig. 3.25 showed no significant correlation at all lags for the cell in the unanesthetized animal, and positive correlation coefficient at low lags for the cell in the anesthetized animal. This again confirmed the bursting nature of the response in the acute preparations.

Evoked responses to electrical stimulation

One experiment was designed to confirm the projection of knee joint cells to VPL. Short electrical pulses (400 mV, .01 msec) were applied to the medial articular nerve, and the evoked responses were recorded in VPL with a microelectrode. The latency to the first burst of spikes was on the order of 14 msec. This compares with a latency of 22 msec when step inputs to the knee are applied. The additional 8 msec is the activation time needed for the receptor to respond.

Figure 3.25. Interspike interval histograms for tonic cells C10-6 and A10-6. (A-C). Cell C10-6 was recorded in an unanesthetized animal. (D-G). Cell A10-6 was recorded in an acute animal. Histograms were plotted from step changes applied to the knee and after the initial transients had died out. MEAN ISI is the mean interspike interval calculated from the histograms. The last bin of the histogram is a catching bin for all intervals longer than the maximum bin. Solid curves in A-C are exponential curves with a time constant equal to the mean discharge rate.

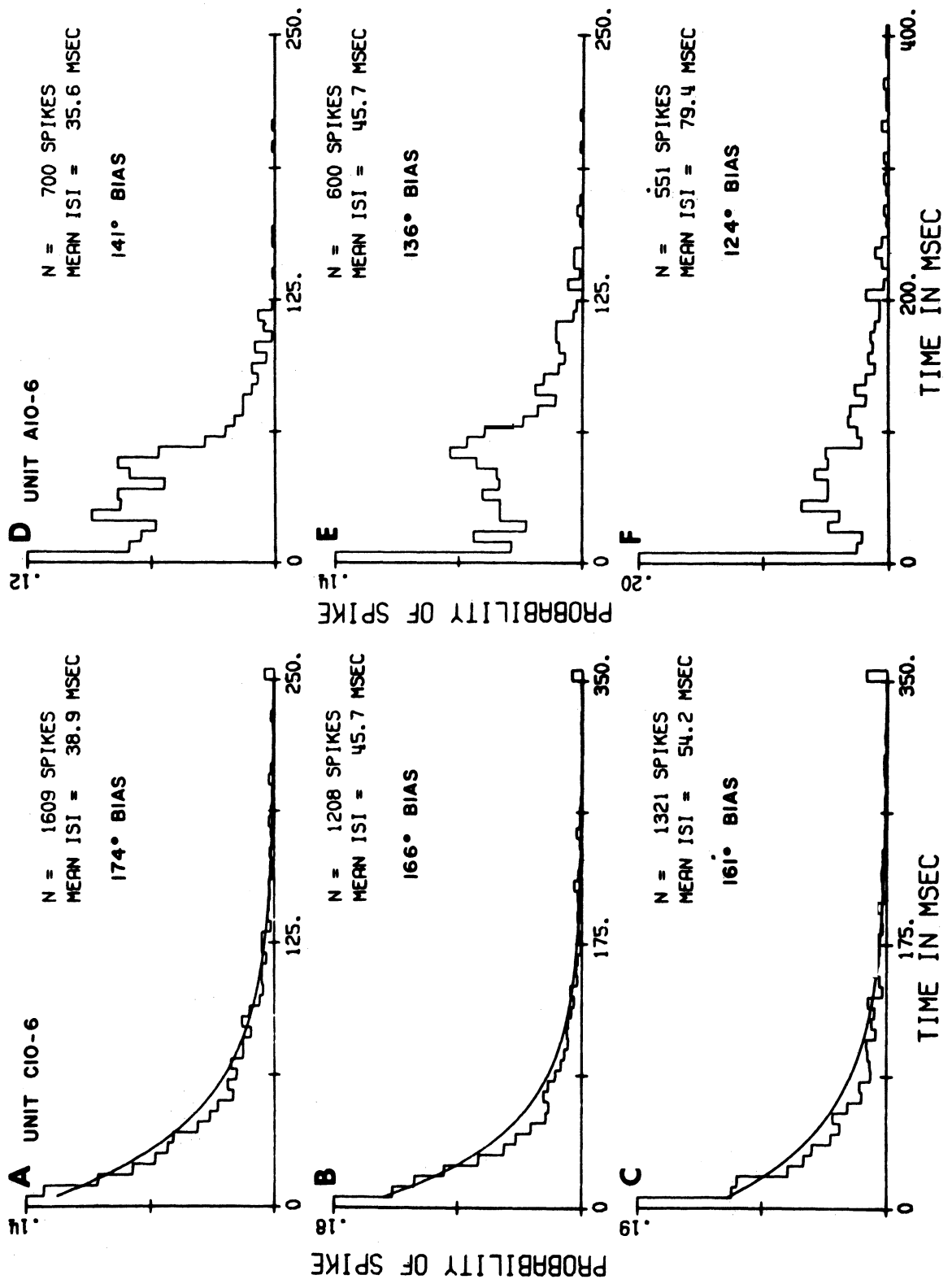
A UNIT C10-6
N = 1609 SPIKES
MEAN ISI = 38.9 MSEC
174° BIAS
B
N = 1208 SPIKES
MEAN ISI = 45.7 MSEC
166° BIAS
C
N = 1321 SPIKES
MEAN ISI = 54.2 MSEC
161° BIAS
D UNIT A10-6
N = 700 SPIKES
MEAN ISI = 35.6 MSEC
141° BIAS
E
N = 600 SPIKES
MEAN ISI = 45.7 MSEC
136° BIAS
F
N = 551 SPIKES
MEAN ISI = 79.4 MSEC
124° BIAS
PROBABILITY OF SPIKE
TIME IN MSEC

Figure 3.25

Histology

Histological verification of the site of recordings was made in nine animals in which knee joint cells were found. For several of these units a lesion was made at the end of the recording session in order to help identify the site. In some cases lesions were not made or could not be found. In these animals the site of recording was identified by comparing the location of electrode tracks with actual penetrations with the microelectrode. In all cases cells were in the rostral-lateral pole of the VPL. The units were generally located between Horsley-Clarke AP 9.0-10.5 and LR 7.0-8.0. Figs. 3.26 and 3.27 show the results from two of the preparations.

Properties of VPL cells

Although the primary goal of this study was to study the dynamics of knee joint cells in VPL, there was also an opportunity to make observations on the properties of other cells in VPL that were found in the course of the experiments. In fact, knee joint cells proved to be rather difficult to find out of the wide variety of responses in VPL and much of the time was spent observing cells not responsive to joint stimulation.

A cell was classified into one of four modalities according to its adequate stimulus: hair, touch, deep, and knee joint. Joint cells other than knee joint were classified as deep cells. No cell was found that responded to more than one stimulus modality, but this is a weak statement because a cell that possibly responded to stimulation of both the hairs and the skin would be classified as hair-sensitive since it was difficult to stimulate the skin without also stimulating the hairs. In addition the cells were classi-

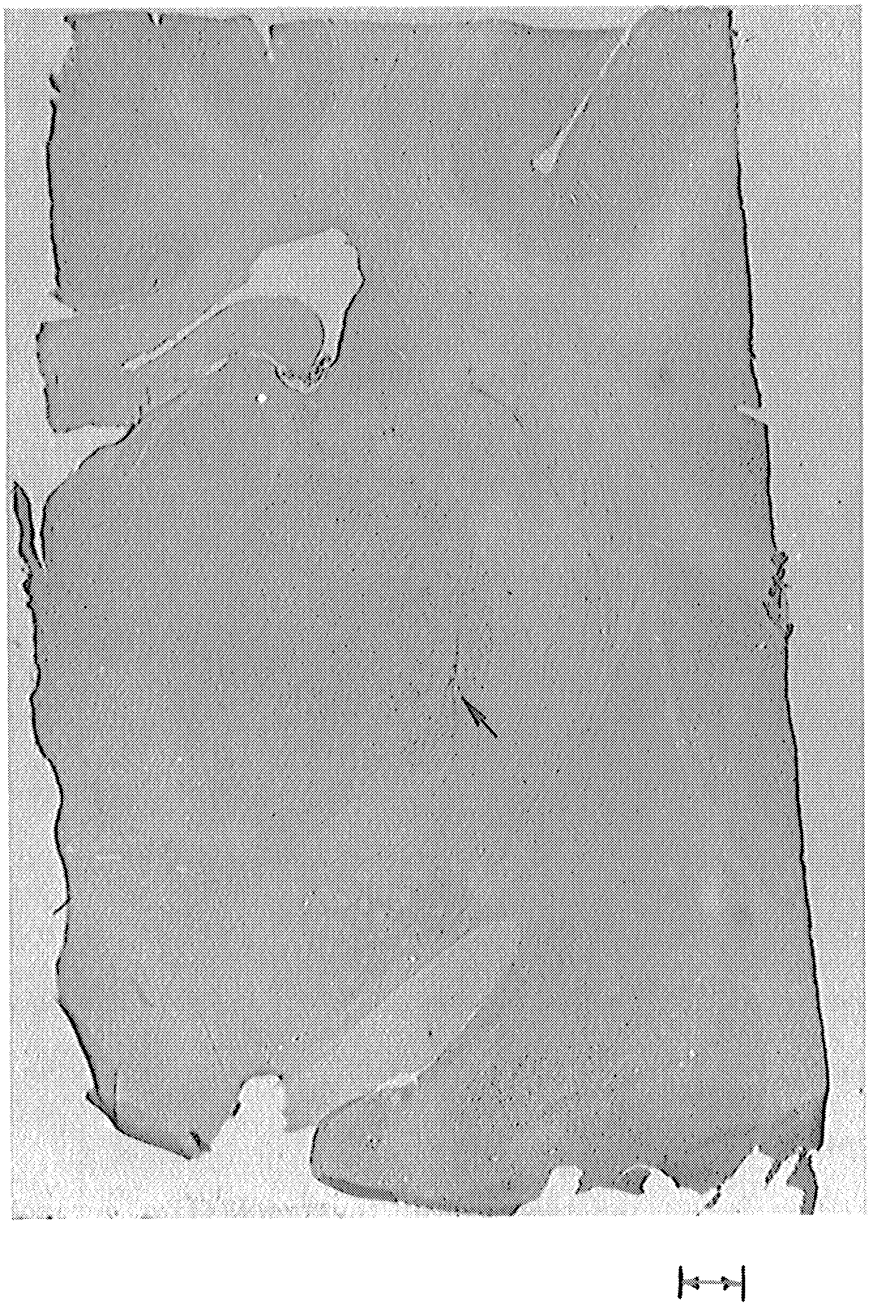

Figure 3.26. Histological section of cat C8. This is a coronal section of the right hemisphere through the diencephalon. An electrode tract and a small lesion are visible in the lateral regions of the VPL at the arrow. This section is at approximately the level of AP 9.9. The calibration mark represents 1 mm. The stain is cresyl violet.

Figure 3.27. Histological section of cat C12. This is a coronal section of the right hemisphere through the diencephalon. An electrode tract is visible passing through the lateral portion of the VPL. This section is approximately at the level of AP 9.2. The calibration mark represents 1 mm. The stain is cresyl violet.

fied by the size of their receptive field. Table 3.1 shows a chart of the cells classified in this manner and separated into acute and semi-chronic preparations. No significant differences were found in the sample of the receptive field properties between the two kinds of preparations. Out of the 387 cells whose receptive fields were identified, 44% were hair, 18% touch, and 38% deep.

Although histological verification was not done on all of the animals, the presence of cells that could be stimulated by gentle cutaneous stimulation and usually located with a distinct topographical relation to each other was taken to be a reliable indicator that the microelectrode was in the VPL. Most of the cells showed an orderly topographical organization as the microelectrode was moved about. In many cases the topographical map described by Mountcastle and Henneman (1949) was used to move the microelectrode to the area with cells sensitive to hind limb stimulation. No dorsal-ventral segregation of deep and tactile cells was observed. The dorsal and ventral limits of VPL were usually clearly delimited by the presence of high spontaneous activity. Forelimb cells were located medial and caudal in VPL while hindlimb cells were lateral and rostral.

A small percentage of cells were found that deviated from the observations made above. Some of these cells did not obey the general topographical organization. Six hair-sensitive cells were observed that had a bilateral receptive field. The sensitivity on the ipsilateral field was weaker than on the contralateral field, but there was no question that the cell responded to ipsilateral

Table of receptive field size and modality

of VPL neurons in acute and semi-chronic preparations

Anesthetized preparations

	Modality				
RF size	Hair	Touch	Deep	Bilateral	Knee joint
Small	18	13	5		Tonic 1
Medium	22	10	16		Phasic 19
Large	9	2	1	1	
Total	49	25	22	1	20

Unanesthetized preparations

	Modality				
RF size	Hair	Touch	Deep	Bilateral	Knee joint
Small	44	33	39		Tonic 6
Medium	38	9	42		Phasic 16
Large	32	3	3	5	
Total	114	45	84	5	22

Table 3.1

stimulation.

DISCUSSION

One reason for determining the frequency response of a sensory system is to provide information about the ability of the organism to respond to dynamic stimulation. As will be seen in the following chapter, it can also give insights into the properties of the neural communication system. The results presented above show that at the level of the thalamus the cat somatosensory system can relay information about movements of the knee joint. Unfortunately because of the small sample of slowly adapting cells found, the study does not shed much light on the dynamic properties of these neurons. The following discussion is an interpretation of the results in relation to other studies of sensory systems and an examination of the functional implications of the findings.

Rapidly adapting response

The frequency response curves for the phasic joint cells showed that the thalamic afferents were sensitive to the higher derivatives of the position of the joint. All units exhibited a high pass filter characteristic in the gain curve with a concomitant leading phase angle that gradually decreased at higher frequencies. This decrease in the phase lead was seen in all of the cycle histogram data as a gradual lag in the peak of the phase-locked response (Fig. 3.9) as well as in all of the frequency response curves. Only part of this decrease could be attributed to a conduction delay between the application of the stimulus to the joint receptors and the response in VPL. The additional phase lag could be indicative of

a low pass filtering effect somewhere in the communication link. In the next chapter it will be seen that this filtering is taking place in the thalamus.

The steep slope of the gain curves is similar to the frequency response of many mechanoreceptors. In particular the primary muscle spindle (Matthews and Stein, 1969; Poppele and Bowman, 1970), cockroach tactile spine (Pringle and Wilson, 1952; Chapman and Smith, 1963; French et al., 1972), and phasic joint receptors (Farias, 1973) have dynamic response curves similar to the ones reported here. The increased gain at higher frequencies means that the phasic neurons are very sensitive to even the slightest rapid movement of the joint but are relatively insensitive to even large slow movements. This feature of the phasic units has a natural adaptive value in warning the animal about sudden movements of the limb. The phasic cells are believed to be afferents in the dorsal column system (see Chapter IV). These results can support the hypothesis set forward by Wall (1970a, 1970b) that the dorsal column system serves as an alarm to gate the central nervous system to signals traveling on other channels.

In the gracile nucleus Williams et al. (1973) found two classes of phasic knee joint cells: one was more common and could be modeled as an acceleration-sensitive cell between input frequencies of 1 -7 Hz and the other could be modeled as a velocity-sensitive cell in that bandwidth. In the VPL there was no such clear differentiation of cell responses. Despite the presence of many common characteristics the response curves from one cell to another exhibited deviations between models that could be termed acceleration-

sensitive and velocity-sensitive, and there was sufficient variability to preclude fitting all of the data with a single tranfer function.

On the other hand, one of the striking aspects of the data was the similarity in the general behavior. From one cell to another the similarities of the response profiles far outnumber the differences. An attempt was made to obtain an estimate of the population response of the VPL phasic cells. The assumptions implicit in calculating the population response from the single unit data are the following: that a large number of thalamic joint cells impinge upon a single cortical joint cell, that the synaptic weighting factor for each synapse is equal, that the cell integrates EPSP's linearly, and the critical one that for a cortical cell sensitive to, say, extension the thalamic cells that respond upon extension of the limb are excitatory and the thalamic cells sensitive to flexion are inhibitory. There is some indirect evidence that the latter assumption is true in the observation that the percentage of bidirectional cells decreases as the signal progresses from the periphery up the central nervous system. If the interconnections between joint cells were random then one would expect an increase in the number of bidirectional cells at higher levels. Fig 3.28 shows the results of normalizing and averaging together the frequency response curves obtained from the phasic cells to get an estimate of the dynamic response of the depolarization potential of a cortical joint cell, i.e. it estimates the dynamic signal transmitted by the population of VPL joint cells. The variation in responses is evident in the standard deviation while the large number of cells averaged together means that the best estimate of

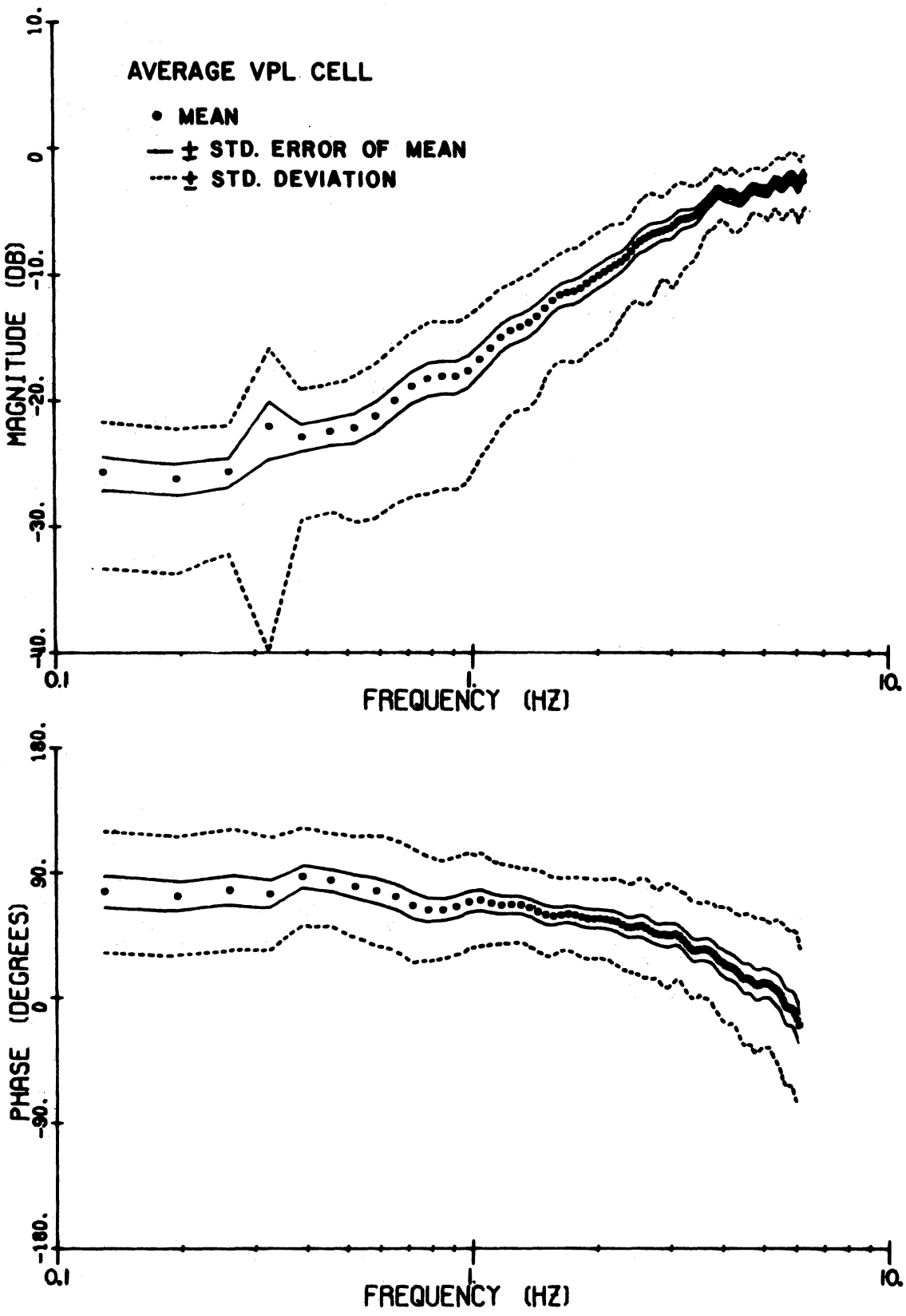

Figure 3.28. Average frequency response of 20 VPL phasic knee joint cells. All individual magnitude curves were normalized to the maximum value before averaging. The solid curves represent the standard error of the mean, assuming a Gaussian distribution of response variations. The dashed curves represent the standard deviation.

the mean has little standard error, assuming a Gaussian distribution of responses.

Fig. 3.29 shows that this "average" VPL cell is best described by a model of the form (3.11), i.e. it can convey the velocity of the input stimulus between .1 and 7. Hz. This does not mean that the nervous system necessarily uses this information to monitor the velocity of the joint, but based on these results the ability to do so in the population response is present at the cortical level. Further studies at that level would be needed to confirm this. There does not seem to be any evidence at the thalamic level for narrow band filters or tuning curves such as found in the visual system (Campbell and Robson, 1968) or the auditory system Kiang, 1965). Most likely, though, the nervous system uses the information in these channels to detect movements, especially rapid movements, of the limb.

The phase-locking response exhibited by most of the phasic cells is evidence of nonlinear behavior. This characteristic has been reported to some extent in most sensory receptors that have been stimulated by cyclic waveforms, particularly at high frequencies (Talbot et al., 1968; Spekreijse, 1969; Poppele and Bowman, 1970; Lavine, 1971; French et al., 1972; Farias, 1973). Rescigno et al. (1970) have shown that a "leaky integrator" model of a neuron will display phase-locked behavior when periodic stimuli are applied. The model consists of an RC network for integrating a depolarization current and a threshold detector that emits a pulse and resets the integrator. This is a reasonable model of the encoding properties of nerve cells, and it will be shown in

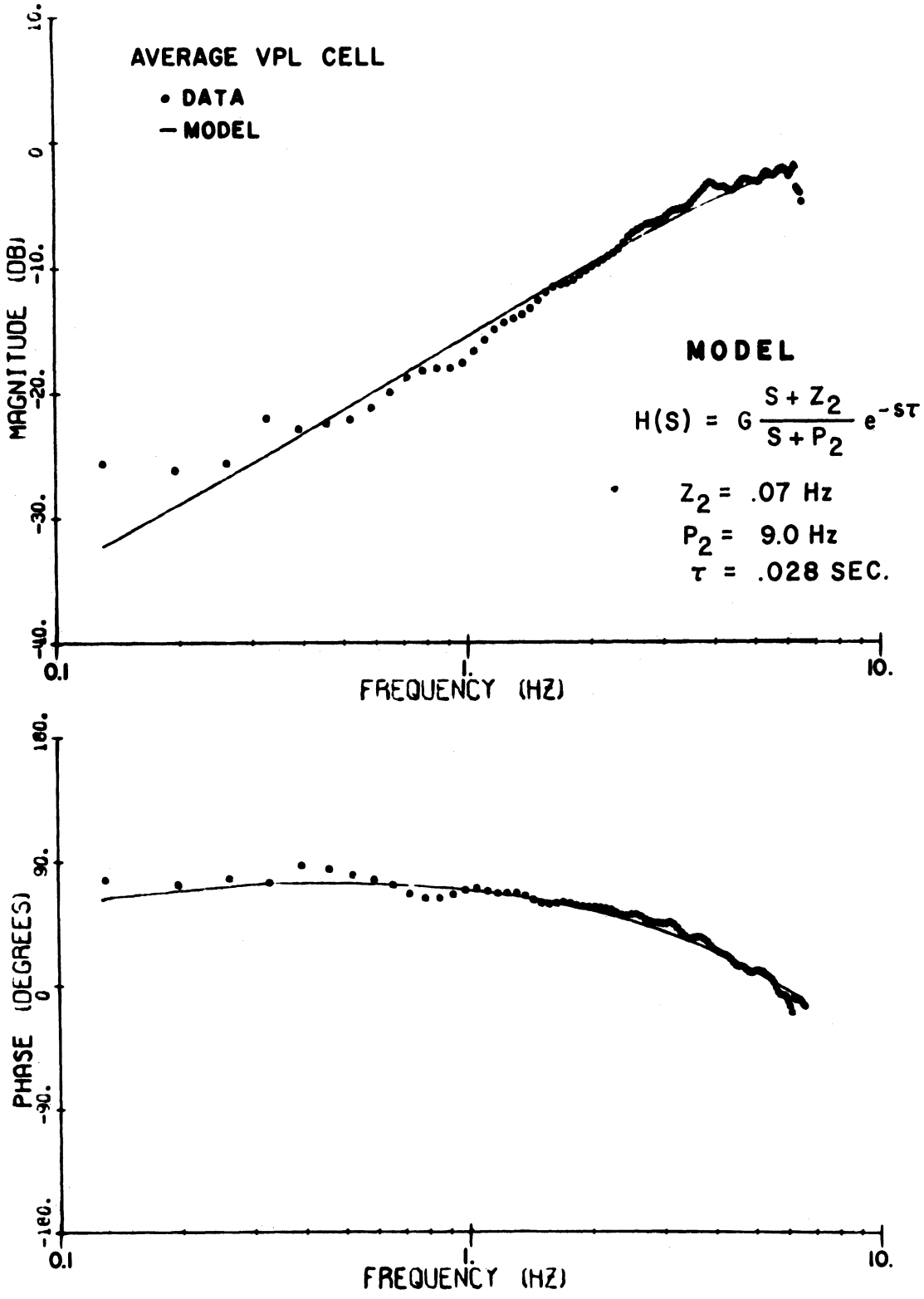

Figure 3.29. Average frequency response curve fit by a linear transfer function. The data points are taken from figure 3.28. The solid curve is a model with transfer function and optimized parameters as shown. See text for details.

the next chapter that the encoder element of the thalamic neurons can be described by a leaky integrator.

As the neural signal in the visual system is transmitted from the retina to the cortex, the cells at each succeeding level become more and more specialized and require successively more specific stimuli to excite them. The only evidence of specialization of this sort in the results reported here is a smaller percentage of VPL rapidly adapting cells with a bidirectional response as compared with the phasic receptors and joint cells at the gracile level (Williams et al., 1973; Farias, 1973). Cells with a bidirectional response will be unable to code the direction of movement. By a process similar to lateral inhibition the nervous system can eliminate a bidirectional response (Bayly et al., 1971). This appears to be the case in the joint receptor system, and most thalamic cells can convey direction of movement.

Within the range of input amplitudes used in this study, the describing function at the thalamic level is approximately linear (Fig. 3.18, 3.19). This linear behavior for the fundamental response provides some more justification for the use of describing function analysis. There is some evidence of a threshold non-linearity for very small $\Delta\Theta$ and a saturation effect for large $\Delta\Theta(>10°)$. These nonlinearities are also present at the receptor level for the tonic joint receptors (McCall et al., 1973). However, the gain is less sensitive to bias angle and excursion angle at the thalamic level than at the gracile level (Williams et al., 1973) indicating that the spatial and temporal integration may tend to cancel out nonlinearities.

Independence of response to condition of the preparation

Generally the dynamic response of the rapidly adapting cells in unanesthetized and anesthetized animals was very similar, which indicated that the dynamic response was relatively resistant to anesthetic agents. This was a somewhat surprising result given the findings of Angel (1969) who showed that anesthetic had a depressant effect at the thalamic level on the response to the second of a pair of pulses applied to the periphery. However, the overall level of spontaneous activity of the cells in anesthetized animals was decreased relative to the activity in chronic animals as seen in Fig. 3.16, which confirmed the findings of many investigators working with chronic preparations (Evarts, 1963; Hayward et al., 1964; Baker, 1971). Apparently, the transient component of the response is unaltered by anesthetic agents at this level while the static phase is suppressed. Similarly Fig. 3.17 shows that the phasic response is similar in awake and sleeping preparations. This is further evidence of the secure synaptic relations of the cells in VPL whose response is not dependent upon the spontaneous activity. It indicates that the spontaneous discharge may be unimportant in the transmission of dynamic inputs.

On the other hand Appendix E shows that for a cell with a Poisson or random carrier the dynamic signal-to-noise ratio is directly proportional to the mean rate of discharge of the cell. Thus, the higher discharge rates seen in the unanesthetized animals could indicate that the central nervous system uses this mechanism to enhance the signal transmission in the awake animal and to suppress these signals in the sleeping or anesthetized

animal. However, this should be reflected in a larger coherence function in unanesthetized animals; and no such difference was observed. So the conjecture remains unproved. The nature of the tonic discharge was, however, altered considerably as seen in Fig. 3.25. The tendency of the cells to respond with bursts of spikes in the anesthetized state is consistent with observations made by others in barbiturate animals (Anderson et al., 1964a; Nakahama et al., 1966; Baker, 1971).

Slowly adapting response

The most disappointing aspect of this research was the paucity of slowly adapting knee joint cells that could be found. By contrast, 26% of the cells in the unanesthetized, paralyzed monkey VPL were tonic joint cells in the study by Mountcastle et al. (1963). Even in the unanesthetized preparations a very small percentage of the cells that were isolated were tonic knee joint cells, though there were more tonic cells found in the chronic animals than in the acute animals. Furthermore, the tonic cells that were identified seemed to be more difficult to hold for long periods of time. As a result only one cell was held long enough to complete a set of the experimental paradigm. There are several possible explanations for the differences in the results described here and in the study of Mountcastle et al. (1963). One, there are simply fewer joint cells in the cat knee joint than in the monkey knee joint (Skoglund, pers. comm. by Mountcastle). Given the different uses that the two species make of their limbs, this is not surprising. Two, the tonic cells may be smaller and more difficult to find than the phasic neurons. There is some support for this in the observation

that the tonic cells were harder to hold for long periods of time. Three, the tonic cells may project to a different region of the nucleus. In the early experiments the VPL was searched in a uniform manner. Since most of the cells followed the topographical arrangement, the later experiements concentrated on finding the knee joint area in the rostral-lateral pole of VPL. It is possible, then, that the later experiments missed knee joint cells in other regions of VPL. However, this does not seem to be a likely possibility given the topographical organization for all other modalities. Four, Mountcastle et al. (1963) studied the static curve of joint cells sensitive to position of any of the joints whereas only knee joint cells were sought in this study. By limiting the sample to a single joint, the possible sample size was severely limited.

There is no question that there are more slowly adapting knee joint receptors than rapidly adapting ones. At the thalamic level, though, the relative proportion of slowly and rapidly adapting joint neurons seems to be the reverse of the situation at the periphery. Mountcastle (1962) has also observed this apparent transformation in the proportion of phasic to tonic cells as the neural signal propagates from the periphery to the central nervous system. One possibility for this transformation is that the central neurons utilize the excitatory and inhibitory synapses to function like differential amplifiers thereby becoming sensitive only to transient changes in the stimulus. This is a reasonable conjecture if the spontaneous activity can be considered to be noise. However, in the tonic receptors the tonic rate is presumably coding the absolute joint angle. Furthermore, the response of the phasic VPL cells is much

more sensitive to the dynamics of the input, e.g. the gain curve is 30 db/decade, than the tonic receptors, which have a 5 db/decade slope in the gain curve. If the tonic receptors were being transformed to phasic afferents by synaptic inhibitory processes, the dynamic phase of the response should be similar. Since it is not, then this does not appear to be taking place in the joint afferent system. It is known that joint afferents ascend in the dorsal spinocerebellar tracts to the cerebellar cortex (Lindström and Takata, 1972). Until the pathway for the slowly adapting joint cells to the cerebral cortex is identified, this will remain a difficult question to resolve.

The frequency response of the tonic VPL cells is similar in character to the response of the receptors. The active angle of the unit (35°) is smaller than the average active angle (73°) of monkey joint cells and the static curve does seem to follow the power law though the exponent is larger (1.0 vs .7) than for the monkey joints (Mountcastle et al., 1963). These observations must be tempered, though, by sample size.

The overall population of cells identified in the VPL is very much like the findings of Baker (1971) in a similar preparation. The small number of cells with bilateral, large, and discontinuous receptive fields agrees with observations made in chloralose animals (Harris, 1970; Jabbur et al., 1972). The spinothalamic system is believed to mediate responses of this type. These findings indicate that a small component of this system probably projects to VPL.

CHAPTER IV

DYNAMIC TRANSFER CHARACTERISTICS OF THALAMIC SENSORY NEURONS

INTRODUCTION

All sensory information from peripheral receptors is conducted to the sensory cortex through several synaptic relays. It is believed that these relays can perform complex spatial and temporal processing of the afferent information. By comparing the characteristics of the afferent signal to a higher order neuron with the efferent signal transmitted by the neuron, it is possible to determine the transformations imposed by the neuron upon the signal. The transformations related to the spatial properties of the higher order cells, e.g. topography and modality of receptive fields, have been studied in many sensory systems. Much less is known about the transformations of the afferent impulse trains in the temporal domain.

Each neuron can be considered to be a communication chain: it receives inputs from many dendritic and somatic synapses, demodulates and sums the excitatory and inhibitory postsynaptic potentials, and re-encodes the signal as a pulse train that is transmitted out the axon. In order to study the temporal processing properties of neurons, previous investigators have applied precise signals or monitored the physiological signal at one link in the chain and recorded the neural signal at another link further along the chain. In recent years the dynamic properties of these neural links have been analyzed by studying the properties of these elements in the frequency domain (Terzuolo, 1969). The frog neuromuscular junction

(Landau and Lass, 1973), mammalian lateral geniculate body (Maffei and Rizzolatti, 1967), Limulus photoreceptor (Dodge et al., 1970), and crayfish stretch receptor (Terzuolo and Bayly, 1968) have been studied by the application of systems analysis techniques. The approach in this study is similar to that of Maffei and Rizzolatti (1967) who applied sinusoidally-varying intensities of light to the retina of the cat and recorded the response of cells in the lateral geniculate body. The response at the output of the lateral geniculate was compared with the input to the lateral geniculate, which was assumed to be the response of the retinal ganglion cells, to identical stimuli found in a previous experiment (Hughes and Maffei, 1965). The transfer property of the lateral geniculate was found to have the characteristics of a low pass filter.

In this chapter the filtering characteristics of thalamic cells in the somatosensory joint receptor system will be found by comparing the frequency response of cells in the VPL (see Chapter III) with the response of cells in the gracile nucleus under identical stimulation conditions (Williams et al., 1973). The major result is that a low pass filtering effect is also found in this system. First some theoretical considerations of neural communication will be discussed.

THEORY

The statistical analysis of neuronal pulse trains has been a subject of increasing interest in recent years due to the development of small digital computers capable of on-line processing (Moore et al.,

1966), If each impulse is treated as a discrete event, a pulse train can be considered to be a stochastic point process (Perkel et al., 1967; Lewis, 1972). Renewal processes, in which the intervals between events are independent and identically distributed random variables, are a subject of particular interest, both because they are mathematically tractable and because they are found frequently in nature. A special case of a renewal process is the Poisson process in which the intervals are distributed exponentially. Let $f_1(t)$ be the probability density function (pdf) for the non-negative random variable t corresponding to interspike intervals. For a Poisson process

$$f_1(t) = \lambda\, e^{-\lambda t} \qquad t \geq 0 \qquad (4.1)$$

where λ is the mean rate. Let $f_2(t)$ be the pdf for the random variable derived from the above Poisson process by considering an event to occur at every other event in the Poisson stream. Since the random variables are independent, the pdf for the sum of two successive intervals is given by the convolution of the individual pdf's. By induction the nth order pdf is given by n - 1 successive convolutions of $f_1(t)$ and is the well-known gamma distribution.

$$f_n(t) = \int_0^\infty f_1(u) f_{n-1}(t - u)\, du \qquad (4.2)$$

$$= \frac{\lambda(\lambda t)^{n-1}\, e^{-\lambda t}}{(n - 1)!} \qquad (4.3)$$

As $n \to \infty$, $f_n(t)$ approaches a Gaussian distribution. The mean m and standard deviation σ of the distribution are

$$m = n/\lambda \tag{4.4}$$

$$\sigma = \sqrt{n}/\lambda \tag{4.5}$$

The ratio of the standard deviation to the mean is known as the coefficient of variation CV; and it measures the amount of regularity in the point process, very regular processes have small CV. For the gamma distribution

$$CV = 1/\sqrt{n} \tag{4.6}$$

Thus, $\{f_i(t)\}$ represents a family of pdf's ranging from the irregular Poisson (n = 1, CV = 1) to a very regular Gaussian (n large, CV small).

The superposition of point processes is an important mechanism for consideration in neurophysiology. Fig. 4.1 shows a simple case of the superposition of 3 point processes. The pooled output is a series of events in which an event occurs at time t if and only if an event occurs at t in one of the p component processes. The fundamental result was shown by Cox and Smith (1954) and states, briefly, that as p gets large, the pooled output locally approaches the characteristics of a Poisson process, more or less regardless of the form of the component processes, provided that they are mutually independent.

The neurophysiological analogy is clear. If many afferents converge upon a higher order cell and each presynaptic impulse gives rise to a postsynaptic pulse, then the postsynaptic pulse train will be a Poisson process provided that the afferent pulses on different axons are independent. If it takes n presynaptic spikes to bring the postsynaptic potential to threshold, then the output pulse train

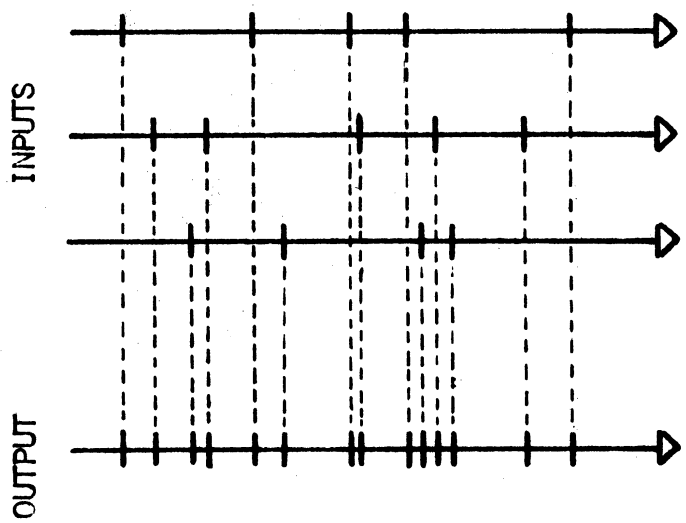

Figure 4.1. Superposition of three point processes.

will be described by an nth order gamma distribution. This model is applicable to a neuron that simply counts the number of presynaptic spikes with no decay in the EPSP's and a constant threshold. If each EPSP has an exponential decay with time constant τ_m, then the model is equivalent to a leaky integrator with a constant threshold. If τ_m is large with respect to the average interspike interval, then the output will approach the form of (4.3). Otherwise no general solution is available. Figure 4.2 shows these simplified models of a higher-order neuron. Some of these concepts are discussed by Stein (1967) and Stein et al. (1972). The point of this discussion is to point out how Poisson, gamma, and Gaussian density functions may arise in the central nervous system.

Many peripheral receptors discharge at a very steady rate (small coefficient of variation) when stimulated with a constant stimulus. Muscle spindles (Matthews and Stein, 1969), slowly adapting knee joint receptors (McCall et al., 1973), type I and II mechanoreceptors in hairy skin (Petit and Burgess, 1968), and vestibular receptors (Goldberg and Fernandez, 1971) all show this general characteristic. This type of discharge will be termed integral pulse frequency modulation (IPFM) since it can be generated by a linear transducer and integrator coupled to a threshold detector that resets the integrator. In striking contrast to the IPFM nature of the receptors, the spontaneous response of thalamic and other higher-order cells is very irregular (Werner and Mountcastle, 1963; Fig. 3.25). Higher-order cells in other sensory systems also show a random nature that can often be characterized as Poisson or gamma processes (Wallφe, 1968;

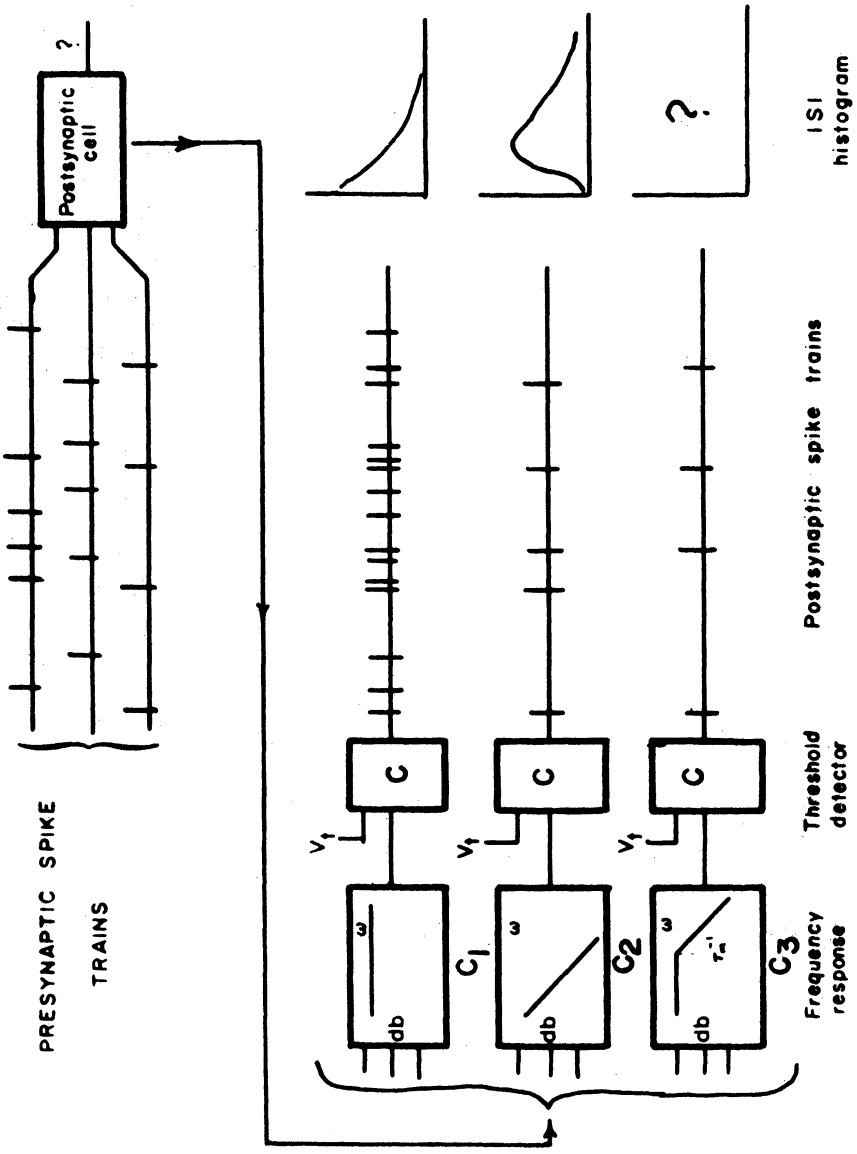

Figure 4.2. Schematic diagram of three possible models of a postsynaptic cell. V_t is the threshold voltage for initiating an action potential. C is a comparator that emits a pulse whenever the two signals on its input are equal. For illustrative purposes the cell is shown with three presynaptic pulse trains converging on it. C_1 is a cell that fires a spike for every presynaptic spike and has an interspike interval histogram that approaches an exponential as the number of presynaptic fibers increase. C_2 is a cell that fires a spike for every third presynaptic spike; its interval histogram approaches a third order gamma function. C_3 is a cell with a leaky integrator with time constant τ_m.

Škavřil et al., 1971). This is in accord with the simple models generated by the superposition of point processes discussed above. In Fig. 4.3 the discharge of a slowly adapting knee joint receptor recorded at the medial articular nerve is compared with the discharge of a cell in the VPL sensitive to knee joint stimulation. Notice the steady discharge at the receptor level that is modulated by the sinusoidal input. In contrast the thalamic discharge shows much more variability. Fig. 3.25 gives evidence that the response of the slowly adapting joint cells in VPL of unanesthetized cats is Poisson in nature. Poggio and Viernstein (1964), however, found that not all of the interspike interval histograms of the tonic cells in VPL of the macaque could be classified as exponential or gamma in character. Furthermore, they found that the intervals were not independently distributed.

When time-varying stimuli are applied, the characteristics of the discharge are most conveniently studied in the frequency domain. The power spectral density for frequency modulated pulse trains has been derived both for the case of a regular carrier (IPFM) (Bayly, 1968) and for the case of a random carrier (Knox, 1970; Gestri, 1971). Appendix E contains a new derivation for the power spectrum of a frequency modulated Poisson point process. For the IPFM process modulated by a sinusoidal signal, the spectrum of the pulse train consists of a DC component, a sinusoidal component at the modulation frequency f_m, components at the carrier rate λ_o and at multiples of the carrier rate, and infinite sidebands about the carrier frequency and its multiples, as shown in Fig. 4.4a

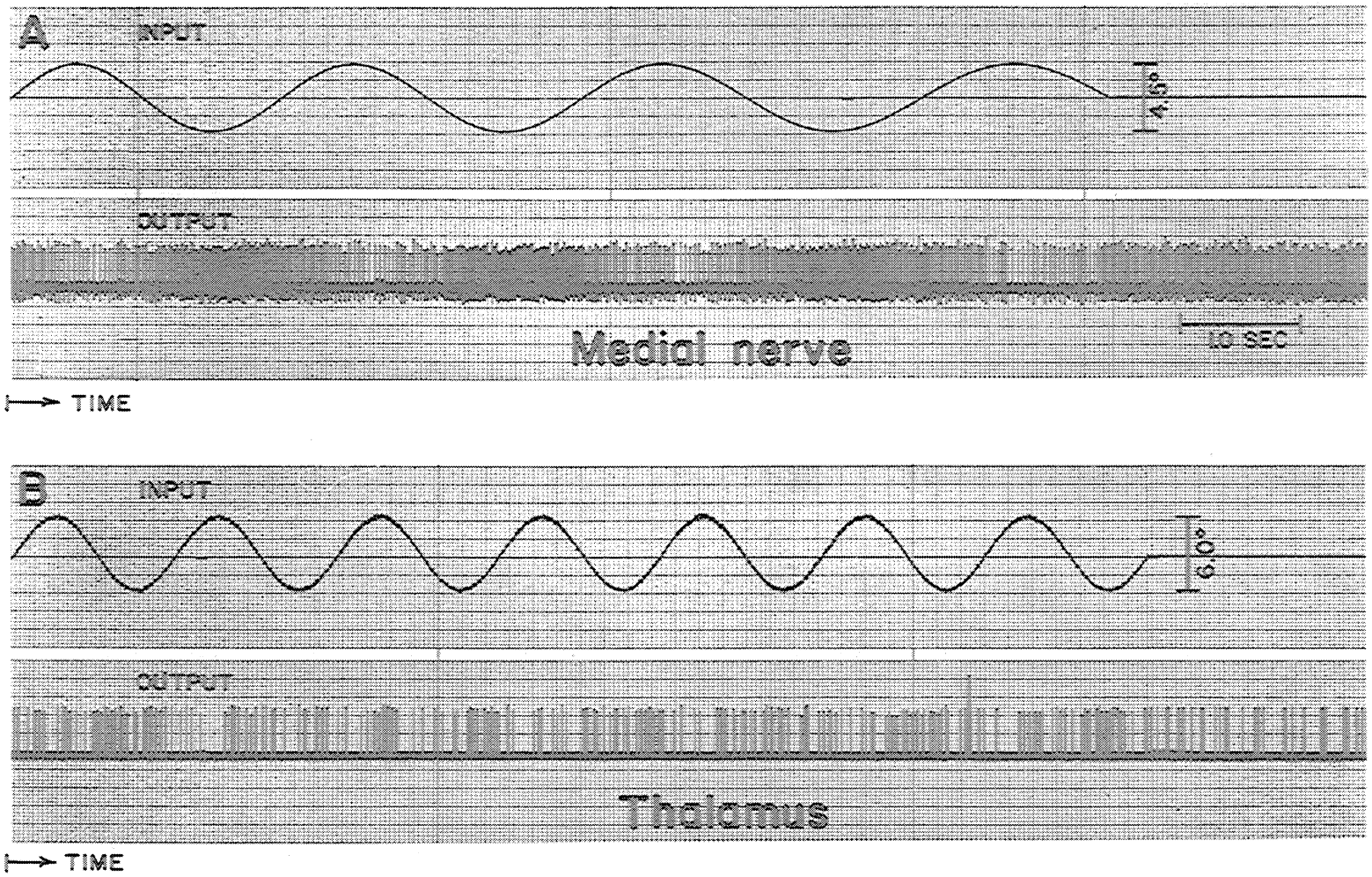

Figure 4.3. Examples of the response of knee joint afferents at two different levels of the nervous system. A). Response of a typical slowly adapting knee joint receptor recorded by silver wire electordes on the medial articular nerve. Courtesy M.A.C. Farias. B). Response of a slowly adapting thalamic knee joint afferent (C10-6) recorded by a microelectrode in the VPL to .74 Hz stimulus. Pulses in B) are the output of the discriminator used to separate out single units.

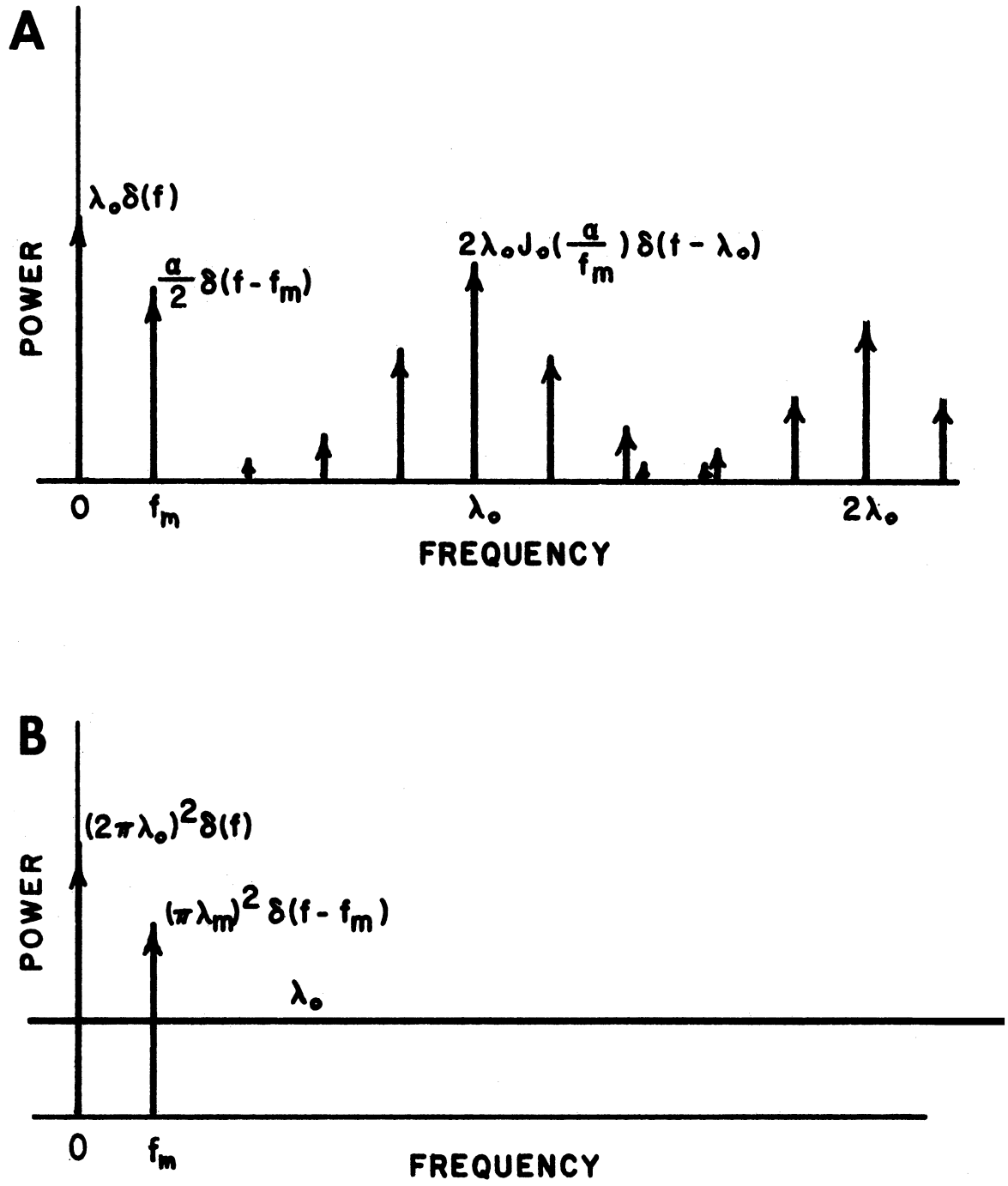

Figure 4.4. Power spectral densities for frequency modulated pulse trains with a regular and random carrier. A). Carrier is a constant frequency λ_o and is modulated with a sinusoidal waveform of frequency f_m and depth of modulation α. B). Carrier is a random Poisson point process and is modulated with a sinusoidal waveform of frequency f_m. The average pulse rate is λ_o. Impulses are assumed to be Dirac-delta functions. A) is adapted from Bayly (1968); B) from Knox (1970) and Appendix E.

$$S(f) = \lambda_o \delta(f) + \frac{\alpha}{2} \delta(|f| - f_m) + 2\lambda_o \sum_{k=1}^{\infty} \sum_{n=-\infty}^{\infty} J_n\left(\frac{k\alpha}{f_m}\right) \left(1 + \frac{nf_m}{k\lambda_o}\right) \delta(|f| - k\lambda_o + nf_m) \quad (4.7)$$

where $\alpha = \lambda_m/\lambda_o$ is the depth of modulation and J_n is a Bessel function of first kind. The signal component can be recovered by low pass filtering if the depth of modulation and modulation frequency are sufficiently small. However sidebands will distort the signal if, for example, f_m becomes too large with respect to λ_o. On the other hand the spectra for a modulated Poisson point process has a DC component, a component at f_m, and noise components with a constant density as shown in Fig. 4.4b (Knox, 1970; Appendix E).

$$S(f) = \lambda_o + (2\pi \lambda_o)^2 \delta(f) + (\pi \lambda_m)^2 \delta(|f| - f_m) \quad (4.8)$$

This signal will always be corrupted by a constant noise power, but unlike the IPFM spectra there are no signal-dependent sidebands. Thus, the randomness of the carrier has made the system impervious to the characteristics of the input signal. The signal can always be demodulated in the random case by low pass filtering provided the depth of modulation is sufficient. Appendix F contains a more general discussion of frequency domain analysis of renewal processes. The spectra for a gamma process can be found, but a general expression for the spectra of a modulated gamma process is not yet known. Evidence will now be given that the VPL cells may demodulate the afferent signals by low pass filtering.

METHODS

The data presented here were obtained from the results of two experiments. The data from the gracile nucleus were recorded from 36

cats in the study of Williams et al. (1973), and the thalamic data were obtained from the 37 cats in the study described in Chapter III. The surgery, recording techniques, and data analysis have been described earlier. The same experimental paradigms were applied in both of the experiments so that the results could be comparable. Since no slowly adapting joint cells were found in the gracile nucleus, the results described here are limited only to the rapidly adapting responses at each level. All of the gracile data were obtained from cats anesthetized with sodium pentobarbital whereas the thalamic data were obtained from both anesthetized and unanesthetized cats.

RESULTS

The describing functions for the rapidly adapting knee joint cells recorded at the level of the gracile nucleus are qualitatively very similar to the responses for the rapidly adapting knee joint cells recorded at the thalamus. Fig. 4.5 shows the response of an acceleration-sensitive joint cell in the gracile nucleus from the study of Williams et al. (1973). The majority (54/59) of joint cells at the gracile nucleus showed a similar response. The gain curve has the same steep slope (≃30 db/decade between 1 - 7 Hz) as the thalamic cells described in Chapter III. The phase curve also begins with a prominent lead but does not have the marked decrease at higher frequencies that is present in the thalamic data, e.g. Fig. 3.11. In this respect the unit shown in Fig. 4.5 lies at one extreme in that most gracile cells did exhibit at least a gradual phase lag at higher frequencies that was larger than the conduction delay would

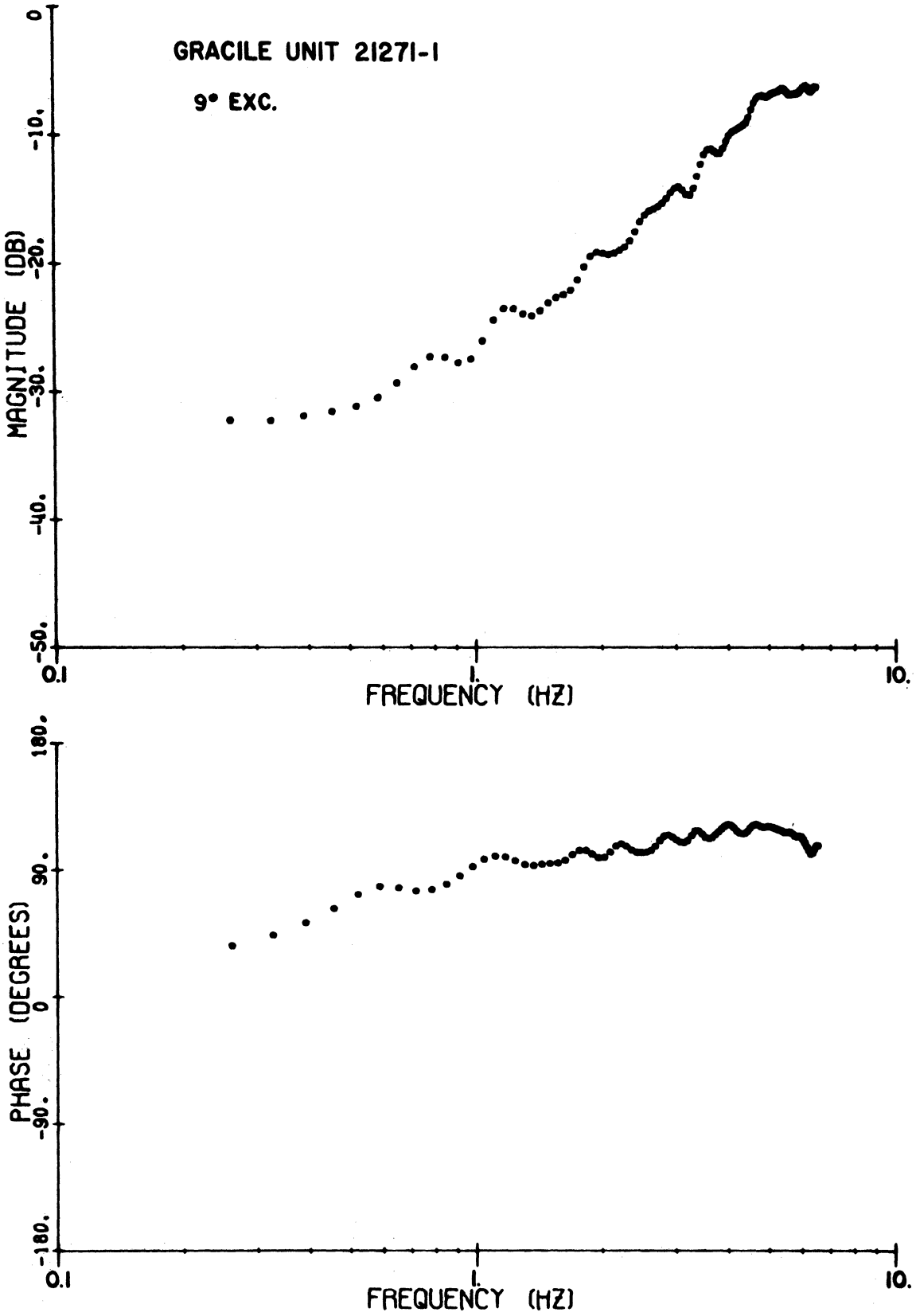

Figure 4.5. Describing function for a typical gracile joint cell. db represents 8.5 pps/deg. (From Williams et al., 1973).

predict. However, the phase lag observed in the thalamic cells was invariably larger than in the gracile cells.

It is known that fibers from the dorsal column nuclei project primarily to the VPL (Boivie, 1971b). Given the similarity in the response patterns of the gracile joint cells and the rapidly adapting VPL joint cells, a critical assumption was made that these gracile cells synapse onto the VPL cells in which a similar response was found. If the cells in VPL are indeed modality specific (Poggio and Mountcastle, 1963), then the knee joint cells in VPL must receive inputs from knee joint afferents of the gracile nucleus. The dynamic characteristic of the signal relayed to VPL by these knee joint afferents can be obtained by averaging the describing functions for all of the gracile joint cells, just as was done for VPL cells in Fig. 3.28. The average gracile knee joint cell response is shown in Fig. 4.6. This is assumed to represent the characteristics of the input signal to the VPL joint cells and includes an estimate of the spatial integrating properties of the cell.

When the characteristics of an average VPL joint cell were compared with an average gracile joint cell (fig. 3.28 and Fig. 4.6), it was even more apparent that the responses were quite similar since the averaging procedure canceled out individual differences between cells. The frequency response curves were, however, not exactly alike. If the VPL functioned as a passive relay in the temporal domain, one would expect the dynamic transfer function of the VPL to be the same as that of the gracile nucleus. Any differences in the frequency response curves can be attributed to filtering properties of the VPL cell itself.

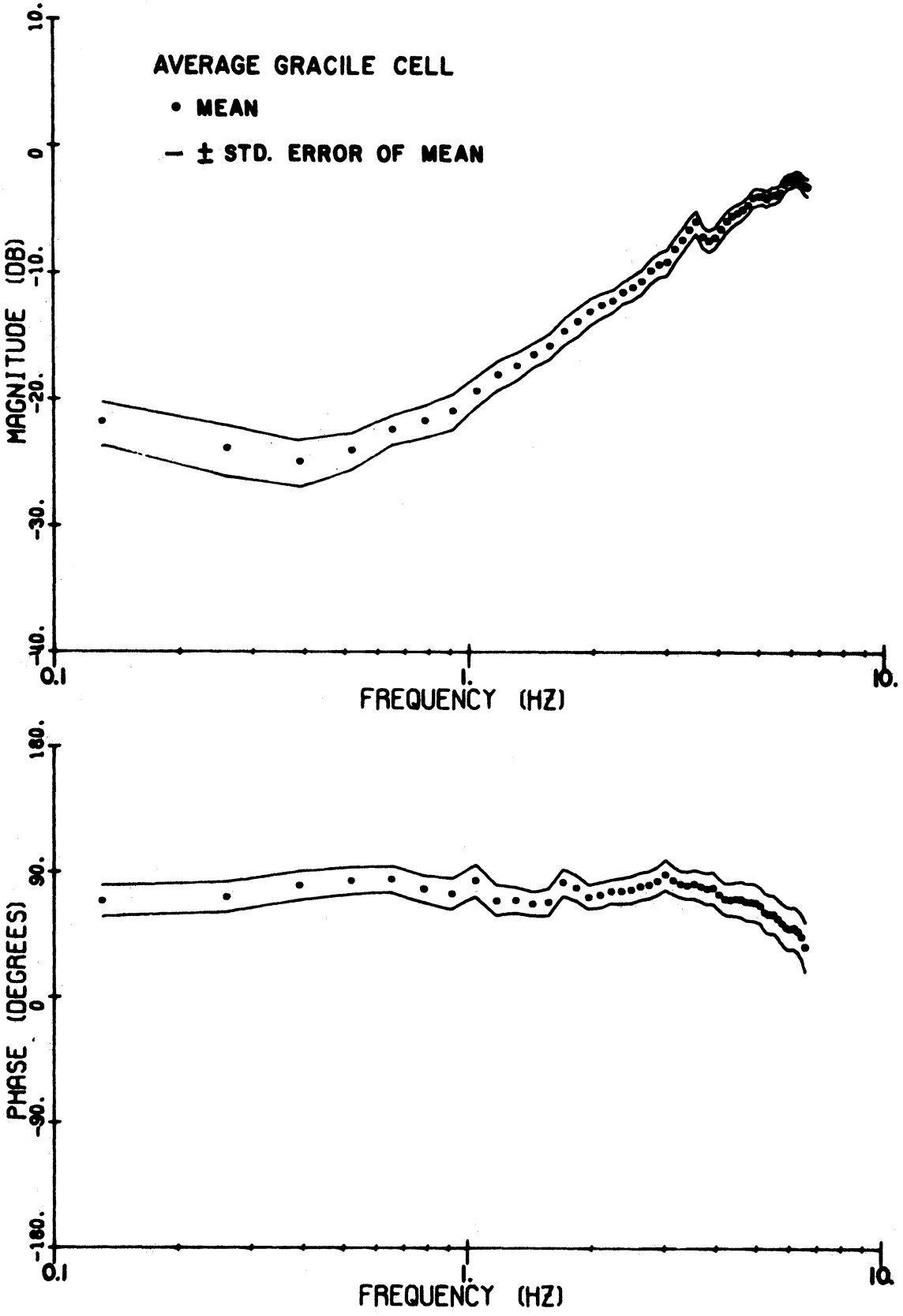

Figure 4.6. Average frequency response of 27 gracile knee joint cells. Data was taken from the study of Williams et al. (1973) and s averaged with the same procedure as described for Fig. 3.28.

A block diagram of the system is given in Fig. 4.7. The transfer function of the signal from the receptor to the level of the gracile nucleus is designated as $G(j\omega)$. The overall transfer characteristic of the signal to the level of the VPL is $H(j\omega)$. The transfer function imposed by the VPL cell itself is $V(j\omega)$. If the system is linear for the range of input amplitudes used, then

$$H(j\omega) = G(j\omega)\, V(j\omega) \tag{4.9}$$

$$V(j\omega) = H(j\omega)/G(j\omega) \tag{4.10}$$

The results of calculating (4.10) are shown in Fig. 4.8. The curve labeled "model" is the optimized fit of the data points with a linear transfer function of the form

$$V(s) = K \frac{e^{-s\tau}}{(s + p)} \tag{4.11}$$

Thus the transfer properties of the VPL cells are fit very well by a single pole low pass filter plus a time delay. The pole is located at 6.0 Hz and corresponds to a time constant of 26.5 msec. The 8 msec time delay is in good agreement with the 8-12 msec difference between latencies in response to step inputs as measured at the gracile and VPL levels. Because of physical limitations the highest input frequency used was 7.0 Hz. As a result the gain curve of Fig. 4.8 does not show much attenuation and it is impossible to ascertain whether or not there are more poles or zeroes beyond 7 Hz from the asymptotic behavior of the gain and phase curves. It is clear, though, that the VPL cell does introduce a significant phase lag over and above the expected time delays.

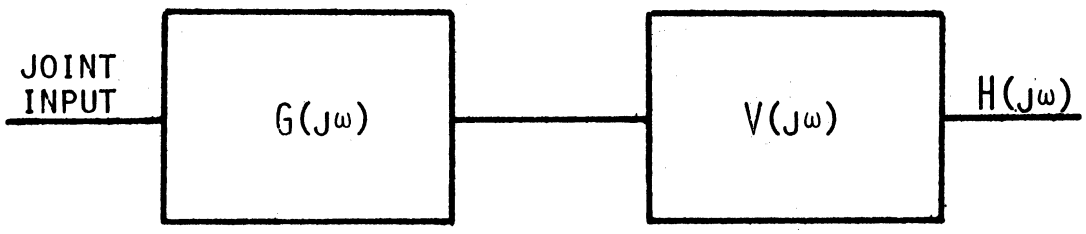

Figure 4.7. Block diagram of knee joint system. This is a simplified diagram of the system for rapidly adapting knee joint cells to the thalamus. G(jω) is the transfer function of the gracile cells, H(jω) is the frequency response of the entire pathway to the thalamus, and V(jω) is the transfer properties of the thalamic cells themselves.

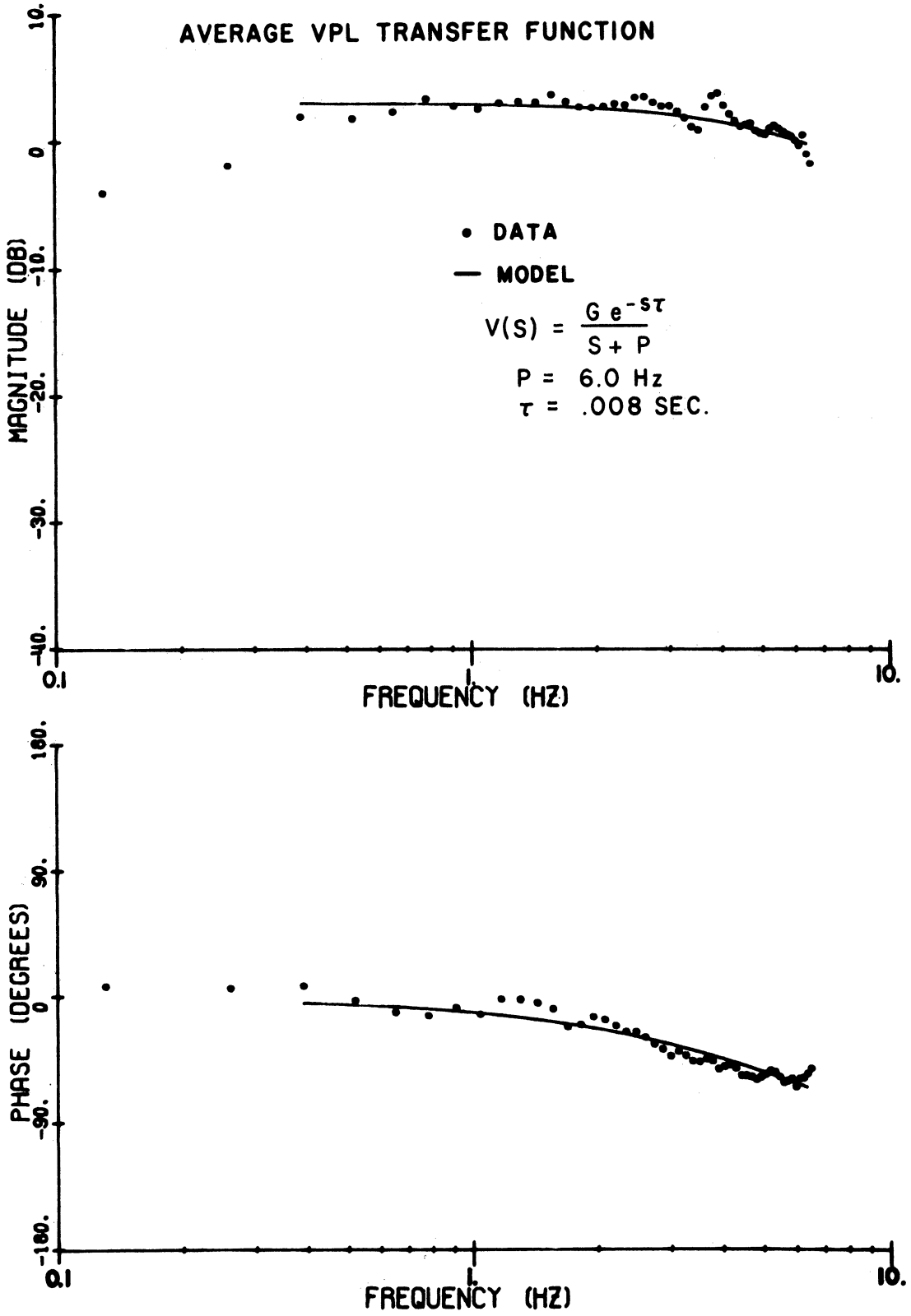

Figure 4.8. Average transfer function of the VPL cells. The data points were obtained from the data of Figs. 3.28 and 4.6. The solid curve is a model with transfer function and optimized parameters as shown. See text for details.

DISCUSSION

The major result of this chapter is the demonstration that the transfer characteristic of the VPL cell itself can be modeled by a simple low pass filter. This low pass feature represents the decoding and subsequent re-encoding properties of the VPL cells and is equivalent to an operation of integration in the time domain.

From the evidence given here it is not possible to determine whether the low pass characteristic is due to the decoder or encoder portion of the neuron. For several reasons I believe it is the decoding mechanism that has the low pass characteristic. First, at the frog neuromuscular junction Landau and Lass (1973) found that the decoding mechanism has a low pass filter response by stimulating the motor nerve with frequency modulated pulse trains and measuring the intracellular end plate potentials (e.p.p.). Second, in the crayfish stretch receptor where a similar low pass characteristic was found, Terzuolo and Bayly (1968) found that the frequency response of the encoder element was relatively flat. They were able to discriminate between the decoding and encoding properties of the cell by impaling it with a microelectrode and introducing sinusoidally-varying intracellular currents. Third, the postsynaptic membrane can be modeled by an RC network that is equivalent to a low pass filter (Hodgkin, 1964), and the geometry and cable properties of the dendritic tree can produce low pass filter effects (Rall, 1962). Also, latency dispersion caused by differences in the conduction velocity from gracile to VPL can also cause low pass effects, though these effects are probably small for this small distance (Williams, 1971). Thus, the physical properties of the cell would predict that the dynamic response of the presynaptic

pulse trains will be demodulated by low pass filtering at the synapses, and the filtered signal will be re-encoded and transmitted to the next level.

The time constant calculated from the data in Fig. 4.7 is greater than the time constants observed in some studies of intracellularly recorded EPSPs. Maekawa and Purpura (1967) show EPSP's in the VPL of cats with time constants in the range of 3-10 msec and IPSPs with time constants of about 15-20 msec. They found that by initially hyperpolarizing the cell, longer time constants were obtained and the increased duration was attributable to an additional depolarization component with the same time course as the IPSPs. Landau and Lass (1973) also found a low pass filter for the demodulating element of neuromuscular junctions with a time constant much larger than the measured e.p.p. decay time. By including facilitatory effects, especially one with only a 15% amplitude gain but a long 260 msec decay time, they were able to simulate the increased attenuation in the response at low frequencies. The facilitation was such that each e.p.p. caused succeeding e.p.p.'s to be increased in amplitude by an exponential factor with a long time constant. A rationale for the facilitatory effects that had to be included in the Landau and Lass simulation may then be provided by the Maekawa and Purpura study. If each action potential causes an after-hyperpolarization of the membrane, then the EPSP's occuring during this hyperpolarization will be of longer duration and time constant. The equivalent time constant of the EPSP's will be increased. Intracellular recordings of EPSP's in the lateral geniculate (Creuzfeldt et al., 1966) and in the ventrolateral nucleus (Uno et al., 1970)

have found time constants of about 40 msec and 32 msec, respectively, which are in the range of values required by the frequency response results reported here.

The results of this study are similar to findings in the lateral geniculate by Maffei and Rizzolatti (1967). A single pole low pass filter with a time constant of 16 msec was found between the response of the retinal ganglion cells and the lateral geniculate cells. However, their data was based on a much smaller sample of cells, with considerably fewer data points in the bandwidth of interest, and on transfer functions that were fit by eye with no apparent consideration for conduction delays. On the other hand, with visual stimuli they were able to stimulate the cells with a much broader bandwidth of sinusoidal signals and their transfer function shows a correspondingly better definition at high frequencies.

It appears then that the VPL cells can temporally integrate the afferent pulse trains with a low pass filter that probably resides in the decoding element of the cell membrane. From the discussion in the THEORY section, it can be seen that a low pass filter can extract the signal component from a frequency modulated pulse train, particularly if the pulse train has the random character seen in many higher-order neurons.

CHAPTER V

GENERAL SUMMARY AND CONCLUSIONS

The frequency response characteristics of cells sensitive to knee joint stimulation in the somatosensory thalamus of both anesthetized and unanesthetized cats have been studied by the use of single unit and linear systems analysis. The response of these thalamic cells has been compared with characteristics of the cells in the gracile nucleus that are thought to synapse upon them in order to study the properties of neural transmission. This chapter summarizes these results and discusses the implications of the findings.

DYNAMIC RESPONSE OF VPL CELLS

The majority of knee joint cells in VPL are rapidly adapting and respond only when the limb is in motion. The describing functions for these cells can be characterized as high pass filters, i.e. they are much more sensitive to high than to low frequency stimuli. This characteristic is common to many mechanoreceptors and reflects the need of the organism to know about rapid movements of the limb, which are potentially harmful. Although the individual cells cannot all be described by a single transfer function, the general features of the response profiles are very similar. The population response, obtained by averaging the individual VPL cell responses, is best fit by a transfer function that can be termed velocity-sensitive. However, it is uncertain whether or not the nervous system actually uses this information to detect the velocity of the input stimulus, though the capacity to do so is present in the thalamic population. Several

untested assumptions are needed in order to obtain the population responses from the average of the single cell responses.

The joint receptors are part of a complex reflex arc that involves muscle afferents and the vestibular system to maintain postural balance. Although the fast compensatory components of the reflex arc are spinal, there is, no doubt, a slower, more precise feedback loop involving the cerebral cortex. For this latter system the phasic joint receptors can possibly provide the velocity information necessary for derivative feedback. Since the time delays in the system are quite significant, the derivative feedback can be important in maintaining the stability of the system. However, it must be kept in mind that at least at the single cell level of the thalamus, the cells are nonlinear transducers of joint movement. The phase-locking and occasional bi-directional behavior are highly nonlinear. The assumption that the nervous system operates with the fundamental component of the response must be examined at the cortical levels.

The rapidly adapting cells cannot convey position sense information. However, they are, no doubt, important in the perception of movements of the limb. It has been known since the work of Goldscheider (1898) that detection of liminal excursions of joints are much more sensitive for higher velocities of joint movement. The steep slope of the frequency response curves of the phasic joint receptors provides for this increased sensitivity at high frequencies. This characteristic was secure enough to be insensitive to anesthetic or to the waking state of the animal.

A very small number of slowly adapting knee joint cells were found in the VPL, even though they were the primary target of the

investigation. This finding, coupled with the large number of tonic knee joint receptors and the fact that the tonic cells do not ascend in the dorsal columns, makes the functional role of the tonic joint cells open to question. It is known that some of the tonic receptors project to the cerebellum via the dorsal spinocerebellar tract. The others may project to the cerebral cortex via some, as yet unknown, pathway. The dynamic response of the tonic joint cell found in the VPL was similar to the response of the tonic joint receptors, but there were not enough data to make any general statement. The activity of the tonic cells seemed to be more susceptible to anesthetic interference.

TRANSFER PROPERTIES OF VPL

By comparing the frequency response of the VPL joint cells with the gracile joint cells, the transfer characteristic of the thalamic cell was found to be that of a low pass filter. This corresponds neatly with the notion that the higher order cells in the central nervous system are sensitive to the average rate of discharge of the cells impinging upon them and that they demodulate the activity by low pass filtering. The filtering is believed to be due to the time constant of the post-synaptic membrane, the filtering processes of the dendritic tree, latency dispersion, and the synaptic transmission processes themselves. The average time constant of the filter is 26 msec, which is somewhat longer than those found by recording EPSP's intracellularly, but not out of reason.

The low pass characteristic of the higher order cells can be important in filtering out the noise components of the signal. For

an IPFM process such as seen frequently at the periphery, the noise components are caused by the carrier rate and its sidebands. For a random process the Poisson nature of the discharge contributes a constant noise power over all frequencies. In both of these cases low pass filtering can extract the signal component. In addition the high pass characteristic of the receptors requires that there be some low pass filtering along the transmission path in order to keep the high frequency noise from interfering with the signal. This is a common consideration in the design of systems that utilize velocity or acceleration transducers.

SUGGESTIONS FOR FUTURE RESEARCH

There are several natural directions in which this research can progress. In order to clarify the functional importance of the joint receptor system, it is necessary to study joint cells in the cortex and to find the location of the second order cell for the tonic receptors. The goal of much of this line of research is to correlate psychophysical measures with the neurophysiological events thought to be essential to them. In order for these results to be clinically useful, it is necessary to know the pathways involved on the way to the cortex and to design the proper psychophysical tests to measure the performance of a certain class of receptors and their central projections. For example, if, as it now appears, the pathways for the slowly adapting and rapidly adapting joint receptors utilize different spinal tracts, then psychophysical tests that can test differentially for static position sense (assumed to be at least partially mediated by the tonic joint receptors) and for joint

movement (assumed to be mediated by the phasic receptors) will be able to localize spinal lesions in different spinal tracts. For this reason a clarification of the pathway for the tonic cells and of their functional importance in conveying position sense is important.

However, the cat knee joint may not be the most fruitful area to pursue, despite the large body of literature already available. For one thing feline and primate joint receptor systems may be different. Since the eventual goal is to provide information for clinical use, the primate joint system would be more likely to match the human joint system. Also, there are more receptors in the primate joints than in the feline joints, thereby possibly alleviating to some extent the tedium of looking for the small population of joint afferents. For the same reason the elbow joint may be technically easier to study than the knee joint, though for clinical reasons the toe joint would be the most useful.

Several extensions of the work on the dynamic response of joint afferents could be useful in elucidating the properties of neural transmission. Sinusoidal inputs are not a natural form of stimulation. Band-limited white noise or sine waves superimposed upon white noise would more closely approximate the natural stimulus. A chronic preparation with a means of monitoring the joint angle in a naturally moving animal, say, running on a treadmill or playing with a ball would be an extremely interesting experiment. The correlation and spectral analysis techniques can be used in these experiments since no restrictions are placed on the

form of the input stimulus except that it cover the relevant bandwidth.

In order to determine the source of the low pass filtering, i.e. whether it is taking place in the decoding or encoding element of the cells, intracellular recordings could be used. If the postsynaptic potential shows the same dynamic response as the output pulse trains then the filtering mechanism must be in the decoder and the encoder would have a flat frequency response. However, this is a most difficult experiment since the intracellular recordings must be held long enough to obtain a frequency response function. In this respect the correlation and spectral analysis techniques would be a distinct advantage because of the increase in the data acquisition in comparison to traditional methods.

APPENDIX A

CORRELATION AND SPECTRAL ANALYSIS

Let x(t) be the input to a linear, time-invariant system with impulse response h(t) and additive noise n(t) as shown below.

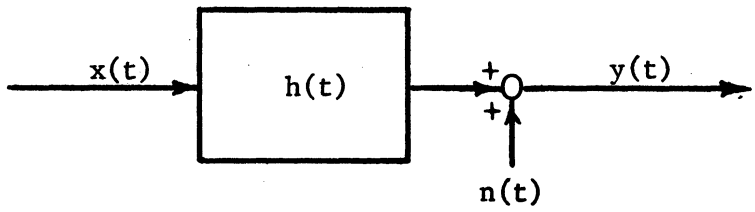

Figure A.1

From a well-known relation the output y(t) is given by the convolution integral of x(t) and h(t) plus the noise term

$$y(t) - \bar{y} = \int_0^\infty h(\alpha)(x(t - \alpha) - \bar{x})\, d\alpha + n(t) \qquad (A.1)$$

For real-time problems only a finite estimate of the sample means $\bar{x}$ and $\bar{y}$ are available, e.g.

$$\bar{x} = \frac{1}{T}\int_0^T x(t)\, dt \qquad (A.2)$$

The general problem is to identify the system response h(t) given x(t) and y(t). It will be shown here that the function h(t) that produces the least integrated square error satisfies the Wiener-Hopf integral equation.

First assume for conveniences sake that the sample means $\bar{x}$ and $\bar{y}$ are zero. It can easily be shown that these constants are simply carried through the calculations. Let the integrated square error be

$$E = \int_0^T n^2(t)\, dt = \int_0^T [y(t) - \int_0^\infty h(\alpha)\, x(t - \alpha)\, d\alpha]^2\, dt \qquad (A.3)$$

$$E = \int_0^T y^2(t)\,dt - 2\int_0^T [y(t)\int_0^\infty h(\alpha)x(t-\alpha)\,d\alpha\,]\,dt$$

$$+ \int_0^T [\int_0^\infty h(\alpha)x(t-\alpha)\,d\alpha \int_0^\infty h(\beta)x(t-\beta)\,d\beta\,]\,dt \qquad (A.4)$$

Interchanging the order of integration

$$E = \int_0^T y^2(t)\,dt - 2\int_0^\infty h(\alpha)[\int_0^T y(t)x(t-\alpha)\,dt]\,d\alpha$$

$$+ \int_0^\infty h(\alpha)\int_0^\infty h(\beta)[\int_0^T x(t-\alpha)x(t-\beta)\,dt]\,d\alpha d\beta \qquad (A.5)$$

For two functions $x(t)$ and $y(t)$ the cross-correlation function $R_{xy}(\tau)$ is given by

$$R_{xy}(\tau) = \lim_{T\to\infty} \frac{1}{2T}\int_{-T}^{T} y(u)x(u-\tau)\,du \qquad (A.6)$$

For real-time calculations this can be written

$$R_{xy}(\tau) = \frac{1}{T}\int_0^T y(u)x(u-\tau)\,du \qquad (A.7)$$

(A.5) can now be written in terms of cross-correlation functions

$$E = TR_{yy}(0) - 2T\int_0^\infty h(\alpha)R_{xy}(\alpha)\,d\alpha + T\int_0^\infty h(\alpha)\int_0^\infty h(\beta)R_{xx}(\alpha-\beta)\,d\alpha d\beta \qquad (A.8)$$

Note that the integrated square error is a function only of $h(\alpha)$, i.e. $E(h(\alpha))$. Using calculus of variations the $h(\alpha)$ that minimizes E can be found. In particular let $\hat{h}(\alpha)$ be the value that minimizes E. Then if

$$h(\alpha) = \hat{h}(\alpha) + kf(\alpha) \qquad (A.9)$$

then $E(h(\alpha))$ is a minimum when $k = 0$, or

$$\frac{\partial E(h(\alpha))}{\partial k} = 0, \ (k = 0) \text{ and } \frac{\partial^2 E(h(\alpha))}{\partial^2 k} > 0, \ (k = 0) \qquad (A.10)$$

then,

$$E(h(\alpha)) = TR_{yy}(0) - 2T\int_0^\infty [\hat{h}(\alpha) + kf(\alpha)]R_{xy}(\alpha)\, d\alpha$$

$$+ T\int_0^\infty\int_0^\infty [\hat{h}(\alpha) + kf(\alpha)][\hat{h}(\beta) + kf(\beta)]R_{xx}(\alpha - \beta)\, d\alpha d\beta \quad (A.11)$$

From (A.10)

$$\frac{\partial E(h(\alpha))}{\partial k}\Big|_{k=0} = -2T\int_0^\infty f(\alpha)R_{xy}(\alpha)\, d\alpha$$

$$+ T\int_0^\infty\int_0^\infty [f(\alpha)\hat{h}(\beta) + f(\beta)\hat{h}(\alpha)]R_{xx}(\alpha - \beta)d\beta d\alpha \quad (A.12)$$

$$= 0$$

Since $R_{xx}(\alpha - \beta) = R_{xx}(\beta - \alpha)$, the last term in (A.12) can be written as $T\int_0^\infty\int_0^\infty 2f(\alpha)\hat{h}(\beta)R_{xx}(\alpha - \beta)\, d\alpha d\beta$, and (A.12) becomes

$$0 = -2T\int_0^\infty f(\alpha)[R_{xy}(\alpha) - \int_0^\infty \hat{h}(\beta)R_{xx}(\alpha - \beta)\, d\beta]\, d\alpha \quad (A.13)$$

But (A.13) must hold for all $f(\alpha)$, therefore $\hat{h}(\alpha)$ must satisfy

$$R_{xy}(\alpha) = \int_0^\infty \hat{h}(\beta)R_{xx}(\alpha - \beta)\, d\beta \quad (A.14)$$

which is the Wiener-Hopf integral equation and also a convolution integral of $h(\alpha)$ and $R_{xx}(\alpha)$. The second condition of (A.10) can be shown by

$$\frac{\partial^2 E(h(\alpha))}{\partial^2 k} = 2\int_0^\infty\int_0^\infty f(\alpha)f(\beta)R_{xx}(\alpha - \beta)\, d\beta d\alpha \quad (A.15)$$

$$R_{xx}(\alpha - \beta) = \frac{1}{T}\int_0^T x(t - \alpha)x(t - \beta)\, dt \quad (A.16)$$

$$\frac{\partial^2 E(h(\alpha))}{\partial^2 k} = \frac{2}{T}\int_0^\infty\int_0^\infty f(\alpha)f(\beta)\int_0^T x(t - \alpha)x(t - \beta)dt d\beta d\alpha \quad (A.17)$$

Interchanging the order of integration

$$\frac{\partial^2 E(h(\alpha))}{\partial^2 k} = \frac{2}{T}\int_0^T \left[\int_0^\infty f(\alpha)x(t-\alpha)\,d\alpha \int_0^\infty f(\beta)x(t-\beta)\,d\beta\right] dt \quad (A.18)$$

$$= \frac{2}{T}\int_0^T \left|\int_0^\infty f(\alpha)x(t-\alpha)\,d\alpha\right|^2 dt > 0 \quad (A.19)$$

Thus, both conditions of (A.10) are proved and (A.14) is the relation for $\hat{h}(\alpha)$ such that it has the least square error. Note that this proof holds even for non-stationary processes. If the inputs and outputs are stationary, a similar proof based on mean square error can be shown.

Equation (A.14) can be transformed into the frequency domain by the help of the Wiener-Khinchine relation that the Fourier transform of the correlation function $R_{xy}(\tau)$ is the power spectral density $S_{xy}(\omega)$. Taking the Fourier transform of both sides of (A.14), we get

$$\int_{-\infty}^{\infty} R_{xy}(\alpha)\, e^{-j\omega\alpha}\, d\alpha = \int_{-\infty}^{\infty}\int_0^{\infty} \hat{h}(\beta)R_{xx}(\alpha-\beta)\,d\beta\, e^{-j\omega\alpha}\, d\alpha \quad (A.20)$$

From the Wiener-Khinchine relation and with an interchange in the order of integration and a change of variables, $\mu = \alpha - \beta$

$$S_{xy}(\omega) = \int_0^\infty \hat{h}(\beta)\, e^{-j\omega\beta} \int_{-\infty}^{\infty} R_{xx}(\mu)\, e^{-j\omega\mu}\, d\mu d\beta \quad (A.21)$$

$$= \left[\int_0^\infty \hat{h}(\beta)\, e^{-j\omega\beta}\, d\beta\right] S_{xx}(\omega) \quad (A.22)$$

$$S_{xy}(\omega) = \hat{H}(\omega)\, S_{xx}(\omega) \quad (A.23)$$

This is the basic relation that is used to find the frequency response function $H(\omega)$. This is done by finding the correlograms $R_{xx}(\tau)$ and $R_{xy}(\tau)$ using Fast Fourier Transform (FFT) techniques. Then the correlograms are also FFT to get the appropriate power spectral densities. In principle if the noise term $n(t)$ is uncorrelated with the input $x(t)$

a sufficiently long correlogram will reduce the least square noise to zero since from (A.1)

$$R_{xy}(\tau) = \int_0^\infty h(\alpha) R_{xx}(\tau - \alpha)\, d\alpha + R_{xn}(\tau) \tag{A.24}$$

$R_{xn}(\tau) \to 0$ as $T \to \infty$, if $x(t)$ and $n(t)$ are uncorrelated.

The frequency response $H(j\omega)$ is, in general a complex function that can be expressed as a magnitude $H(\omega)$ and a phase $\phi(\omega)$ such that

$$H(j\omega) = H(\omega)\, e^{j\phi(\omega)} \tag{A.25}$$

If the input is a sine wave, the output is also a sine wave with a change in amplitude and phase expressed by $H(j\omega)$

$$x(t) = \lambda_i \sin \omega t \tag{A.26}$$

$$y(t) = \lambda_m(\omega) \sin(\omega t + \phi(\omega)) \tag{A.27}$$

$$H(j\omega) = \lambda_m(\omega)/\lambda_i$$

For these inputs the powerful noise rejecting properties of correlation techniques can also be used to find the amplitude and phase. The cross-correlation of $x(t)$ and $y(t)$ is given by

$$R_{xy}(\tau) = \frac{1}{T}\int_0^T \lambda_i \sin \omega t\, \lambda_m(\omega) \sin(\omega t + \phi(\omega))\, dt \tag{A.28}$$

$$= \frac{\lambda_i \lambda_m(\omega)}{T} \int_0^T \sin \omega t \sin(\omega t + \phi(\omega))\, dt \tag{A.29}$$

$$= \frac{\lambda_i \lambda_m(\omega)}{2} \cos(\omega t + \phi(\omega)) \tag{A.30}$$

From the cross-correlation function (A.30) of the input and output the magnitude and phase of the response can be found.

APPENDIX B

DESCRIBING FUNCTION ANALYSIS AND SIMULATION

From (3.1) the response of a linear system is given by the convolution of the impulse response h(t) with the input x(t). Likewise, the response for the non-linear system is the convolution of the describing function impulse response $h_1(t)$ and input x(t) plus an additive noise term. If this noise term is uncorrelated with the input, then the system is identical to a linear system with additive uncorrelated noise (Appendix A). Harmonically-related noise can be eliminated by choosing a sampling window T_w that is short enough such that the second and higher harmonics are not correlated. The logarithmically swept sine waveform used in this study is superior to a linearly swept sine because the logarithmic sweep lengthens the sweep time in the lower frequencies where there is the greatest chance of distortion. If the logarithmic sweep has a bandwidth from f_o to f_h and a sweep length of T_s, then the following hold

$$f_h = f_o e^{aT_s} \tag{B.1}$$

$$a = (1/T_s) \ln (f_h/f_o) \tag{B.2}$$

The frequency f_1 at any time t_1 is

$$f_1 = f_o e^{at_1} \tag{B.3}$$

and the second harmonic $2f_1$ appears at time t_2

$$2f_1 = f_o e^{at_2} \tag{B.4}$$

$$t_2 - t_1 = (1/a) (\ln(2f_1/f_o) - \ln(f_1/f_o)) \tag{B.5}$$

$$= (1/a) \ln 2 \tag{B.6}$$

The criterion for rejecting higher harmonics is $T_w < t_2 - t_1$ since the logarithmic sweep passes through equal intervals of frequency in equal time increments. For this study I have used $f_o = .1$ Hz, $T_s = 150$ sec.,

T_w = 7.67 sec., so that $t_2 - t_1$ = 24.4 sec. Thus the criterion is easily satisfied and the second harmonics are not correlated into the signal. This shows that with the logarithmic sweep input the same relationships developed for finding the frequency response of a linear system can be used to find the describing function for a non-linear system. This technique was used for all of the swept frequency inputs.

To test the data analysis procedure, a simulation was performed with a model receptor. The block diagram of the simulation system is shown in Fig. B.1. A lead filter with frequency response

$$H(s) = \frac{s + a}{s + b} \qquad (B.7)$$

was simulated with operational amplifiers and the appropriate RC feedback networks. The input to the lead filter was a logarithmically swept frequency waveform with T_s = 150 sec. and bandwidth .1 - 15 Hz. This was considered to be the input to the system. The output of the lead filter was used to drive a linear voltage controlled oscillator (VCO) whose output was a frequency modulated pulse train with a constant carrier, The output of the VCO was then used as the clock frequency to a pseudo-random pulse generator whose output was a frequency modulated pulse train with a Poisson or random carrier. The random pulse generator was built by B.F. Belanger. See Appendix C for a more complete description of the device. The output of the random pulse generator was taken to be the output of the receptor. The average pulse rate λ_o could be varied with a Bernoulli sampler that preserved the statistical properties of the Poisson pulse train. Despite the high depth of modulation (α = .8), the modulating signal was not easy to discriminate aurally once it was randomized by the random pulse generator, particularly

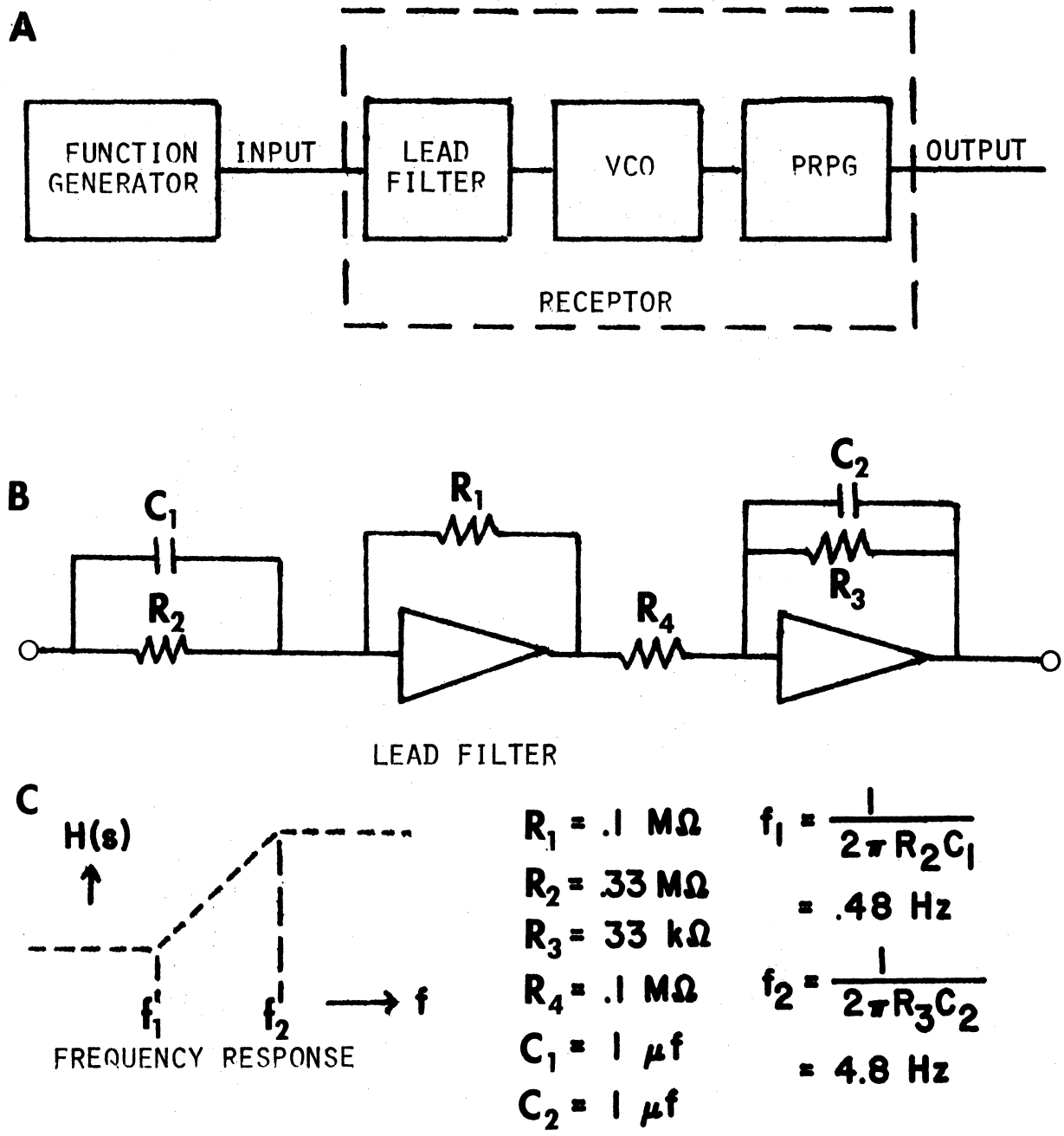

Figure B.1. Block diagram of the simulation. A) Overall block diagram of the simulation. Logarithmically swept sinusoidal waveforms were used as the input signal. The output signal was a frequency modulated pulse train with a random carrier. B). Diagram of the lead filter. C). Response characteristics and parameters of the lead filter.

for low λ_o.

The filter characteristics of the receptor were then extracted by the same procedure described in the Data analysis section (page 40) and compared with the known filter response function. The corner frequency of the low pass filter used to demodulate the pulse train was set at 15 Hz. Fig. B.2 shows the results of the frequency response extraction. The curve labeled "analog" is the true frequency response of the filter found by cross-correlating directly across the lead filter. As can be seen, the characteristics of the filter are very precisely found. At low λ_o the response shows greater deviation in both magnitude and phase from the model. This is a result of the smaller signal-to-noise ratio for low λ_o and is more evident in the coherence functions shown in Fig. B.3. See Appendix E for a full discussion of the signal-to-noise ratio for frequency modulated pulse trains with random carriers. The coherence function for the analog signal is very close to 1.0 as expected for a linear, noise-free system. For λ_o = 75 pps, the theoretical value for $\tilde{\gamma}^2(\omega) = 0.38$; for λ_o = 33 pps, $\tilde{\gamma}^2(\omega) = 0.21$; and for λ_o = 10 pps, $\tilde{\gamma}^2(\omega) = 0.08$. The results of the simulation show reasonably good correspondence to these theoretical values.

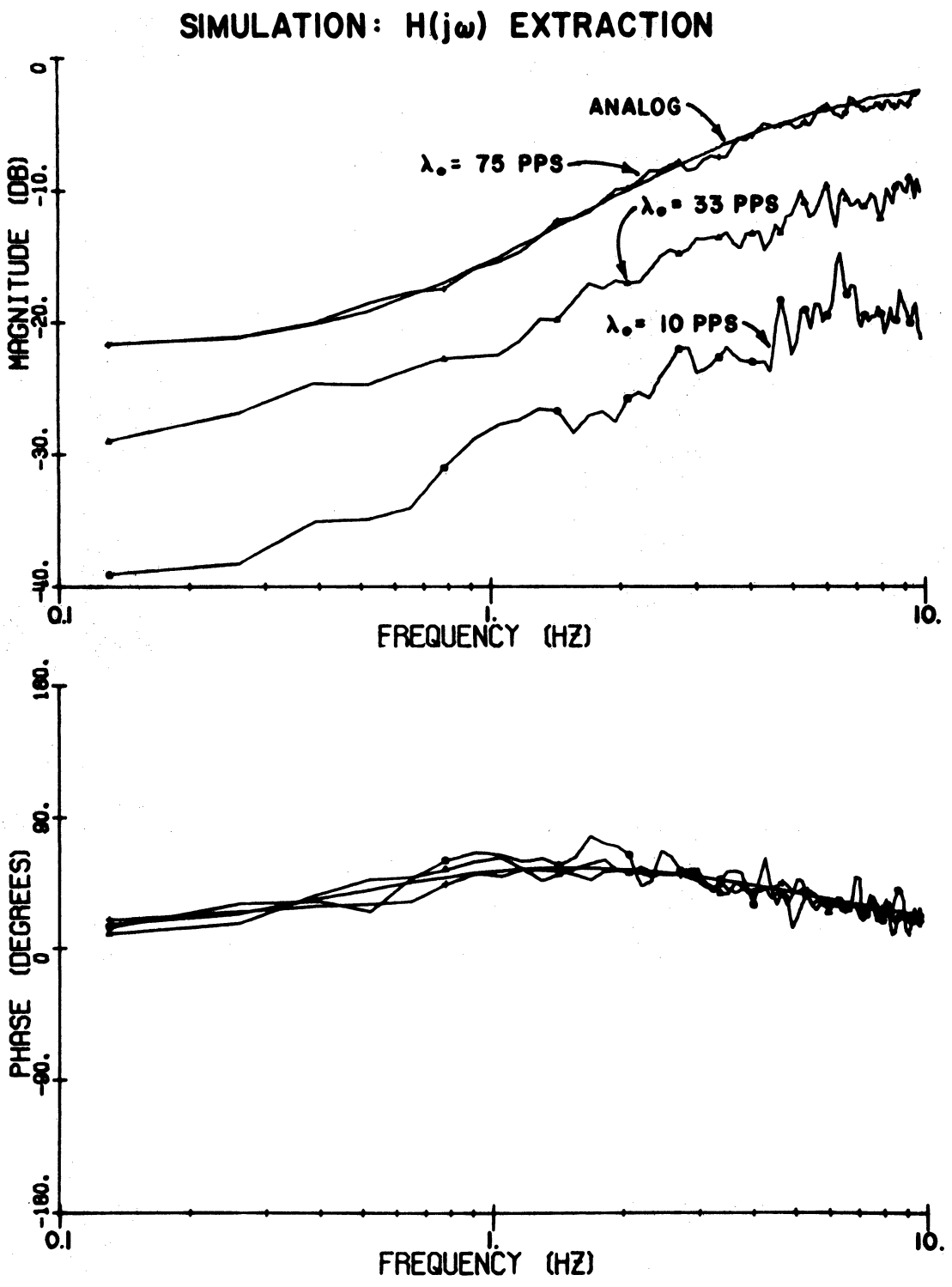

Figure B.2. Simulation results for frequency response extraction technique. The curve labeled "analog" is the characteristic of the lead filter of Fig. B.1b. Average pulse rate λ_o of the pseudo-random pulse generator is set at three different values as shown. See text for details.

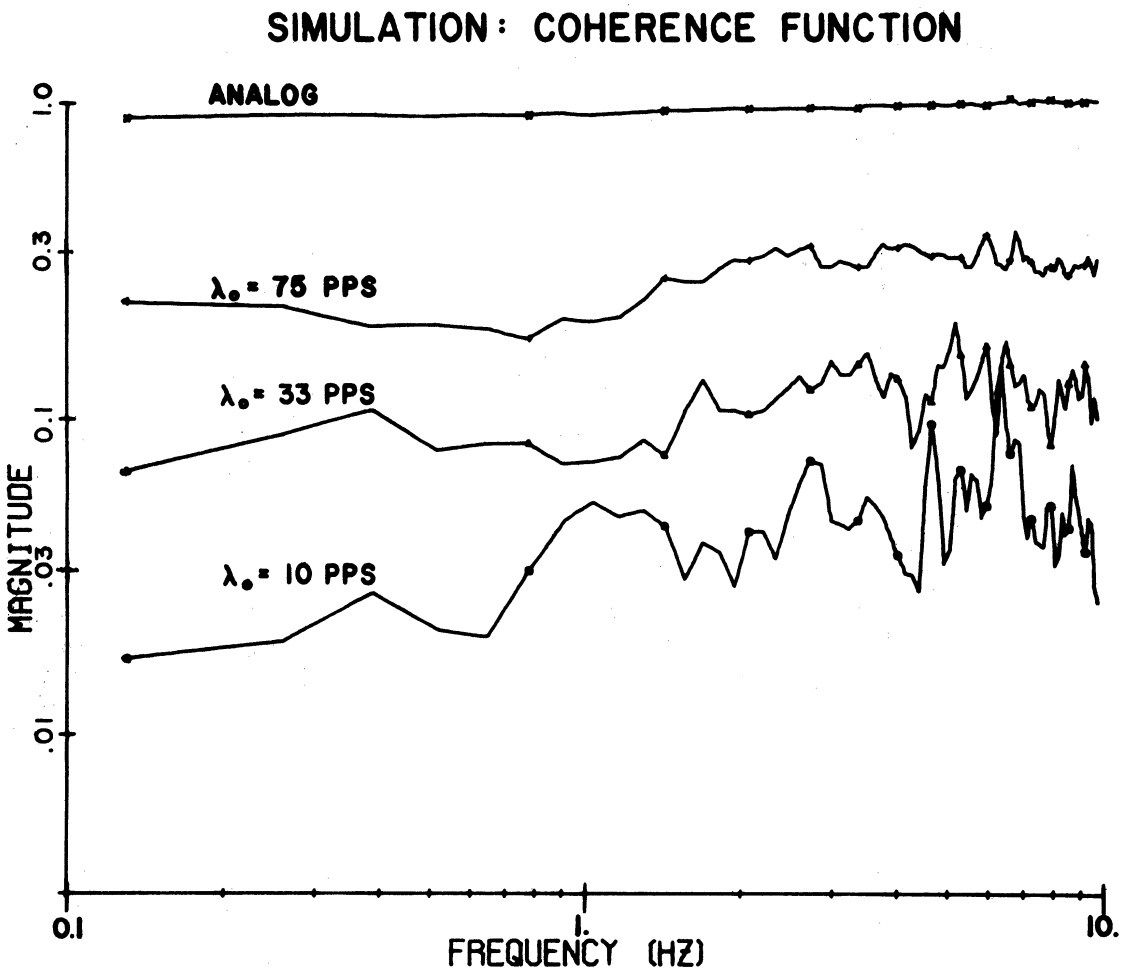

Figure B.3. Coherence functions for the simulation described in the text. The corresponding frequency response functions are shown in Fig. B.2.

APPENDIX C

PSEUDO-RANDOM PULSE GENERATOR

This appendix is a brief description of the pseudo-random pulse generator that is used in the simulation described in Appendix B. Fig. C.1 shows a block diagram of the generator. The basic device is a fifteen-stage shift register with linear modulo-two feedback. Pulses occurring on the clock line at point A trigger shifts in the state of each flip-flop so that the output of the shift register at point B is a pseudo-random telegraph wave. With the proper feedback the sequence of state changes is periodic (hence, pseudo-random) with period $2^{15} - 1$, or 32,766, clock pulses. Within this period the occurrence of zeroes or ones is equally likely and independent. By ANDing the random telegraph wave with the clock, a pseudo-random pulse train is obtained at point C.

Two additional properties make this device a useful tool for simulating neurophysiological phenomena. The average pulse rate of the output can be altered without affecting the statistics of the pulse train by a Bernoulli-type sampler. This is accomplished by ANDing the pulse train with the output of a multivibrator that has a variable pulse width (point E). The frequency of the multivibrator is made very large and asynchronous with respect to the clock rate so that the Bernoulli trials approach a Poisson process. In addition since the mean rate of the output is directly proportional to the clock frequency, it can be modulated by making the clock rate a frequency modulated pulse train. This is accomplished by putting the modulating signal into a voltage-controlled oscillator and using the output for the clock train. For a more detailed description, see Belanger, B.F., Williams, W.J., and Yin, T.C.T. (to be published).

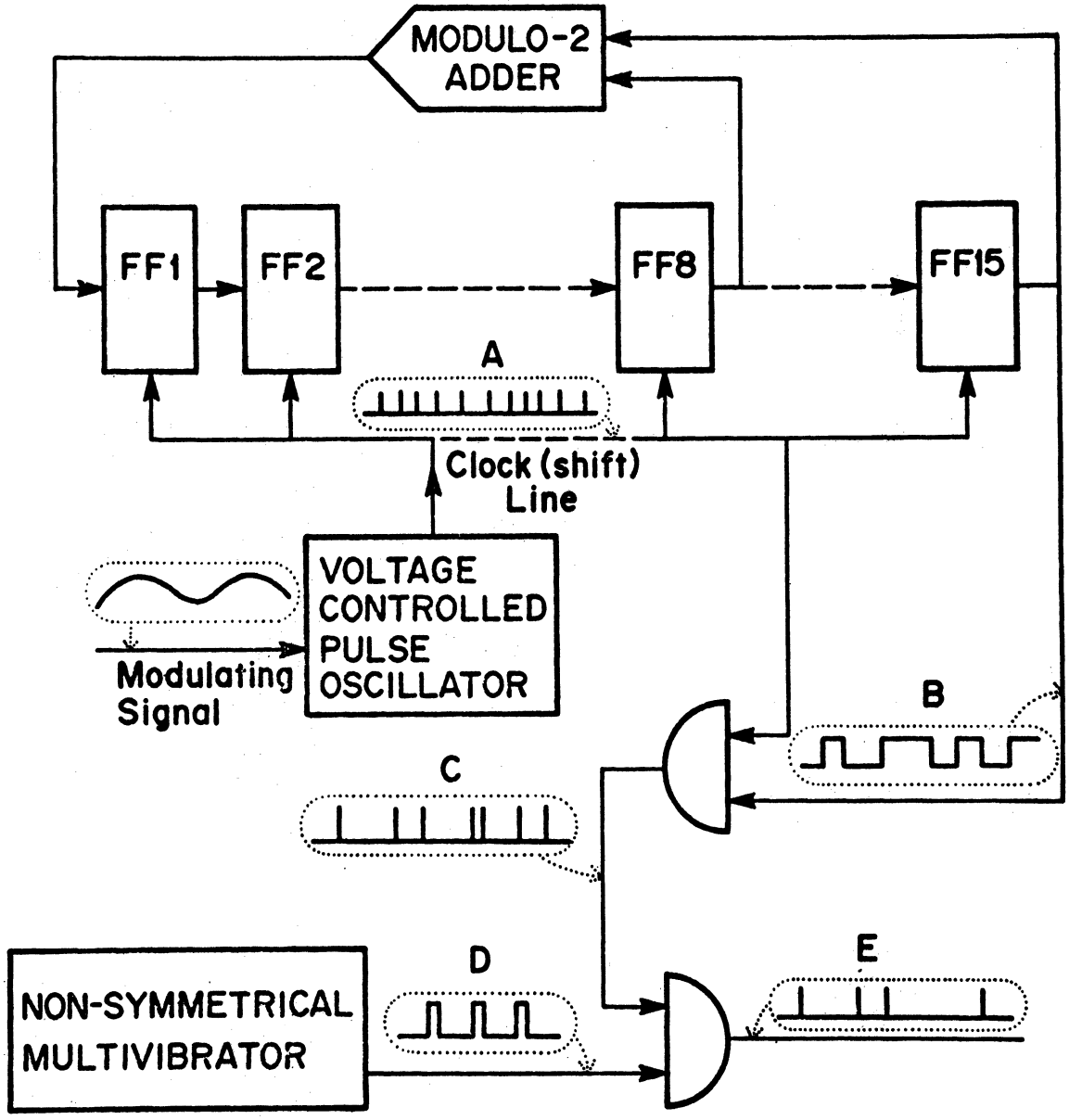

Figure C.1. Block diagram of the pseudo-random pulse generator. FF1 to FF15 is a 15 stage shift register. (From Belanger et al., 1973).

APPENDIX D

LINEARITY OF SCATTER DIAGRAM ORDINATE

This appendix is a demonstration that the frequency axis on the scatter diagrams is linear, at least for the subset of logarithmic sweeps that were used in this experiment. Let f_i be the instantaneous frequency of the swept input waveform determined by taking the reciprocal of the ith period, e.g. f_1 is the reciprocal of the first period. f_o and f_h are the lower and upper limits of the bandwidth and T_s is the total sweep time.

The logarithmic sweep is governed by the following relation

$$f(t) = f_o e^{at} \tag{D.1}$$

To determine a, we use the boundary condition

$$f_h = f_o e^{aT_s} \tag{D.2}$$

$$\ln (f_h/f_o) = aT_s \tag{D.3}$$

$$a = (1/T_s) \ln (f_h/f_o) \tag{D.4}$$

Now let $x = a/f_o$ and we get for the first few periods

$$f_1 = f_o \tag{D.5}$$

$$f_2 = f_o e^{a/f_o} = f_o e^x \tag{D.6}$$

$$f_3 = f_o e^{a(1/f_o + 1/f_2)} = f_o e^x e^{xe^{-x}} \tag{D.7}$$

$$f_4 = f_o e^{a(1/f_o + 1/f_2 + 1/f_3)}$$

$$= f_o e^x e^{xe^{-x}} e^{xe^{-xe^{-x}}} \tag{D.8}$$

$$f_5 = f_o e^{a(1/f_o + 1/f_2 + 1/f_3 + 1/f_4)}$$

$$= f_o e^x e^{xe^{-x}} e^{xe^{-xe^{-x}}} e^{xe^{-xe^{-xe^{-x}}}} \tag{D.9}$$

.
.
.
.

Since each row on the scatter diagram corresponds to a separate period of the swept frequency input, the frequency axis will be linear if the $\{f_i\}$ are linear in i. Assume that the value of x is small so that the following assumptions can be made

$$e^{x} = 1 + x + \frac{x^2}{2} \tag{D.10}$$

$$e^{-x} = 1 - x + \frac{x^2}{2} \tag{D.11}$$

The $\{f_i\}$ are linear in i if the difference between successive f_i are all equal, i.e. if $f_{i+1} - f_i = f_{n+1} - f_n$ for all i and n. To check this use the relations (D.5-- D.9) and throw out all third order terms.

$$\begin{aligned} f_2 - f_1 &= f_o e^{x} - f_o \\ &= f_o(1 + x + \frac{x^2}{2} - 1) = f_o(x + \frac{x^2}{2}) \end{aligned} \tag{D.12}$$

$$\begin{aligned} f_3 - f_2 &= f_o e^{x}(e^{xe^{-x}} - 1) \\ &= f_o(1 + x + \frac{x^2}{2})((1 + x + \frac{x^2}{2})(1 - x^2) - 1) \\ &= f_o(1 + x + \frac{x^2}{2})(x - \frac{x^2}{2}) \\ &= f_o(x + \frac{x^2}{2}) \end{aligned} \tag{D.13}$$

$$\begin{aligned} f_4 - f_3 &= f_o e^{x} e^{xe^{-x}} (e^{xe^{-x}e^{-xe^{-x}}} - 1) \\ &= f_o(1 + x + \frac{x^2}{2}) e^{x-x^2} (e^{x(1 - x + \frac{x^2}{2})(1 - x + \frac{x^2}{2})(1 + x^2)} - 1) \\ &= f_o(1 + 2x - x^2)(e^{x - 2x^2} - 1) \\ &= f_o(1 + 2x - x^2)(x - \frac{3x^2}{2}) \\ &= f_o(x + \frac{x^2}{2}) \end{aligned} \tag{D.14}$$

$$\begin{aligned} f_5 - f_4 &= f_o e^{x} e^{xe^{-x}} e^{xe^{-x}e^{-xe^{-x}}} (e^{xe^{-x}e^{-xe^{-x}}e^{-xe^{-x}}e^{-xe^{-x}}} - 1) \\ &= f_o(1 + 3x - \frac{x^2}{2})(e^{x(1 - 2x + 2x^2)e^{-x + 2x^2}} - 1) \\ &= f_o(1 + 3x - \frac{x^2}{2})(x - \frac{5x^2}{2}) = f_o(x + \frac{x^2}{2}) \end{aligned} \tag{D.15}$$

From (D.12 - D.15) it can be seen that the lower order f_i are linear in i. It can be shown (ardously!) that the relationship holds for all f_i as well. Thus, the frequency axis will be linear provided that the assumptions regarding x in (D.10) and (D.11) are true. For the values used in this experiment, the approximations in (D.10) and (D.11) are true to better than .0004%. In general x will be small provided that the bandwidth is not wide and the sweep time is long.

APPENDIX E

POWER SPECTRUM FOR A FREQUENCY MODULATED RANDOM PULSE TRAIN

This appendix gives a new derivation for the power spectrum of a frequency modulated pulse train with a Poisson or random carrier. The proof is an extension of the work of Bayly (1968) who first derived the power spectrum of a frequency modulated pulse train with a steady carrier. Knox (1970) has previously found the result given here by a different method adapted from Bartlett (1963). The proof offered here has the attribute of being easy to conceptualize and is adapted from one given by Lee (1960) for a non-modulated Poisson process.

Let x(t) be a Poisson point process with a time-varying rate parameter, i.e. the probability of a spike in time dt is given by $\lambda(t)dt$, i.e. $P_{\xi}(\xi = \text{a spike in time dt}) = \lambda(t)dt$ where $\lambda(t)$ is the modulating signal. Let $\lambda(t)$ be a periodic waveform of period T and average value λ_o. It can be written as

$$\lambda(t) = \lambda_o + \lambda_m(t,\phi) \tag{E.1}$$

where

$$\lambda_o = \frac{1}{T}\int_0^T \lambda(t)\ dt \text{ and } \frac{1}{T}\int_0^T \lambda_m(t,\phi)\ dt = 0 \tag{E.2}$$

$\lambda_m(t,\phi)$ is the time-varying component of $\lambda(t)$ and is a function of t and ϕ, the phase angle of $\lambda(t)$ with respect to t = 0. Further assume that the auto-correlation function $R_{xx}(\tau)$ is given by the ensemble average auto-correlation

$$R_{xx}(\tau) = \iint_{x_1 x_2} x_1 x_2\ P_{\xi_1\xi_2}(x_1,x_2,\tau)\ dx_1 dx_2 \tag{E.3}$$

where $P_{\xi_1\xi_2}(x_1,x_2,\tau)$ is the joint probability that the variables $\xi_1 = x_1$

and $\xi_2 = x_2$ in time τ. Assume that the pulse train consists of ideal pulses such that the variables ξ_1 and ξ_2 can take on only two values A and 0. The pulses are of amplitude A and width dt such that as $A \to \infty$ and $dt \to 0$, $Adt = 1$. The continuous probability densities of (E.3) can now be written as discrete densities

$$R_{xx}(\tau) = \sum_i \sum_j x_{1i} x_{2j} P_{\xi_1 \xi_2}(x_{1i}, x_{2j}, \tau) \qquad \text{(E.4)}$$

x_{1i} and x_{2j} are the set of possible realizations of the variables ξ_1 and ξ_2. Since there are two possible realizations for ξ_1 and ξ_2, namely A and 0, then there are only four possible values for x_{ij}, i.e. $x_{11} = 0$, $x_{12} = A$, $x_{21} = 0$, and $x_{22} = A$. The only non-zero product term that is possible is when $\xi_1 = \xi_2 =$ A and $x_{12}x_{22} = A^2$. Thus (E.4) becomes

$$R_{xx}(\tau) = x_{12} x_{22} P_{\xi_1 \xi_2}(x_{12}, x_{22}, \tau) \qquad \text{(E.5)}$$

Assume that an arbitrary point in time is picked for $\tau = 0$ such that $\lambda(\tau)$ has phase ϕ at $\tau = 0$. ϕ is a random variable with a uniform density over (0,T) since it is chosen randomly.

Take the two cases for $\tau = 0$ and $\tau \neq 0$ separately. For $\tau = 0$

$$\begin{aligned} R_{xx}(\tau,\phi)\Big|_{\tau=0} &= x_{12} x_{22} P_{\xi_1 \xi_2}(x_{12}; x_{22}) \\ &= A^2 \left[\lambda_o + \lambda_m(\phi)\right] d\tau \Big|_{\substack{A\to\infty \\ d\tau\to 0}} \\ &= A\lambda_o + A\lambda_m(\phi)\Big|_{A\to\infty} \\ &= \lambda_o \delta(\tau) + \lambda_m(\phi)\delta(\tau) \end{aligned} \qquad \text{(E.6)}$$

where $\delta(\tau)$ is the Dirac-delta function. For $\tau \neq 0$, rewrite the joint probability as a product of conditional probabilities.

$$P_{\xi_1 \xi_2}(x_{12}; x_{22}, \tau) = P_{\xi_1}(x_{12}) P_{\xi_2 | \xi_1}(x_{22} | x_{12}, \tau) \qquad \text{(E.7)}$$

$$P_{\xi_1}(x_{12}) = [\lambda_o + \lambda_m(\phi)]\, d\tau \tag{E.8}$$

$$P_{\xi_2|\xi_1}(x_{22}|x_{12},\tau) = [\lambda_o + \lambda_m(\phi,\tau)]\, d\tau \tag{E.9}$$

From (E.7-E.9)

$$\begin{aligned} R_{xx}(\tau,\phi)\Big|_{\tau\neq 0} &= x_{12}x_{22}P_{\xi_1}(x_{12})P_{\xi_2|\xi_1}(x_{22}|x_{12},\tau) \\ &= A^2[\lambda_o + \lambda_m(\phi)]\, d\tau\, [\lambda_o + \lambda_m(\tau,\phi)]\, d\tau \Big|_{\substack{A\to\infty \\ d\tau\to 0}} \\ &= \lambda_o^2 + \lambda_o[\lambda_m(\phi) + \lambda_m(\tau,\phi)] + \lambda_m(\phi)\lambda_m(\tau,\phi) \end{aligned} \tag{E.10}$$

From (E.6) and (E.10) the auto-correlation for all τ is

$$\begin{aligned} R_{xx}(\tau,\phi) = {} & \lambda_o\delta(\tau) + \lambda_m(\phi)\delta(\tau) + \lambda_o^2 + \lambda_o[\lambda_m(\phi) + \lambda_m(\tau,\phi)] \\ & + \lambda_m(\phi)\lambda_m(\tau,\phi) \end{aligned} \tag{E.11}$$

But this is the auto-correlation for a particular value of ϕ at $\tau = 0$. In order to find the true ensemble averaged auto-correlation $R_{xx}(\tau)$, the expected value of $R_{xx}(\tau,\phi)$ must be taken over ϕ.

$$\begin{aligned} R_{xx}(\tau) &= E_\phi[R_{xx}(\tau,\phi)] \\ &= \frac{1}{T}\int_0^T R_{xx}(\tau,\phi)\, d\phi \\ &= \frac{1}{T}\int_0^T \{\lambda_o\delta(\tau) + \lambda_m(\phi)\delta(\tau) + \lambda_o^2 + \lambda_o[\lambda_m(\phi) + \lambda_m(\tau,\phi)] \\ &\qquad + \lambda_m(\phi)\lambda_m(\tau,\phi)\}\, d\phi \end{aligned} \tag{E.12}$$

But from (E.2) all integrals of the form

$$\frac{1}{T}\int_0^T \lambda_m(\tau,\phi)\, d\phi = \frac{1}{T}\int_0^T \lambda_m(\phi)\, d\phi = 0 \tag{E.13}$$

Therefore

$$R_{xx}(\tau) = \lambda_o\delta(\tau) + \lambda_o^2 + \frac{1}{T}\int_0^T \lambda_m(\phi)\lambda_m(\tau,\phi)\, d\phi \tag{E.14}$$

The last term of (E.14) is simply the time auto-correlation of $\lambda(t)$

$$R_{xx}(\tau) = \lambda_o \delta(\tau) + \lambda_o^2 + R_{\lambda\lambda}(\tau,\phi) \tag{E.15}$$

If the process $\lambda(\tau)$ is stationary, this reduces to

$$R_{xx}(\tau) = \lambda_o \delta(\tau) + \lambda_o^2 + R_{\lambda\lambda}(\tau) \tag{E.16}$$

By using the Wiener-Khinchine relation, the power spectral density for the frequency modulated Poisson point process is given by

$$S_{xx}(\omega) = \lambda_o + \lambda_o^2 \delta(\omega) + S_{\lambda\lambda}(\omega) \tag{E.18}$$

For a sinusoidal modulating signal

$$\lambda(t) = \lambda_o + \lambda_m \cos \omega_m t \tag{E.19}$$

$$R_{xx}(\tau) = \lambda_o \delta(\tau) + \lambda_o^2 + \frac{\lambda_m^2}{2} \cos \omega_m \tau \tag{E.20}$$

$$S_{xx}(\omega) = \lambda_o + 2\pi\lambda_o^2 \delta(\omega) + \frac{\pi}{2} \lambda_m^2 \, \delta(|\omega| - \omega_m) \tag{E.21}$$

This spectra is shown in Fig. 4.4b. If a perfect low pass filter with passband f_b is used to demodulate the signal, then the signal-to-noise ratio is given by

$$S/N = \frac{\frac{\pi}{2} \lambda_m^2}{2\pi f_b \lambda_o} = \frac{\lambda_m^2}{4\lambda_o f_b} \tag{E.22}$$

Let $\alpha = \lambda_m/\lambda_o$ be the depth of modulation

$$S/N = \frac{\alpha^2 \lambda_o}{4 f_b} \tag{E.23}$$

so that the S/N is a linear function of the average pulse rate λ_o.

The generalization of this derivation to all periodic functions was suggested by W.J. Williams.

APPENDIX F

POWER SPECTRUM AND AUTO-CORRELATION FOR RENEWAL POINT PROCESS

This appendix gives a derivation of the power spectrum and auto-correlation for a renewal point process that has a gamma probability density function (pdf) and is unmodulated. The proof is not meant to be rigorous, but rather to be illustrative of certain principles in renewal processes.

Recall that a renewal point process is one in which the intervals are independent and identically distributed random variables drawn from a pdf. We consider mth order gamma functions as the pdf's. The rationale for choosing gamma functions is that they appear quite often in the neurophysiological literature and that as m varies from 1 to ∞, the spike trains described by these pdf's varies from random to essentially constant.

Let the pdf for an mth order gamma function be $f_1(t)$ where

$$f_1(t) = \frac{\lambda(\lambda t)^{m-1}}{\Gamma(m)} \; e^{-\lambda t} \qquad \text{(F.1)}$$

where λ = the mean rate. Let m be an integer in which case $\Gamma(m) = (m-1)!$

Let $f_n(t)$ be the pdf for higher order intervals of the gamma process described by $f_1(t)$, e.g. $f_3(t)$ is the pdf for intervals derived from $f_1(t)$ by taking every third spike. Since the intervals are independent and the pdf of the sum of random variables is given by the convolution of the individual pdf's,

$$f_n(t) = \int_0^\infty f_1(u)\, f_{n-1}(t - u)\, du \qquad \text{(F.2)}$$

Let g(t) be the renewal density, which is the pdf for a spike occurring at time t, given a spike at t = 0, and regardless of any intervening spikes. Assume that the pulses are ideal Dirac-delta functions $\delta(t)$

$$g(t) = \sum_{n=1}^{\infty} f_n(t) \tag{F.3}$$

The **auto-correlation** function $R(\tau)$ is given by

$$R(\tau) = g(t) + \lambda\delta(t) \tag{F.4}$$

Take the LaPlace transform of (F.1)

$$F_1(s) = \left(\frac{\lambda}{s + \lambda}\right)^m \tag{F.5}$$

Since the LaPlace transform of the convolution of two functions is given by the product of the individual transforms, by induction on (F.2)

$$F_n(s) = \left(\frac{\lambda}{s + \lambda}\right)^{nm} \tag{F.6}$$

From (F.3)

$$G(s) = \sum_{n=1}^{\infty} F_n(s) = \sum_{n=1}^{\infty} \left(\left[\frac{\lambda}{s + \lambda}\right]^m\right)^n \tag{F.7}$$

Since $\sum_{n=1}^{\infty} u^n(x) = \frac{u(x)}{1 - u(x)}$ for $u(x) < 1$, (F.7) becomes

$$G(s) = \frac{(\lambda^m/(s + \lambda)^m}{1 - \lambda^m/(s + \lambda)^m} = \frac{\lambda^m}{(s + \lambda)^m - \lambda^m} \tag{F.8}$$

The auto-correlation function $R(\tau)$ can be found by taking the inverse LaPlace transform of (F.8) for the particular value of m and using (F.4).

BIBLIOGRAPHY

1. Amassian, V.E., Macy, J. Jr., Waller, H.J., Leader, H.S., and Swift, M. Transformation of afferent activity at the cuneate nucleus. Inf. Proc. in the Nervous System 12th International Congress. Leiden. 235-254, 1962.

2. Amassian, V.E., Berlin, L., Macy, J. Jr., and Waller, H.J. Simultaneous recording of the activities of several individual cortical neurons. Trans. N.Y. Acad. Sci. 21: 395-405, 1959.

3. Andersen, P., Brooks, C.M., Eccles, J.C., and Sears, T.A. The ventrobasal nucleus of the thalamus: potential fields, synaptic transmission and excitability of both presynaptic and post-synaptic components. J. Physiol., London 174: 348-369, 1964a.

4. Andersen, P., Eccles, J.C., and Sears, T.A. The ventrobasal complex of the thalamus: types of cells, their responses and their functional organization. J. Physiol., London 174: 370-399, 1964b.

5. Andrew, B.L. The sensory innervation of the medial ligament of the knee joint. J. Physiol., London 123: 241-250, 1954.

6. Andrew, B.L. and Dodt, E. The deployment of sensory nerve endings at the knee joint of the cat. Acta physiol. scand. 28: 287-296, 1953.

7. Angel, A. Cortical responses to paired stimuli applied peripherally and at sites along the somato-sensory pathway. J. Physiol., London 191: 427-448, 1967.

8. Angel, A. The central control of sensory transmission and its possible relation to reaction time. Acta psychol. 30: 339-357 1969.

9. Baker, M.A. Spontaneous and evoked activity of neurones in the somatosensory thalamus of the waking cat. J. Physiol., London 217: 359-379, 1971.

10. Bartlett, M.S. The spectral analysis of point processes. J. Roy. Stat. Soc. B 25: 264-281, 1963.

11. Bava, A., Fadiga, E., and Manzoni, T. Interactive potentialities between thalamic relay nuclei through subcortical commissural pathways. Arch. Sci. Biol. 50: 101-133, 1966.

12. Bayly, E.J. Spectral analysis of pulse frequency modulation in the nervous system. IEEE Trans. Bio-Med. Engin. 15: 257-265, 1968.

13. Bayly, E.J., Cervetto, L., Fiorentini, A., and Maffei, L. On and off retinal cells in parallel channel communication. Kybernetik 8: 52-58, 1968.

14. Bell, C. On the nervous circle that connects voluntary muscles with the brain. Phil. Trans. Roy. Soc. London, Part II. 163-173, 1826.

15. Bendat, J.S. and Piersol, A.G. Measurement and Analysis of Random Data. New York: Wiley, 1966.

16. Boivie, J. The termination of the cervicothalamic tract in the cat. An experimental study with silver impregnation methods. Brain Res. 19: 333-360, 1970.

17. Boivie, J. The termination of the spinothalamic tract in the cat. An experimental study with silver impregnation methods. Exp. Brain Res. 12: 331-353, 1971a.

18. Boivie, J. The termination in the thalamus and the zona incerta of fibres from the dorsal column nuclei (DCN) in the cat. An experimental study with silver impregnation methods. Brain Res. 28: 459-490, 1971b.

19. Boyd, I.A. The histological structure of the receptors in the knee joint of the cat correlated with their physiological response. J. Physiol., London 124: 476-488, 1954.

20. Boyd, I.A. and Roberts, T.D.M. Proprioceptive discharges from the stretch receptors in the knee joint of the cat. J. Physiol., London 122: 38-58, 1953.

21. Brindley, G.S. and Merton, P.A. The absence of position sense in the human eye. J. Physiol., London 153: 127-130, 1960.

22. Brown, M.C. and Stein, R.B. Quantitative studies on the slowly adapting stretch receptor of the crayfish. Kybernetik 3: 175-185, 1966.

23. Browne, K., Lee, J., and Ring, P.A. The sensation of passive movement at the metatarso-phalangeal joint of the great toe in man. J. Physiol., London 126: 448-458, 1954.

24. Burgess, P.R. and Clark, F.J. Dorsal column projection of fibres from the cat knee joint. J. Physiol., London 203: 301-315, 1969a.

25. Burgess, P.R. and Clark, F.J. Characteristics of knee joint receptors in the cat. J. Physiol., London 203: 317-335, 1969b.

26. Campbell, F.W. and Robson, J.G. Application of Fourier analysis to the visibility of gratings. J. Physiol., London 197: 551-566, 1968.

27. Chapman, K.M. and Smith, R.S. A linear transfer function underlying impulse frequency modulation in a cockroach mechanoreceptor. Nature 197: 699-701, 1963.

28. Cohen, L.A. Activity of knee joint proprioceptors recorded from posterior articular nerve. Yale J. Biol. and Med. 28: 225-232, 1955.

29. Cook, A.W. and Browder, E.J. The function of posterior columns in man. Arch. Neurol. 12: 72-79, 1965.

30. Cox, D.R. and Smith, W.L. On the superposition of renewal processes. Biometrika 41: 91-99, 1954.

31. Creuzfeldt, O., Fuster, J.M., Herz, A., and Straschill, M. Some problems of information transmission in the visual system. In: Brain and Conscious Behavior. Ed. J.C. Eccles. New York: Springer Verlag. 138-164, 1966.

32. Crosby, E.C., Humphrey, T. and Lauer, E.W. Correlative Anatomy of the Nervous System. New York: MacMillan, 1962.

33. Dobry, P.J.K. and Casey, K.L. Roughness discrimination in cats with dorsal column lesions. Brain Res. 44: 385-397, 1972.

34. Dodge, F.A., Shapley, R.M., and Knight, B.W. Linear systems analysis of the Limulus retina. Behav. Sci. 15: 24-36, 1970.

35. Eldred, E., Yellin, H., Gadbois, L., and Sweeney, S. Bibliography on muscle receptors: their morphology, pathology, and physiology. Exp. Neurol. Suppl. 3: 1-154, 1967.

36. Evarts, E.V. Photically evoked responses in visual cortex units during sleep and waking. J. Neurophysiol. 26: 229-248, 1963.

37. Farias, M.A.C. Static and dynamic characteristics of cat knee joint receptors. Ph.D. thesis, Univ. of Michigan, 1973.

38. Freeman, M.A.R. and Wyke, B. Articular contributions to limb muscle reflexes. The effects of partial neurectomy of the knee joint on postural reflexes. Brit. J. Surgery 53: 61-69, 1966.

39. Freeman, M.A.R. and Wyke, B. The innervation of the knee joint. An anatomical and histological study in the cat. J. Anat. 101: 505-532, 1967.

40. French, A.S., Holden, A.V., and Stein, R.B. The estimation of the frequency response function of a mechanoreceptor. Kybernetik 11: 15-23, 1972.

41. Gardner, E. The distribution and termination of nerves in the knee joint of the cat. J. Comp. Neurol. 80: 11-33, 1944.

42. Gardner, E. Pathways to the cerebral cortex for nerve impulses from joints. Acta anat., Basel 73: Suppl. 56, 203-216, 1969.

43. Gardner, E. and Noer, R. Projection of afferent fibers from muscles and joints to the cerebral cortex of the cat. Am. J. Physiol. 168: 437-441, 1952.

44. Gelfan, S. and Carter, S. Muscle sense in man. Exp. Neurol. 18: 469-473, 1967.

45. Gesink, J.W. and Williams, W.J. A servo-contolled linear actuator for bio-system studies. Proc. 21st A.C.E.M.B. 10: 18.5, 1968.

46. Gestri, G. Pulse frequency modulation in neural systems. A random model. Biophys. J. 11: 98-109, 1971.

47. Glees, P. and Soler, J. Fiber content of the posterior columns and synaptic connections of the nucleus gracilis. Z. Zellforsch. 36: 381-400, 1951.

48. Goldberg, J.M., Adrian, H.O., and Smith, F.D. Response of neurons of the superior olivary complex of the cat to acoustic stimuli of long duration. J. Neurophysiol. 27: 706-749, 1964.

49. Goldberg, J.M. and Fernandez, C. Physiology of peripheral neurons innervating semicircular canals of the squirrel monkey. I. Resting discharge and response to constant accelerations. J. Neurophysiol. 34: 635-660, 1971.

50. Goldscheider, A. Physiologie des Muskelsinnes. Leipzig: Barth, 1898.

51. Goodwin, G.M., McCloskey, D.I., and Matthews, P.B.C. Proprioceptive illusions induced by muscle vibration: contribution by muscle spindles to perception? Science 175: 1382-1384, 1972a.

52. Goodwin, G.M., McCloskey, D.I., and Matthews, P.B.C. The persistence of appreciable kinesthesia after paralysing muscle afferents. Brain Res. 37: 326-329, 1972b.

53. Grant, G., Boivie, J., and Silfvenius, H. Course and termination of fibers from the nucleus Z of the medulla oblongata. An experimental light microscopical study in the cat. Brain. Res. 55: 55-70, 1973.

54. Ha, H. and Liu, C.N. Spinal afferents to lateral cervical nucleus and their terminals. Anat. Rec. 142: 237-238, 1962.

55. Ha, H. and Liu, C.N. Organization of the spino-cervico-thalamic system. J. Comp. Neurol. 127: 445-470, 1966.

56. Harris, F.A. Population analysis of somatosensory thalamus in the cat. Nature 225: 559-562, 1970.

57. Hayward, J.N., Fairchild, M.D., Stuart, D.G., and Deemer, J.A. A stereotaxic platform for microelectrode studies in chronic animals. Electroenceph. clin. Neurophysiol. 16: 522-524, 1964.

58. Helmholtz, H. Handbuch der physiologischen Optik, Leipzig: Voss, 1897.

59. Hodgkin, A.L. The Conduction of the Nervous Impulse. Liverpool: Liverpool Univ. Press, 1964.

60. Hughes, G.W. and Maffei, L. Retinal ganglion cell response to sinusoidal light stimulation. J. Neurophysiol. 29: 333-352, 1965.

61. Jabbur, S.J., Baker, M.A., and Towe, A.L. Wide-field neurons in thalamic nucleus ventralis posterolateralis of the cat. Exp. Neurol. 36: 213-238, 1972.

62. James, W. The Principles of Psychology, Vol. 2, Chap. XXVI. London: MacMillan, 1890.

63. Jasper, H.H. and Ajmone-Marsan, C. A Stereotaxic Atlas of the Diencephalon of the Cat. Ottawa: National Research Council. 1954.

64. Jenkins, G.M. and Watts, D.G. Spectral Analysis and Its Applications. San Francisco: Holden-Day, 1968.

65. Jones, G.M. and Milsum, J.H. Characteristics of neural transmission from the semicircular canal to the vestibular nuclei of cats. J. Physiol., London 209: 295-316, 1970.

66. Kiang, N.Y.-S. Discharge Patterns of Single Fibers in the Cat's Auditory Nerve. Research Monograph M.I.T. Press, 1965.

67. Kirkwood, P.A. The frequency response of frog muscle spindles under various conditions. J. Physiol., London 222: 135-160, 1972.

68. Kitai, S.T., Ha, H., and Morin, F. Lateral cervical nucleus of the dog: anatomical and microelectrode studies. Am. J. Physiol. 209: 307-311, 1965.

69. Kitai, S.T. and Morin, F. Microelectrode study of dorsal spinocerebellar tract. Am. J. Physiol. 203: 799-802, 1962.

70. Kitai, S.T. and Weinberg, J. Tactile discrimination study of the dorsal column-medial lemniscal system and spino-cervico-thalamic tract in cat. Exp. Brain. Res. 6: 234-246, 1968.

71. Knox, C.K. Signal transmission in random spike trains with applications to the statocyst neurons of the lobster. Kybernetik 7: 167-174, 1970.

72. Körner, L. and Landgren, S. Projections of low threshold joint afferents to the cerebral cortex of the cat. Acta physiol. scand. 76: 5A-7A, 1969.

73. Krause, W. Histologische notizen. Zentbl. med. Wiss. 12: 211-212, 1874.

74. Kruger, L., Siminoff, R., and Witkovsky, P. Single neuron analysis of dorsal column nuclei and spinal nuclei of trigeminal cat. J. Neurophysiol. 24: 333-349, 1961.

75. Landau, E.M. and Lass, Y. Synaptic frequency response: the influence of sinusoidal changes in stimulation frequency on the amplitude of the end-plate potential. J. Physiol., London 228: 27-40, 1973.

76. Landgren, S., Nordwall, A., and Wengström, C. The location of the thalamic relay in the spinocervico-lemniscal path. Acta physiol. scand. 65: 164-175, 1965.

77. Landgren, S. and Silfvenius, H. Nucleus Z, the medullary relay in the projection path to the cerebral cortex of group I muscle afferents from the cat's hind limb. J. Physiol., London 218: 551-571, 1971.

78. Lashley, K.S. The accuracy of movement in the absence of excitation from the moving organ. Am. J. Physiol. 43: 169-194, 1917.

79. Lavine, R.A. Phase locking in response of single neurons in cochlear nuclear complex of the cat to low frequency stimuli. J. Neurophysiol. 34: 467-483, 1971.

80. Lee, Y.W. Statistical Theory of Communication. New York: Wiley 1960.

81. Levitt, M. and Schwartzmann, R. Spinal sensory tracts and two point tactile sensitivity. Anat. Rec. 154: 377, 1966.

82. Lewis, P.A.W. Remarks on the theory, computation and application of the spectral analysis of series of events. J. Sound Vibr. 12: 353-375, 1970.

83. Lewis, P.A.W. (Ed.) Stochastic Point Processes. New York: Wiley Interscience, 1972.

84. Lindström, S. and Norrsell, U. A note on knee joint denervation and postural reflexes in the cat. Acta physiol scand. 82: 406-408, 1971.

85. Lindström, S. and Takata, M. Monosynaptic excitation of dorsal spinocerebellar tract neurones from low threshold joint afferents. Acta phsyiol. scand. 84: 430-432, 1972.

86. Lundberg, A. and Oscarsson, O. Functional organization of the dorsal spinocerebellar tract in the cat. Acta physiol. scand. 50: 356-374, 1960.

87. McCall, W.D., Jr. Dynamic response of slowly adapting cat knee joint receptors. Ph.D. thesis, Univ. of Michigan, 1971.

88. McCall, W.D., Jr., Farias, M.A.C., Williams, W.J., and BeMent, S.L. Static and dynamic responses of slowly adapting joint receptors. Brain Res. 1973. (In press).

89. McIntyre, A.K. Central projections of impulses from receptors activated by muscle stretch. In Symposium on Muscle Receptors, Ed. D. Barker. Hong Kong: Hong Kong Univ. Press, 19-29, 1962.

90. Maekawa, K. and Purpura, D.P. Properties of spontaneous and evoked synaptic activities of thalamic ventrobasal neurons. J. Neurophysiol. 30: 360-381, 1967.

91. Maffei, L. and Rizzolatti, G. Transfer properties of the lateral geniculate body. J. Neurophysiol. 30: 333-340, 1967.

92. Mallart, A. Thalamic projection of muscle nerve afferents in the cat. J. Physiol., London 194: 337-353, 1968.

93. Mannard, A. and Stein, R.B. Determination of the frequency response of isometric soleus muscle in the cat using random nerve stimulation. J. Physiol., London 229: 275-296, 1973.

94. Matthews, P.B.C. Muscle spindles and their motor control. Physiol. Rev. 44: 219-288, 1964.

95. Matthews, P.B.C. Mammalian Muscle Receptors and their Cnetral Actions. Baltimore: Williams and Wilkins, 1972.

96. Matthews, P.B.C. and Stein, R.B. The sensitivity of muscle spindles afferents to small sinusoidal changes of length. J. Physiol., London 200: 723-743, 1969.

97. Merton, P.A. Human position sense and sense of effort. Sym. Soc. Exp. Biol. 18: 387-400, 1964.

98. Millar, J. Joint afferent discharge following muscle contraction in the absence of joint movement. J. Physiol., London 226: 72P, 1972.

99. Moore, G.P., Perkel, D.H., and Segundo, J.P. Statistical analysis and functional interpretation of neuronal spike data. Ann. Rev. Physiol. 28: 493-522, 1966.

100. Morin, F. A new spinal pathway for cutaneous impulses. Am. J. Physiol. 183: 245-252, 1955.

101. Morin, F., Gardner, E., and Kitai, S.T. Microelectrode studies of a new spinal pathway. 12th International Congress. Leiden. 612.831, 1962.

102. Morin, F., Kitai, S.T., Portnoy, H., and Demirjian, C. Afferent projections to the lateral cervical nucleus: a microelectrode study. Am. J. Physiol. 204: 667-672, 1963.

103. Mountcastle, V.B. Modality and topographic properties of single neurons of cats' somatic sensory cortex. J. Neurophysiol. 20: 408-434, 1957.

104. Mountcastle, V.B. In discussion of Inf. Proc. in the Nervous System 12th International Congress. Leiden. 3: 61, 1962.

105. Mountcastle, V.B. (Ed.) Medical Physiology Vol II. St. Louis: C.V. Mosby Co., 1968.

106. Mountcastle, V.B. and Henneman, E. Pattern of tactile representation in thalamus of cat. J. Neurophysiol. 12: 85-100, 1949.

107. Mountcastle, V.B. and Henneman, E. Representation of tactile sensibility in the thalamus of the monkey. J. Comp. Neurol. 97: 409-440, 1952.

108. Mountcastle, V.B., Poggio, G.F., and Werner, G. The relation of thalamic cell response to peripheral stimuli varied over an intensive continuum. J. Neurophysiol. 26: 807-834, 1963.

109. Nakahama, H., Nishioka, S., Otsuka, T., and Aikawa, S. Statistical dependency between interspike intervals of spontaneous activity in thalamic lemniscal neurons. J. Neurophysiol. 19: 921-934, 1966.

110. Oscarsson, O. and Rosen, I. Projection to cerebral cortex of large muscle spindle afferents in forelimb nerves of the cat. J. Physiol., London 169: 924-945, 1963.

111. Oswaldo-Kruz, E. and Kidd, C. Functional properties of neurons in the lateral cervical nucleus of the cat. J. Neurophysiol. 27: 1-14, 1964.

112. Paillard, J. and Brouchon, M. Active and passive movements in the calibration of position sense. In The Neuropsychology of Spatially Oriented Behavior. Ed. S.J. Freedman. Illinois: Dorsey Press. 37-55, 1968.

113. Perkel, D.H., Gerstein, D.L., and Moore, G.P. Neuronal spike trains and stochastic point processes. I. The single spike train. Biophys. J. 7: 391-418, 1967.

114. Petit, D. and Burgess, P.R. Dorsal column projection of receptors in cat hairy skin supplied by myelinated fibers. J. Neurophysiol. 31: 849-855, 1968.

115. Poggio, G.F. and Mountcastle, V.B. The functional properties of ventrobasal thalamic neurons studied in unanesthetized monkeys. J. Neurophysiol. 26: 775-806, 1963.

116. Poggio, G.F. and Viernstein, L.J. Time series analysis of impulse sequences of thalamic somatic sensory neurons. J. Neurophysiol. 27: 517-545, 1964.

117. Poppele, R.E. and Bowman, R. Quantitative description of linear behavior of mammalian muscle spindles. J. Neurophysiol. 33: 59-71, 1970.

118. Pringle, J.W.S. and Wilson, V.J. The response of a sense organ to a harmonic stimulus. J. Exp. Biol. 29: 220-234, 1952.

119. Provins, K.A. The effect of peripheral nerve block on the appreciation and execution of finger movements. J. Physiol., London 143: 55-67, 1958.

120. Rall, W. Electrophysiology of a dendritic neuron model. Biophys. J. 2: 145-167, 1962.

121. Rescigno, A., Stein, R.B., Purple, R.L., and Poppele, R.E. A neuronal model for the discharge patterns produced by cyclic inputs. Bull. Math. Biophys. 32: 337-353, 1970.

122. Rinvik, E. A re-evaluation of the cytoarchitecture of the ventral nuclear complex of the cats' thalamus on the basis of corticothalamic connections. Brain. Res. 8: 237-254, 1968.

123. Rodieck, R.W. Maintained activity of cat retinal ganglion cells. J. Neurophysiol. 30: 1043-1071, 1967.

124. Rose, J.E. and Mountcastle, V.B. Activity of single neurons in the tactile region of cat in response to a transient peripheral stimulus. J. Hopkins Hosp. Bull. 94: 238-282, 1954.

125. Roth, P.R. Effective measurements using digital signal analysis. IEEE Spectrum 8: 62-70, 1971.

126. Samuel, E.P. The autonomic and somatic innervation of the articular capsule. Anat. Rec. 113: 53-70, 1952.

127. Schneider, L.W. Responses of first and second order vestibular neurons to thermal and rotational stimuli. Ph.D. thesis, Univ. of Michigan, 1973.

128. Schwartzmann, R.J. and Bogdonoff, M.D. Proprioception and vibration sensibility discrimination in the absence of the posterior columns. Arch. Neurol. 20: 349-353, 1969.

129. Sherrington, C.S. The muscular sense. In Textbook of Physiology. Ed. Schäfer. London. Vol. 2: 1002-1005, 1900.

130. Skoglund, S. Anatomical and physiological studies of knee joint innervation in the cat. Acta phsyiol. scand. 36: Suppl. 124, 1-101, 1956.

131. Škavřil, J., Radil-Weiss, T., Bohdanecky, Z. and Syka, J. Spontaneous discharge patterns of mesencephalic neurons: interval histogram and mean interval relationship. Kybernetik 9: 11-15, 1971.

132. Spekreijse, H. Rectification in the goldfish retina: analysis by sinusoidal and auxiliary stimulation. Vision Res. 9: 1461-1472, 1969.

133. Spekreijse, H. and Oosting, H. Linearizing: a method for analysing and synthesizing nonlinear systems. Kybernetik 7: 22-31, 1970.

134. Stein, R.B. Some models of neuronal variability. Biophys. J. 7: 37-68, 1967.

135. Stein, R.B., French, A.S., and Holden, A.V. The frequency response, coherence, and information capacity of two neuronal models. Biophys. J. 12: 295-322, 1972.

136. Stevens, S.S. Neural events and the psychophysical law. Science 170: 1043-1050, 1970.

137. Talbot, W.H., Darian-Smith, I., Kornhuber, H.H., and Mountcastle, V.B. The sense of flutter vibration: comparison of the human capacity with response patterns of mechanoreceptive afferents from the monkey hand. J. Neurophysiol. 31: 301-334, 1968.

138. Taub, A. and Bishop, P.O. The spinocervical tract: dorsal column linkage, conduction velocity, primary afferent spectrum. Exp. Neurol. 13: 1-21, 1965.

139. Terzuolo, C.A. (Ed.) Conf. on Systems Analysis Approach to Neurophysiological Problems. Brainerd, Minn.: Univ. Minn. Press, 1969.

140. Terzuolo, C.A. and Bayly, E.J. Data transmission between neurons. Kybernetik 5:83-85, 1968.

141. Thaler, G.J. and Pastel, M.P. Analysis and Design of Nonlinear Feedback Control Systems. New York: McGraw Hill, 1962.

142. Uno, M., Yoshida, M. and Hirota, I. The mode of cerebello-thalamic relay transmission investigated with intracellular recording from cells of the ventrolateral nucleus of cats' thalamus. Exp. Brain Res. 10: 121-139, 1970.

143. Vierck, C.J. Spinal pathways mediating limb position sense. Anat. Rec. 154: 437, 1966.

144. Viernstein, L.J. Dynamic properties of first order afferents responsive to joint rotation. Proc. A.C.E.M.B. 11: 4.7, 1969.

145. Wall, P.D. The sensory and motor role of impulses traveling in the dorsal columns towards cerebral cortex. Brain 93: 505-524, 1970a.

146. Wall, P.D. Sensory role of impulses traveling in the dorsal columns. IEEE Trans. on Man-Machine Systems 11: 39-44, 1970b.

147. Wallφe, L. Transfer of signals through a second order sensory neuron. Ph.D. thesis, Univ. of Oslo, 1968.

148. Werner, G. and Mountcastle, V.B. The variability of central neural activity in a sensory system and its implication for the central reflection of sensory events. J. Neurophysiol. 26: 958-977, 1963.

149. Williams, W.J. Transfer characteristics of dispersive nerve bundles. IEEE Trans. on Systems, Man, and Cybernetics 2: 72-85, 1972.

150. Williams, W.J., BeMent, S.L., Yin, T.C.T., and McCall, W.D., Jr. Nucleus gracilis responses to knee joint motion: a frequency response study. Brain. Res. 1973. (In press).

151. Williams, W.J., Gesink, J.W., and Stern, M.M. Biological system transfer function extraction using swept frequency and correlation techniques. Med. and Biol. Engineering 10: 609-620, 1972.

152. Winter, D.L. N. gracilis of cat. Functional organization and corticofugal effects. J. Neurophysiol. 28: 48-70, 1965.

ABSTRACT

DYNAMIC RESPONSE AND TRANSFER CHARACTERISTICS
OF KNEE JOINT AFFERENTS IN SOMATOSENSORY THALAMUS OF THE CAT

by
Tom Chi Tien Yin

Chairman: William J. Williams

The dynamic response of neurons sensitive to knee joint stimulation in the cat somatosensory thalamus were studied with sinusoidal inputs of joint angle. The input sine waves were applied with a precise voltage-controlled, electromechanical actuator. The average rate of discharge of a single cell was considered as the output parameter. Describing functions of the sensory system were extracted by correlation and spectral analysis techniques. The effects of anesthetic, bias angle, excursion angle, and waking condition of the animal were investigated. Discrete and swept sinusoidal waveforms between .1 and 7 Hz were used as inputs. Both anesthetized and unanesthetized animals were used in the experiment.

The majority of cells in the thalamus were rapidly adapting and had frequency response curves that were characterized as high pass filters. Although the major features of the response curves for individual cells were very similar, they could not all be fit with a single transfer function. The frequency response of all the rapidly adapting cells averaged together was well-fit by a transfer function that could be termed velocity-sensitive in the bandwidth between .1 and 7 Hz. Most of these phasic cells showed a phase-locking tendency, particularly

at high frequencies. The dynamics of the response for the rapidly adapting cells was relatively independent of anesthetic, bias angle, and waking condition of the animal. Threshold and saturation effects were exhibited by some cells for very small (< 2°) and large (> 10°) input amplitudes, respectively. In addition a small percentage (12%) showed a bidirectional response, i.e. responded at both flexion and extension of the limb. The anesthetic had a strong effect in depressing the spontaneous discharge of the cells and seemed to change the character of the tonic response by introducing a bursting response.

However, only 17% of the knee joint sensitive cells were slowly adapting or tonic, and more tonic cells were found in the unanesthetized animals. Only one cell was studied in detail and its dynamic characteristics were similar to that of the slowly adapting joint receptors. In this respect the rapidly adapting and slowly adapting joint cells in the thalamus have strikingly different frequency response curves, the former curves have a much steeper slope in the magnitude.

The response dynamics of the rapidly adapting joint cells in the thalamus were compared to the response found at the gracile nucleus, which is the level just preceding the thalamus for these afferents. At each level an average frequency response curve was found by normalizing and averaging all of the individual responses. The transfer characteristic of the thalamic cells was found to be well-fit by a single pole low pass filter plus a time delay. The corner frequency of the filter was 6.0 Hz and the time delay was 8.0 msec, in good agreement with latency measurements. The major component

of the filtering effect is believed to result from the postsynaptic membrane properties. The thalamic cell can use the low pass filter to demodulate the incoming pulse trains by temporal integration. The effect of the low pass filter may be to reduce the high frequency noise components of the signal that result from the high pass characteristics of the receptors.